



PWR STEAM GENERATOR TUBE REPAIR LIMITS:
TECHNICAL SUPPORT DOCUMENT FOR EXPANSION ZONE
PWSCC IN ROLL TRANSITIONS - REV. 2

NP-6864-L - Rev. 2

Research Projects S404-12, -15, -18, -19, -21, -24, -32, -37, -90, -92, -93

Draft Report
August 1993

NON-PROPRIETARY VERSION

Prepared by

Committee for Alternate Repair Limits for EZ PWSCC

Prepared for
Electric Power Research Institute
3412 Hillview Avenue
Palo Alto, California 94304

EPRI Project Manager
D. A. Steininger

Steam Generator Reliability Project
Nuclear Power Division

9403170081 930903
PDR TOPRP EXIEPRI
B PDR

NOTICE: This report contains proprietary information that is the intellectual property of EPRI. Accordingly, it is available only under license from EPRI and may not be reproduced or disclosed wholly or in part, by any Licensee to any other person or organization.

For further information on licensing terms and conditions for this report, contact the EPRI Office of Commercial Development. (415) 855-2974.

Electric Power Research Institute and EPRI are registered service marks of Electric Power Research Institute, Inc.

Copyright © 1990, 1991 and 1993 Electric Power Research Institute, Inc. All rights reserved.

NOTICE

This report was prepared by the Electric Power Research Institute, Inc. (EPRI). Neither EPRI, members of EPRI, nor any person acting on behalf of any of them: (a) makes any warranty, express or implied, with respect to the use of any information, apparatus, method, or process disclosed in this report or that such use may not infringe privately owned rights; or (b) assumes any liabilities with respect to the use of, or for damages resulting from the use of, any information, apparatus, method, or process disclosed in this report.

COMMITTEE FOR ALTERNATE REPAIR LIMITS FOR EZ PWSCC

Rev. 2

D. A. Steininger, Chairman
S. Brown**
L. Williams
ELECTRIC POWER RESEARCH INSTITUTE

G. Airey
NUCLEAR ELECTRIC

F. Anderson
NORTHEAST UTILITIES

J. Blomgren
COMMONWEALTH EDISON

G. Bollini
SPANISH UTILITIES

J. Engstrom
SWEDISH STATE POWER BOARD

J. Frick
SOUTH CAROLINA ELECTRIC & GAS

P. Hernalsteen**
LABORELEC

J. Hutin
ELECTRICITÉ DE FRANCE

G. Kammerdeiner
DUQUESNE LIGHT COMPANY

G. Kent
PORTLAND GENERAL ELECTRIC

D. Mayes
DUKE POWER

B. Miller
SOUTHERN NUCLEAR OPERATING CO.

R. Pearson
NORTHERN STATES POWER

J. Smith
ROCHESTER GAS & ELECTRIC

C. Smoker
WISCONSIN PUBLIC SERVICE

J. Jensen
AMERICAN ELECTRIC POWER

P. Anderson
ABB-COMBUSTION ENGINEERING

R. Gamble**
SARTREX CORP.

T. Gerber**
STRUCTURAL INTEGRITY ASSOC., INC.

J. Gorman**
DOMINION ENGINEERING, INC.

H. Houseman
R. Vollmer
ZETEC, INC.

J. Begley
J. Houtman**
WESTINGHOUSE ELECTRIC CORP.

J. Snider
BABCOCK & WILCOX

B. Curtis
ALLEN NUCLEAR ASSOCIATES

*Additional participants for document's first issue: S. Green (EPRI), C. Welty, Jr. (EPRI), M. Browne (SCE&G), D. Goetcheus (TVA), S. Leshnoff (GPU), B. Dow (EMSI).

**Document principal authors.

ABSTRACT

Primary water stress corrosion cracking (PWSCC) of alloy 600 steam generator tubes has been diagnosed in the tubesheet expansion zone (EZ) of many PWR steam generators. When existing tube repair limits based on crack depth are applied (such as plug at $\geq 40\%$ through-wall), many tubes may require unnecessary repair. Allowing tubes with axial PWSCC to remain in service can be justified based on a combination of 100% inspection by rotating pancake coil (RPC), a repair limit based on crack length rather than crack depth, a limit on the number of cracked tubes remaining in service, and a reduced primary to secondary allowable leak rate.

This report provides the technical support for a length-based tube repair limit for steam generator tubes in U.S. PWR power plants. In this approach, axial crack length is used as the measure of tube integrity and tube leakage potential, and operation with known through-wall cracks is permitted. An additional repair limit to preclude significant circumferential cracks in combination with axial cracks and modified repair limits for partial-depth rolled tubes are included.

This document has been prepared by a committee of U.S. and foreign industry participants who are experts on the technical and licensing issues associated with development and implementation of steam generator tube repair limits. The document represents the committee's recommended approach, and presents information for use by utilities as a reference or supplement to site-specific analyses for developing revised tube repair limits associated with PWSCC in roll transition expansion zones.

CONTENTS

<u>Section</u>		<u>Page</u>
1	INTRODUCTION AND BACKGROUND	1-1
	1.1 Overview	1-1
	1.2 Compliance With General Design Criteria	1-7
	1.3 Background	1-10
	1.4 Current International Practices	1-13
	1.5 References	1-15
2	CRACKED TUBE BURST DATA	2-1
	2.1 Integrity Criteria	2-1
	2.2 Tube Rupture	2-1
	2.3 References	2-12
3	CRACK LENGTH MEASUREMENT	3-1
	3.1 Background	3-1
	3.2 Rotating Pancake Coil (RPC)	3-1
	3.3 Demonstrated Crack Length Measurement Accuracy	3-6
	3.4 Compensating for Coil Diameter Effects in Measuring Length	3-18
	3.4 References	3-23
4	ALLOWABLE CRACK LENGTH	4-1
	4.1 Approach	4-1
	4.2 Tube Rupture Equation	4-4
	4.3 Loads and Safety Factors	4-6
	4.4 Material Properties and Tube Dimensions	4-6
	4.5 Correction for Tubesheet Constraint	4-7
	4.6 Allowance for Crack Growth	4-11
	4.7 Allowance for Crack Length Measurement Uncertainty	4-13
	4.8 Allowable Crack Length Sample Calculation	4-15
	4.9 References	4-18
5	LEAK RATE CONSIDERATIONS	5-1
	5.1 Leak Rate Under Normal Loads	5-1
	5.2 Leak Rate at Postulated Faulted Loads	5-4
	5.3 References	5-9

6	COMBINATION AXIAL AND CIRCUMFERENTIAL CRACKS	6-1
6.1	Introduction	6-1
6.2	Detection of Circumferential Cracks Between Axial Cracks	6-2
6.3	Pressure Capacity of Tubes With Combination Cracks	6-2
6.4	Additional Repair Limit to Preclude Significant Combination Cracks.	6-3
7	REPAIR LIMITS FOR THE EXPANDED REGION OF PARTIAL- DEPTH ROLLED TUBES	7-1
7.1	Tube Burst and Allowable Crack Length	7-1
7.2	Leak Rate Consideration	7-2
7.3	Summary of Repair Limits for Partial-Depth Rolled Tubes.	7-2
7.4	References	7-3
8	SUMMARY	8-1
8.1	Overview	8-1
8.2	Comparison With European Practices	8-3
APPENDIX A	STEAM GENERATOR DEGRADATION-SPECIFIC MANAGEMENT	A-1
A.1	Steam Generator Management	A-1
A.2	Steam Generator Management Strategy	A-2
A.3	Defense In Depth	A-2
A.4	EZ PWSCC Degradation Management	A-4
A.5	References	A-7
APPENDIX B	BACKGROUND OF PWSCC	B-1
B.1	Causes of Primary Water Stress Corrosion Cracking	B-1
B.2	Plant Experience	B-2
B.3	Impact of Roll Transition PWSCC	B-6
B.4	Remedial Measures for PWSCC in Expanded Areas	B-9
B.5	References	B-12
APPENDIX C	BURST DATA AND STATISTICAL EVALUATION OF DATA FOR THROUGH-WALL FLAWS AND BURST DATA FOR PART-THROUGHWALL-WALL FLAWS	C-1
APPENDIX D	NDE OF ROLL TRANSITIONS - INDUSTRY EXPERIENCE	D-1
D.1	Tube Pull Data	D-1
D.2	Specific Details	D-1
APPENDIX E	CRACK GROWTH RATE DATA	E-1
E.1	Introduction	E-1
E.2	Kiss Roll Data	E-1
E.3	Standard Roll Data	E-5
E.4	References	E-6

APPENDIX F	LEAK RATE DATA FOR STEAM GENERATOR TUBES WITH SCC IN THE EXPANSION ZONE ROLL TRANSITION REGION	F-1
APPENDIX G	ANALYSIS METHOD FOR LEAK RATE CALCULATION	G-1
	G.1 Introduction	G-1
	G.2 Base Deterministic Model	G-1
	G.3 Model Validation	G-5
	G.4 Probabilistic Methodology	G-14
	G.5 Computer Program	G-15
	G.6 References	G-22
APPENDIX H	COMBINATION AXIAL AND CIRCUMFERENTIAL CRACK DETECTION UTILIZING RPC EDDY-CURRENT PROBES	H-1
	H.1 Introduction	H-1
	H.2 NDE Experiments	H-1
	H.3 Results	H-13
APPENDIX I	PRESSURE TESTS OF STEAM GENERATOR TUBES WITH COMBINATION AXIAL AND CIRCUMFERENTIAL CRACKS	I-1
	I.1 Introduction	I-1
	I.2 LABORELEC Data	I-1
	I.3 TECNATOM Data	I-2
	I.4 Westinghouse Data	I-2
	I.5 References	I-3

ILLUSTRATIONS

<u>Figure</u>		<u>Page</u>
1-1	Schematic of EZ Roll Transition Axial Crack	1-2
1-2	EZ-PWSCC Axial Crack Configurations Acceptable for Continued Service Per the Guidance in This Document	1-3
1-3	EZ-PWSCC Axial Crack Configurations That Should be Repaired Per the Guidance in This Document	1-4
1-4	Examples of EZ-PWSCC Crack Configurations With Distinct Circumferential Crack Components for Which This Document Does Not Apply and Therefore Should be Repaired	1-6
2-1	Belgian (BELGATOM) Axial Defect Burst Test Data and Correlation	2-3
2-2	French (EdF/Framatome) Axial Defect Burst Test Data and Correlation	2-5
2-3	Westinghouse Axial Defect Burst Test Data and Correlation	2-6
2-4	Comparison of General Tube Burst Correlations Along With Lower Bound Tube Burst Equation	2-7
2-5	Comparison of Tube Rupture Equation with Data and Best Fit Curve for Axial Throughwall Cracks Having No Sealing System	2-9
2-6	Comparison of Throughwall Crack Tube Burst Relationships with Data for Axial Part-throughwall Cracks	2-11
3-1	Typical Rotating Pancake Coil	3-2
3-2	RPC Data Acquisition/Analysis	3-4
3-3	Zetec SM-15™ Analysis Display	3-5

3-4	Crack Length Prediction - Composite Industry Experience	3-8
3-5	Crack Length Prediction - Electricité de France	3-10
3-6	Crack Length Prediction - Laborelec	3-11
3-7	Crack Length Prediction - Swedish State Power Board	3-12
3-8	Crack Length Prediction - Spanish Utilities	3-13
3-9	Crack Length Prediction - U.S. Utility	3-14
3-10	Comparison of Eddy-Current and Ultrasonic Measurement of Crack Length	3-16
3-11	Eddy-Current Crack Length Measurement Showing Effects of Finite Coil Diameter	3-19
3-12	EdF Data Set Prior to Correction for Coil Diameter	3-21
3-13	EdF Data Set Showing How Coil Diameter Compensation Factor is Determined	3-22
4-1	Illustration of Allowable Crack Lengths for Axial and Inclined Axial Cracks	4-2
4-2	Allowable EZ PWSCC Axial Crack Length Calculation Steps	4-3
4-3	Tube Rupture Equation in Terms of Dimensionless Burst Pressure and Critical Crack Length	4-5
4-4	Allowance for Tubesheet Reinforcement	4-11
4-5	Estimate of EZ PWSCC Average Crack Growth Rate Curves	4-12
4-6	Definition of Crack Length Measurement Correction, a_{NDE}	4-13
5-1	Leak Rate Versus Nominal or Average Axial Crack Length for Steam Generator Tubes With Corrosion Cracks in the Expansion Zone Roll Transition Region, 600°F (Data From Appendix F)	5-2
5-2	Predicted Leak Rate Versus Axial Throughwall Crack Length for Steam Generator Tubes With Corrosion Cracks in the Expansion Zone Roll Transition Region, 515°F	5-8

A-1	Degradation-Specific Management Decision Tree	A-8
A-2	EZ PWSCC Degradation Management Decision Tree	A-9
B-1	Standard and "Kiss" Roll Transitions With Typical PWSCC	B-4
D-1	Ringhals 4 - Tube R22-C97. RPC Isometric - High and Low Sensitivity. Indication Just Below Roll Expansion	D-2
D-2	Ringhals 4 - Tube R22-C97. Comparison of Composite Test Results	D-3
D-3	Dam pierre 1 - Tube L12-C43. Comparison of RPC and Destructive Test Results	D-5
D-4	Doel 2 Tube R13-C30. Comparison of RPC and Destructive Test Results	D-6
D-5	Doel 3 Tubes R27-C52 and R23-C53. Actual Shape of Through-Wall Cracks and Comparison With RPC Length Measurement	D-7
D-6	Ringhals 4 - Tube R47-C50. Axial and Circumferential RPC Indications	D-8
D-7	Ringhals 4 - Tube R47-C50. Axial and Circumferential Cracks	D-9
D-8	Dampierre 1 - Tube L8-C48. Circumferential Cracks in Kiss-Roll Transition Comparison of RPC and Destructive Test Results	D-11
D-9	Ringhals 3 - Tube R18-C79. Short ID Axial Cracking	D-12
D-10	Ringhals 3 - Tube R18-C79. Composite Test Results	D-13
D-11	Ringhals 4 - Tube R17-C81. Multiple RPC Indications	D-14
D-12	Ringhals 4 - Tube R17-C81. Composite Test Results	D-15
E-1	Average Crack Growth Rates Based on LABORELEC Repeated Measurements of Kiss and Standard Roll Transitions with EZ PWSCC Indications.	E-4
G-1	Plastic Component of the Crack Leakage Area	G-3
G-2	Flow Discharge Coefficient Assumptions	G-4

G-3	Leakage Model Validation	G-5
G-4	Comparison of Calculated Leak Areas With Measured Areas, Belgian Data From SCHELLE Tests (Linear Coordinates)	G-6
G-5	Comparison of Calculated Leak Areas With Measured Areas, Belgian Data From SCHELLE Tests (Logarithmic Coordinates)	G-7
G-6	Correlation Between Flow Discharge Coefficient, K, and Mean Crack Width, CW	G-9
G-7	Comparison of Calculated Leak Rates (Eq. 5-1) With Measured Leak Rates From Various Programs	G-11
G-8	Distribution of Initial Crack Lengths	G-18
G-9	Distribution of End of Cycle and Critical Crack Lengths	G-18
G-10	Mean Crack Width as a Function of Crack Length	G-19
G-11	Distribution of Crack Width (For a Inch Long Crack)	G-19
G-12	Contribution of Each Crack Length Category to the Total Leak Rate (Total = gpm)	G-20
G-13	Distribution of Tube Leak Rates	G-20
G-14	Distribution of Steam Generator Leak Rate (mean = gpm)	G-21
H-1	Typical Test Sample Geometry (Expanded Tube With U-Shaped Notch at Roll)	H-2
H-2	Pancake Coil - Diameter, Sample # Z-9300	H-3
H-3	Pancake Coil - Diameter (Shielded), Sample # Z-9300	H-4
H-4	Pancake Coil - Diameter, Sample # Z-9299	H-5
H-5	Pancake Coil - Diameter (Shielded), Sample # Z-9299	H-6
H-6	Pancake Coil - Diameter, Sample # Z-9289	H-7
H-7	Pancake Coil - Diameter (Shielded), Sample # Z-9289	H-8
H-8	Pancake Coil - Diameter, Sample # Z-9231	H-9

H-9	Pancake Coil - Diameter (Shielded), Sample # Z-9281	H-10
H-10	Pancake Coil - Diameter, Sample # Z-9280	H-11
H-11	Pancake Coil - Diameter (Shielded), Sample # Z-9280	H-12
I-1	LABORELEC Combination Notch Geometries	I-7
I-2	LABORELEC Through-Wall Angle Degradation Pressure Tests	I-8
I-3	LABORELEC Through-Wall "L" Shaped Degradation Pressure Tests	I-9
I-4	Spanish Combination Degradation Pressure Test - Specimen Configuration	I-10
I-5	TECNATOM Part-Through-Wall Degradation Pressure Tests	I-11
I-6	Westinghouse Through-Wall "L" Shaped Degradation Pressure Tests	I-12
I-7	Westinghouse Modified Through-Wall and Part-Through-Wall "L" Shaped Degradation Pressure Tests	I-13
I-8	Sketches of Axial and Circumferential Cracks in Westinghouse RP301- 9 Specimens	I-14
I-9	Westinghouse Stress Corrosion Crack Pressure Tests	I-15

TABLES

<u>Table</u>	<u>Page</u>
1-1 Full-Depth Rolled Plants With PWSCC	1-12
3-1 Crack Length Measurement Accuracy	3-7
3-2 Eddy-Current Length Measurement Accuracy	3-15
4-1 Alloy 600 Strength Properties, 3/4 X 0.043-Inch Mill-Annealed Tubing	4-8
4-2 Alloy 600 Strength Properties, 7/8 X 0.050-Inch Mill-Annealed Tubing	4-9
4-3 Sample Calculations of Allowable Crack Length for 7/8-Inch and 3/4-Inch Diameter Tubes	4-17
5-1 Example Crack Distribution from RPC Inspection for Calculation of Leak Rate at Faulted Load for 7/8-Inch Diameter Tubes	5-7
5-2 Estimated Leak Rates for Postulated Faulted Load for Two Example Flaw Distributions	5-7
8-1 Comparison of Length-Based Repair Limits for Axial EZ PWSCC Roll Transition Cracks	8-4
A-1 Definitions	A-10
A-2 Management Options	A-11
B-1 Reported Extent of EZ PWSCC at Plants with >10% Tubes Affected	B-5
B-2 Status of PWSCC at Part-Depth-Rolled Plants in USA	B-7
B-3 Status of PWSCC at Full-Depth-Rolled Plants in USA	B-8
C-1 Normalized Burst Pressure for Non Degraded Tubes ($\lambda = 0$)	C-2
C-2 Westinghouse S/G Tube Burst Data, 70°F. EDM Notches in Roll Transition Region. Axial Through-Wall Cracks	C-3

C-3	NRC Phase II Burst Tests, 600°F, Tubes with Axial SCC	C-4
C-4	CE S/G Tube Burst Data, 565F. Axial IGA Cracks Simulating Those in St. Lucie 1	C-5
D-1	Listing of Tubes Removed for PWSCC	D-17
E-1	LABORELEC Analysis of EZ PWSCC Crack Growth Data From Doel-3 and Tihange-2	E-2
E-2	Crack Growth Data From Belgian Plants With Kiss Rolls	E-3
F-1	CE S/G Tube Leakage Test Results, 600°F Axial Roll Transition and Unrolled Section Cracks, Normal Operating Pressure Differential	F-2
F-2	CE S/G Tube Leakage Test Results, 600°F Axial Roll Transition and Unrolled Section Cracks, Main Steam Line Break Differential Pressure	F-3
F-3	Westinghouse Leak Rate Tests Axial Roll Transition Cracks at 600°F	F-4
F-4	In-Service Leak Rates - Axial Roll Transition Cracks	F-5
F-5	Crack Length and Measured Leak Rate at Normal and Faulted Pressure Differentials for Pulled Tubes with Through-wall PWSCC in the EZ Roll Transition	F-6
F-6	CEGB S/G Tube Leakage Test Results, 560°F, Cracks in Unrolled Tube Sections, Normal Operating Pressure Differential	F-7
G-1	Comparison of Predicted Total Leak Rates with Total Measured Leak Rates	G-13
G-2	Input Data Used for Sample Probabilistic Calculation	G-16
H-1	Test Sample Matrix	H-2
H-2	Summary of Pancake Coil Data	H-13
I-1	LABORELEC Combined Axial and Circumferential Crack Pressure Test Data	I-4
I-2	TECNATOM Combined Axial and Circumferential Crack Pressure Test Data	I-5

NOMENCLATURE

a	=	axial crack length
\bar{a}	=	reference crack length
a_{TS}	=	correction for tubesheet constraint
a_{CC}	=	allowance for crack growth
a_{NDE}	=	allowance for NDE uncertainty
A	=	allowable crack length
b	=	intercept of regression line
c	=	circumferential crack length
c_s	=	circumferential spacing
C_s	=	flow stress coefficient
δ	=	leakage area
E	=	elastic modulus
ρ	=	fluid density
k	=	slope of regression line
K	=	discharge coefficient
λ	=	dimensionless crack length
m	=	stress magnification (bulging) factor
η	=	Poisson's ratio
P	=	tube (differential) pressure
\bar{P}	=	dimensionless pressure
P_{cr}	=	critical pressure
Q	=	volumetric flow rate
R	=	tube mean radius
r	=	correlation coefficient
t	=	tube wall thickness
S_y	=	yield strength
S_u	=	ultimate strength
s	=	standard deviation
σ	=	hoop (circumferential) stress
$\bar{\sigma}$	=	material flow stress
x	=	corrected reference crack length
Y	=	NDE measured crack length
Y_{lb}	=	lower bound y

EXECUTIVE SUMMARY

Primary water stress corrosion cracking (PWSCC) of alloy 600 steam generator tubes has been diagnosed in the tubesheet expansion zone* (EZ) roll transition of steam generator tubes in many PWR power plants. When existing tube repair (plugging/sleeving) limits based on crack depth are applied, many tubes may require repair which is unnecessary from either a safety or reliability standpoint. Allowing tubes with PWSCC to remain in service can be justified based on a combination of enhanced in-service inspection, a repair limit based on crack length rather than crack depth, a limit on the number of cracked tubes remaining in service, and a reduced primary-to-secondary allowable leak rate.

This report provides the technical support for a length-based repair limit for axial PWSCC in roll transition expansion zones of steam generator tubes in U.S. PWR power plants. In this approach, crack length is used as the measure of tube integrity and tube leakage potential, and operation with cracks that may be through-wall is permitted.

The combination of remedial measures, inspection, an acceptable length-based repair limit, and a reduced allowable leak rate, along with several repair options for cracked tubes, provides a series of plant-specific alternatives that can be used to develop the most cost-effective means to maintain safety and acceptable reliability for steam generators experiencing PWSCC. The criteria described in this report are in addition to previous work that established degradation specific evaluation criteria (e.g., P*, F*, wastage, etc.) that provided significant operational benefit while maintaining adequate safety margins.

This document has been prepared by a committee of U.S. and foreign industry participants who are experts on the technical and licensing issues associated with development and implementation of steam generator tube repair limits. The document represents the committee's recommended approach, and presents information for use by utilities as a reference or supplement to site-specific analyses for developing revised tube repair limits associated with axial PWSCC in roll transition expansion zones.

A length-based repair limit approach is currently being used by the Belgian and Swedish utilities. A repair limit relying on the combination of a leak-before-break (LBB) argument and a length-based limit is being employed by Electricité de France

*Expansion zone is that region of the tube from the primary face of the tubesheet up to and including the final roll transition.

(EdF) and a Spanish utility. It is believed that a similar length-based limit approach is viable for those U.S. power plants that now have EZ PWSCC.

The length-based repair limit described in this report has been developed for tubes with full- and partial-depth roll expansion zones. For tubes with full-depth roll expansion zones, crack length is used to determine that adequate leakage limits are maintained at faulted load and there is acceptable margin against tube rupture. For tubes with partial- depth roll expansion zones, confinement of the cracked section of the tube within the tubesheet precludes tube burst at pressure less than that of an unflawed tube and the repair limit is based on maintaining acceptable leakage limits at faulted load for the distribution of cracked tubes.

Field experience indicates that circumferential cracks or combinations of circumferential and axial cracks occasionally occur in tube expansion zones. To provide added assurance that combined axial and circumferential cracks will not reduce margin against tube rupture or increase leakage at faulted load beyond allowable limits, an additional repair limit has been defined. This limit requires the spacing between adjacent axial crack indications to be _____ or more.

This document applies to axial or inclined axial cracks where the axial extent of the inclined crack is greater than the circumferential extent. This document is not applicable for NDE indications evaluated to be distinct circumferential cracks. Tubes with identified distinct circumferential cracks should be repaired.

The elements of the proposed U. S. approach include:

- Application of EZ PWSCC remedies to limit the number of cracks expected in service.
- At each scheduled inspection outage, performance of rotating pancake coil (RPC) eddy-current inspections of 100% of the roll transitions of tube expansion zones in regions of the steam generator (i.e., the hot leg) where the tube expansion zones are susceptible to PWSCC.
- Repair of tubes with axial cracks longer than a conservatively established repair limit which includes the following elements:
 - Use of an experimentally verified tube rupture curve
 - Use of an experimentally verified tube leak rate relationship
 - Application of USNRC Regulatory Guide 1.121 safety factors.
 - Use of lower bound tube material properties.
 - Correction for tubesheet constraint.
 - Allowance for crack growth between inspections.
 - Allowance for eddy-current crack length measurement uncertainty.
 - Restriction on spacing between adjacent axial cracks.

Implementation of the proposed U.S. approach is expected to require the following utility actions:

- Computation of the plant-specific length based repair limit using the information in this report supplemented by available plant-specific data on material properties, crack growth rates and NDE uncertainties.
- Limiting allowable primary to secondary leak rate limit to 150 gpd to provide assurance against abnormal leakage and tube rupture at normal and faulted loads.
- Calculation of the potential leak rate during postulated accident loads from the cracked tubes that remain in service.
- Calculation of maximum allowable site-specific leak rate at postulated faulted load to ensure that 10CFR100 dose limits are maintained.

Implementation of these elements constitutes a defense-in-depth approach that was developed to ensure adequate levels of safety and compliance with applicable General Design Criteria in 10CFR50. The inspection scope and procedures, crack length and distribution limits, and the leak rate limits developed for tubes with EZ PWSCC ensure adequate margins against failure and excessive leakage and meet the requirements specified in the applicable General Design Criteria.

Section 1 of this document summarizes the overall approach, need, and justification for a length-based repair limit for EZ PWSCC. Section 2 provides a discussion of data and criteria that can be used to predict and justify tube burst conditions for EZ PWSCC. Section 3 describes the NDE capability and develops the approach for dealing with inspection uncertainty. Section 4 provides a comprehensive discussion of allowable crack length. Key topics include analyses with safety factors, loads (accidents and normal operation), material properties, crack growth and NDE uncertainty considerations. Section 5 provides a discussion of when/how a leak-before-break argument applies to the recommended U.S. degradation-specific management strategy, and the calculation of the leak rate resulting from postulated accident loads and the cracked tubes that remain in service following an inspection (i.e., tubes with crack lengths below the repair limit). Section 6 defines an additional requirement to ensure that adequate margins for tube rupture and leakage at faulted load are maintained in the unlikely event that combined through-wall axial and circumferential flaws develop simultaneously in service. Repair limits for tubes with partial-depth roll expansion zones are defined in section 7. Section 8 provides a summary of the recommended length-based repair limit approach. Appendices A through I provide additional background and supporting material, and are appropriately referenced in the body of the document.

Section 1

INTRODUCTION AND BACKGROUND

1.1 OVERVIEW

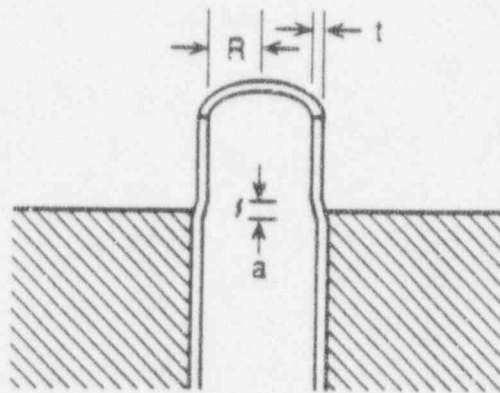
This report documents the justification for a repair limit for axial primary water stress corrosion cracking (PWSCC) that initiates at the tube inside diameter (ID) in the tubesheet expansion zone* (EZ) roll transition of steam generator tubes in U.S. PWR power plants. In this approach, crack length is used as the measure of tube integrity and tube leakage potential, and operation with cracks that may be through-wall is permitted.

Figure 1-1 shows a schematic of a tube and tubesheet along with important geometric parameters for EZ PWSCC roll transition cracks. The tube mean radius and thickness are designated as R and t , respectively. The axial crack length, a , is the extent of the longest crack in the axial direction. As indicated in figure 1-1, there are three possible locations of the EZ roll transition relative to the top of the tubesheet. In case A, the roll transition is at the top of the tubesheet and is typical of a full-depth roll tube. In case B, the roll transition is below the top of the tubesheet. This is the case of a partial depth roll tube or of a tube which has been "under" rolled. In the third case shown in figure 1-1, case C, the roll transition is above the top of the tubesheet. This would be typical of a tube which had been "over" rolled.

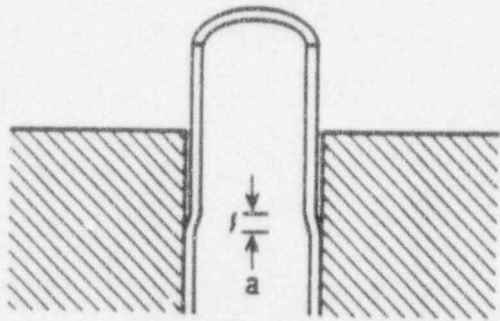
Repair limits have been developed for axial cracks at or above the tubesheet (figure 1-1, cases A and C) and for axial cracks in partial-depth rolled tubes (figure 1-1, case B). For cracks above the top of the tubesheet, limited leakage at faulted load and acceptable crack length are the bases for the repair limit, while limited leakage at faulted load is the basis for the repair limit for partial-depth rolled tubes.

This document can be used to evaluate single or multiple part-through-wall or through-wall axial and inclined axial cracks with configurations shown in figures 1-2 and 1-3.

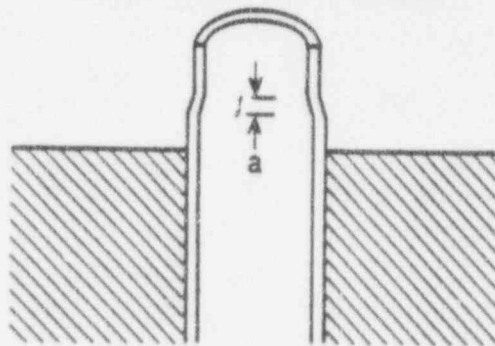
*Expansion zone is that region of the tube from the primary face of the tubesheet up to and including the final roll transition.



Case A. Full depth roll tube



Case B. Partial depth roll tube



Case C. Over-rolled tube

a - axial length of EZ PWSCC crack
 R - tube mean radius
 t - tube thickness

Figure 1-1. Schematic of EZ
 Roll Transition Axial Cracks

Figure 1-2. EZ-PWSCC axial crack configurations acceptable for continued service per the guidance in this document.

Figure 1-3. EZ-PWSCC axial crack configurations that should be repaired per the guidance in this document.

This document does not apply to inclined cracks where the circumferential extent is larger than the axial extent or to NDE indications evaluated to be distinct circumferential cracks or cracks with significant circumferential components, e.g., "L", "T", "U", or "Z" shaped cracks, examples of which are shown in figure 1-4. Tubes with identified distinct circumferential cracks should be repaired.

This length-based repair limit approach is based on tube burst, leak rate, PWSCC growth data, and demonstrated crack length measurement capabilities using rotating pancake coil (RPC) equipment and procedures. Together, these support an alternative to the eddy-current depth-based repair limit used by most U.S. PWRs, and can be used to support site-specific submittals to the U.S. NRC for revision of tube repair limits.

The repair limit will be defined to provide an acceptable margin against tube rupture and will be determined from an experimentally verified correlation between burst pressure and crack length, an experimentally determined adjustment for tube sheet constraint, an adjustment for NDE measurement uncertainty determined from destructive examination of pulled tubes, and a mean crack growth rate determined from successive inservice inspections.

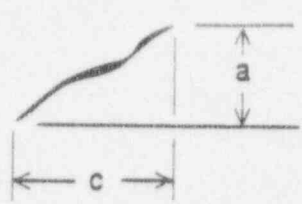
Application of the repair limits developed in this document requires at each scheduled inspection outage, performance of rotating pancake coil (RPC) eddy-current inspections of 100% of the roll transitions of tube expansion zones in regions of the steam generator where the tube expansion zones are susceptible to PWSCC (i.e., the hot leg).

A leak rate analysis will be performed for degraded tubes that do not require repair to determine if the dose rate from leakage at faulted load will remain within of the 10CFR100 limits. If results from the accident leak analysis indicate an excessive leak rate, tubes will be repaired selectively so that the dose rate remains within 10CFR100 limits.

To provide assurance against abnormal leakage and tube rupture at normal and faulted loads, a leak rate of 150 gpd has been established as the allowable primary to secondary leak rate limit during normal operation.

Implementation of this document satisfies the following general requirements:

- Complies with the General Design Criteria.
- Avoids conditions that lead to exceeding a conservative leakage limit of 150 gpd.
- Provides adequate margin against tube rupture under normal operating and postulated accident loads (e.g., steam line break).
- Avoids excessive leakage under postulated accident loads.



Circumferential and predominately circumferential cracks ($c > a$)

Axial cracks with distinct circumferential crack component



"L" Shaped Cracks



"T" Shaped Cracks



"U" Shaped Cracks



"Z" Shaped Cracks

Figure 1-4. Examples of EZ-PWSCC crack configurations with distinct circumferential crack components for which this document does not apply and therefore should be repaired.

1.2 COMPLIANCE WITH GENERAL DESIGN CRITERIA

The repair limit for axial PWSCC in tube expansion zones has been developed to ensure compliance with the applicable General Design Criteria (GDC) in Part 50 of Title 10 of the Code of Federal Regulations (10CFR50). The GDC were reviewed and it was concluded that GDC 14, 15, 30, 31 and 32 are applicable to the development of repair limits for axial PWSCC occurring in steam generator tubes. The remainder of paragraph 1.2 summarizes the bases for compliance with the applicable GDC.

1.2.1 GDC 14

GDC 14 requires the reactor coolant pressure boundary (RCPB) to be designed, fabricated, erected and tested so as to have an extremely low probability of abnormal leakage, of rapidly propagating to failure, and of gross rupture.

R.G. 1.121, "Bases for Removing Degraded PWR Tubes from Service," provides explicit and implied safety margins for tube loading. R.G. 1.121 explicitly states that tube loading should have a safety factor of 3.0 under normal operating conditions. The regulatory guide further states that the margins of safety against tube rupture under postulated conditions should be consistent with the margin of safety determined by the stress limits specified in Section III of the ASME Boiler and Pressure Vessel Code. The repair limits discussed in this report are shown to meet all of the above acceptance criteria.

Following the implementation of the EZ PWSCC tube repair criterion, steam generator tube integrity is maintained both by eddy-current inspection and by measuring steam generator primary to secondary leakage. To further help to ensure adequate margins of safety are maintained during service, in-service inspections are performed for 100% of the affected regions during each refueling outage. Any tubes found to have flaws larger than those necessary to maintain acceptable margins against tube rupture (including consideration of additional flaw growth during service) will be repaired. Service experience indicates leakage levels at plants with through-wall PWSCC in the expansion zone roll transition can be expected to remain at very low levels and range from $\frac{1}{2}$ gpd (1). A maximum leak rate of 150 gpd has been established for normal operation to maintain leakage within acceptable levels during all plant conditions. This level of leakage helps to ensure that the dosage contribution from tube leakage will remain within 10CFR100 limits in the event of a steam generator tube rupture or steam line break event.

1.2.2 GDC 15

GDC 15 requires the reactor coolant system and associated auxiliary, control, and protection systems to be designed with sufficient margin to ensure the design margins of the RCPE are not exceeded during any condition of normal operation, including anticipated operating occurrences.

As the steam generator tubing represents a large portion of the total primary system pressure boundary, to help to ensure that steam generator tube integrity is maintained during normal operation, including anticipated operational occurrences, a factor of safety of three margin on normal pressure loads is used in the alternate repair criterion to define the maximum axial crack length allowed to remain in service. In addition, a maximum leak rate of 150gpd has been established to enhance defense-in-depth and increase the potential for leak-before-break.

1.2.3 GDC 30

GDC 30 requires that components which are part of the reactor coolant pressure boundary shall be designed, fabricated, erected, and tested to the highest quality standards practical. Also, means shall be provided for detecting and, to the extent practical, identifying the location of the source of reactor coolant leakage.

Following implementation of the steam generator tube repair limit, use of the rotating pancake coil (RPC) eddy-current probe is an example of how the reactor coolant pressure boundary will be tested to state-of-the-art quality standards. The eddy-current sample size is 100% of the affected area.

During reactor operation the secondary side of the steam generator will be monitored for radioactivity to detect leaks from cracks in steam generator tubes. If leakage exceeding 150 gpd is detected, the unit will be shutdown and the steam generator tubes will be inspected to determine the source of the leakage.

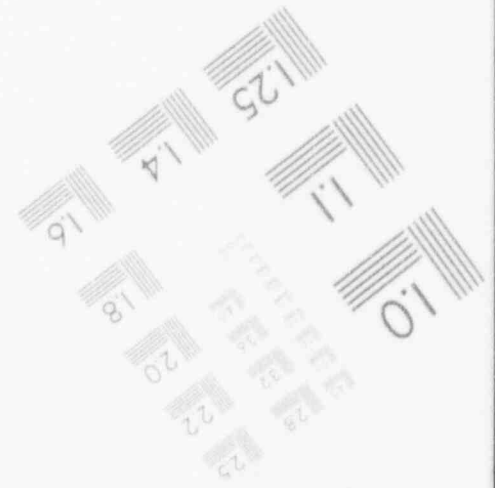
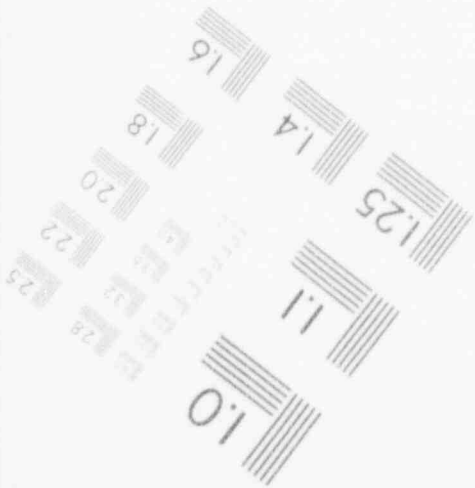
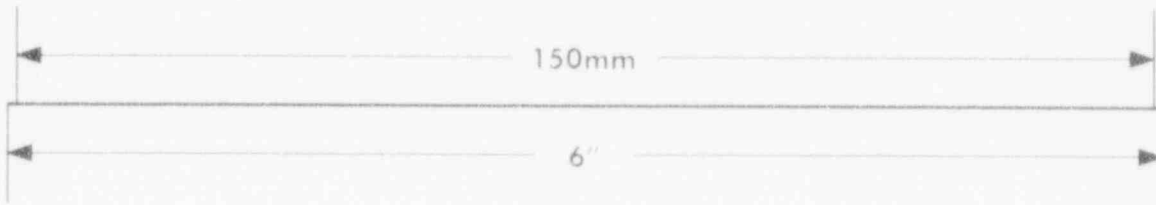
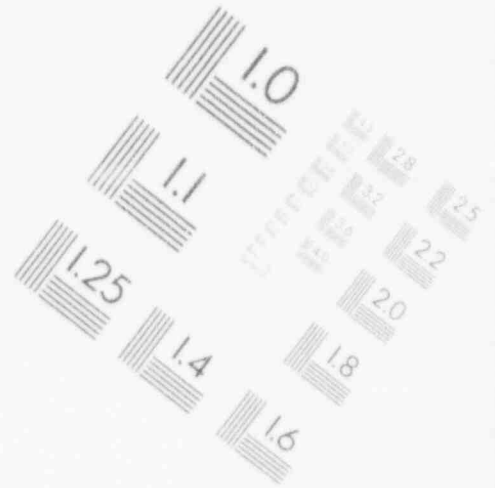
1.2.4 GDC 31

GDC 31 requires the reactor coolant pressure boundary be designed with sufficient margin to ensure that when stressed under operating, maintenance, testing, and postulated accident conditions (1) the boundary behaves in a nonbrittle manner and (2) the probability of rapidly propagating fracture is minimized. The design shall reflect consideration of service temperatures and other conditions of the boundary material under operating, maintenance, testing and postulated accident conditions and the uncertainties in determining (1) material properties, (2) irradiation effects on material properties, (3) residual, steady state and transient stresses, and (4) size of flaws.

To ensure that the tubes behave in a nonbrittle manner and the probability of rapidly propagating fracture is minimized during operating, maintenance, testing and postulated accident conditions, the tubes are manufactured from ductile materials and conservative margins are applied to normal, maintenance, testing and postulated accident loads. These margins have been confirmed from experiments with tubes experiencing EZ PWSCC. This testing has been accredited for use in the development of the tube repair criterion.

2

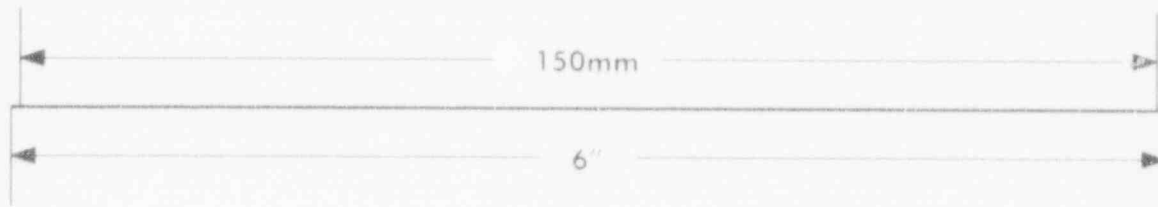
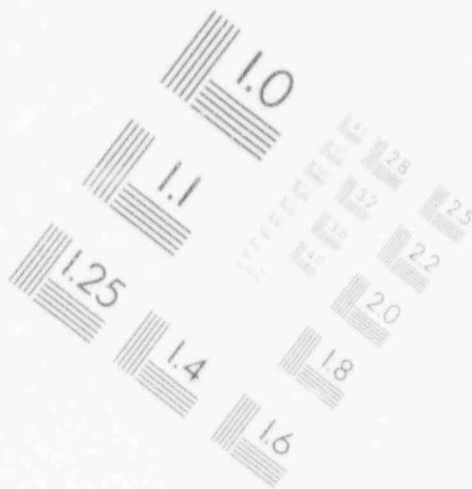
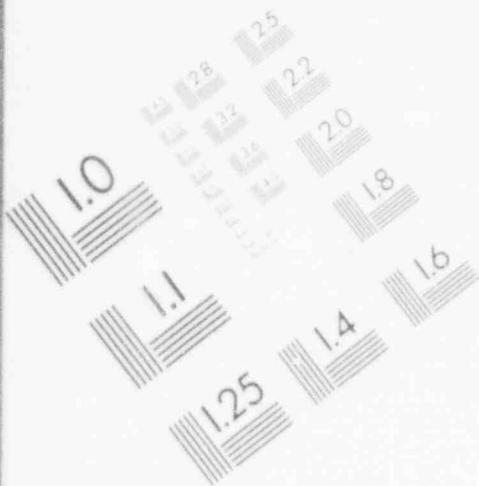
IMAGE EVALUATION TEST TARGET (MT-3)



PHOTOGRAPHIC SCIENCES CORPORATION
770 BASKET ROAD
P.O. BOX 338
WEBSTER, NEW YORK 14580
(716) 265-1600

2

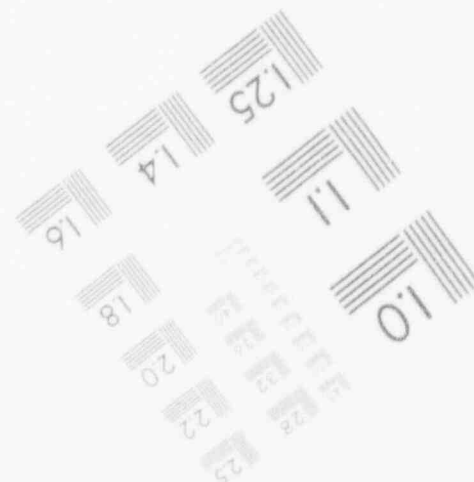
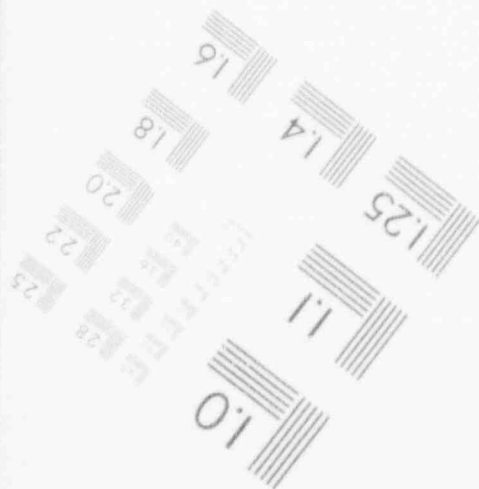
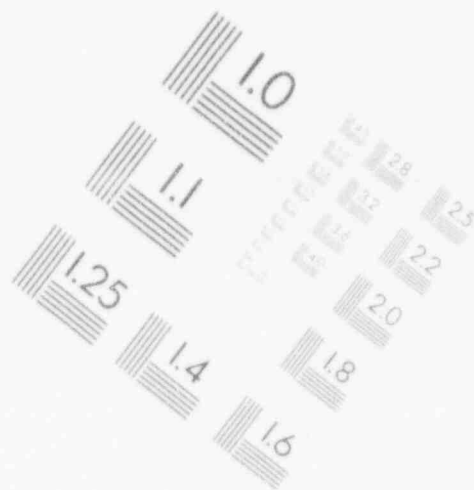
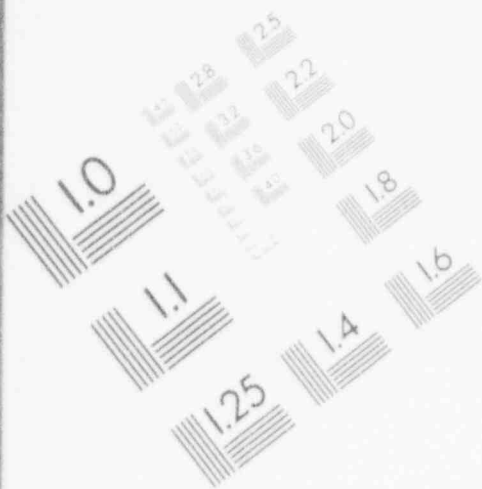
IMAGE EVALUATION TEST TARGET (MT-3)



PHOTOGRAPHIC SCIENCES CORPORATION
770 BASKET ROAD
P.O. BOX 338
WEBSTER, NEW YORK 14580
(716) 265-1600

2

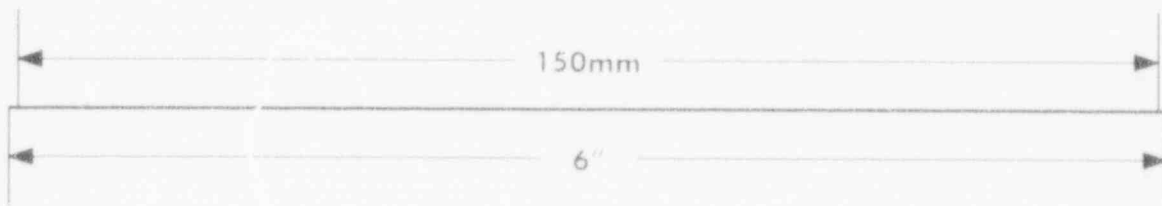
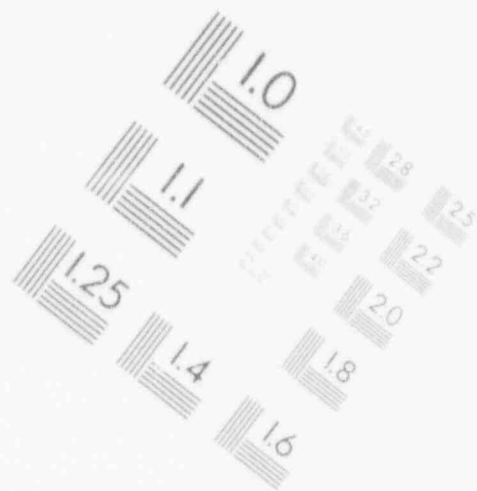
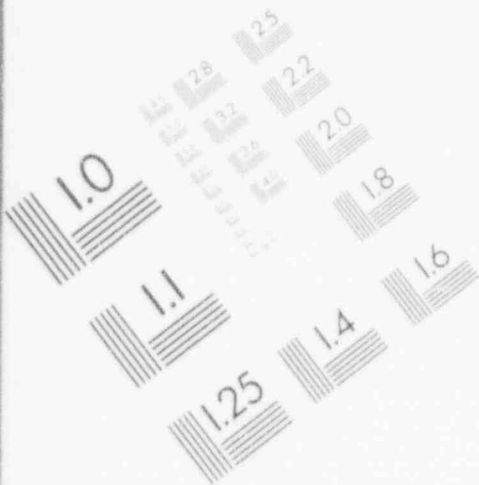
IMAGE EVALUATION TEST TARGET (MT-3)



PHOTOGRAPHIC SCIENCES CORPORATION
770 BASKET ROAD
P.O. BOX 338
WEBSTER, NEW YORK 14580
(716) 265-1600

2

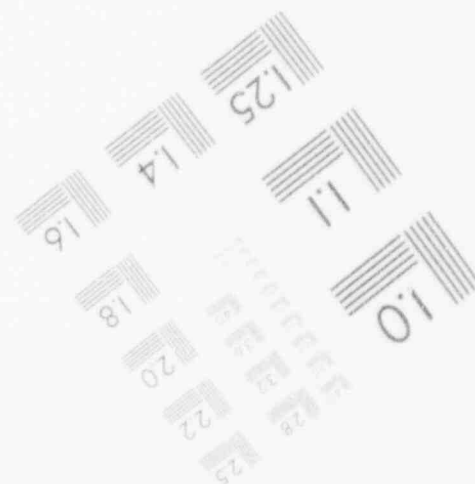
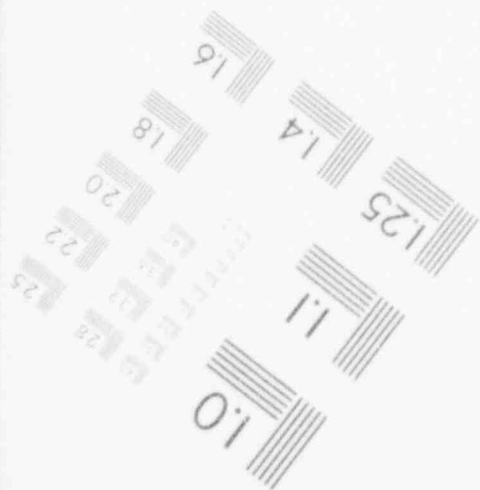
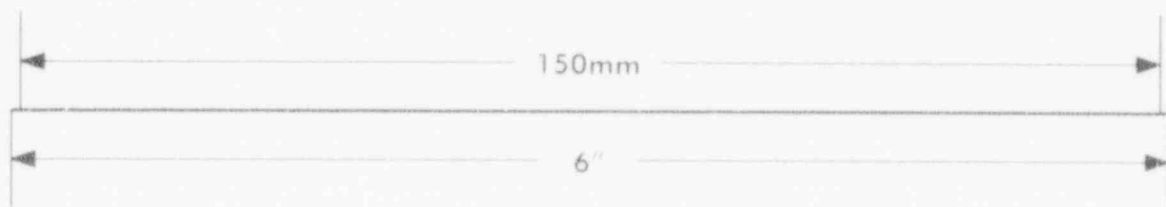
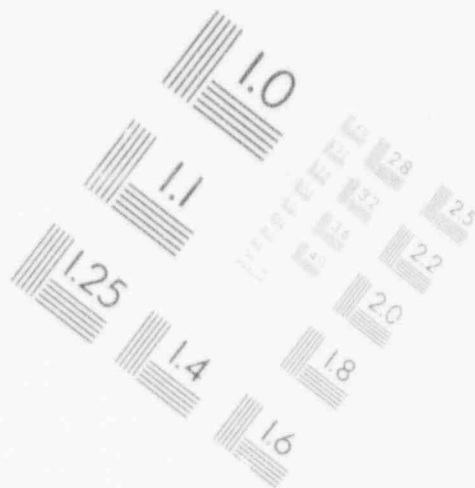
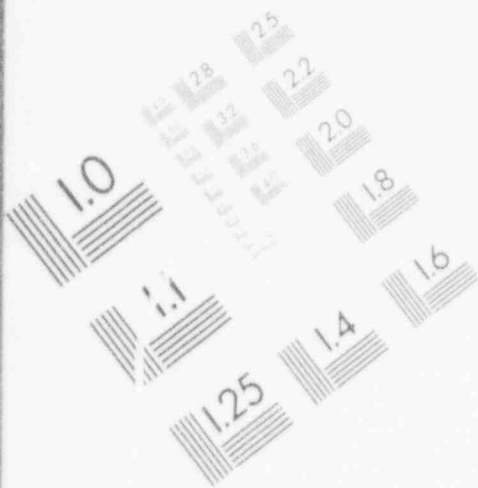
IMAGE EVALUATION TEST TARGET (MT-3)



PHOTOGRAPHIC SCIENCES CORPORATION
770 BASKET ROAD
P.O. BOX 338
WEBSTER, NEW YORK 14580
(716) 265-1600

2

IMAGE EVALUATION TEST TARGET (MT-3)



PHOTOGRAPHIC SCIENCES CORPORATION
770 BASKET ROAD
P.O. BOX 338
WEBSTER, NEW YORK 14580
(716) 265-1600

The margins have been determined considering the temperature and pressures at normal and postulated accident loads, and the uncertainties associated with material properties, stresses, flaw size, flaw length measurement error, and in-service crack growth. Conservative values and margins for these variables have been used to account for these uncertainties. Again as noted above, upon implementation of the criterion, the margins are in compliance with those specified in Regulatory Guide 1.121, the ASME Code, and the individual plant Final Safety Analysis Report. Where plant specific measured values for these variables are unavailable, conservative values have been used.

1.2.5 GDC 32

GDC 32 requires that components which are part of the reactor coolant pressure boundary be designed to permit inspection and testing of important areas and features to assess their structural and leak-tight integrity.

The presence of multiple, axial, (potential) through-wall cracks in the EZ region does not adversely affect the ability of an eddy-current analyst to interpret the eddy current signal and categorize the condition of the tube. Eddy-current inspections using the RPC probe will be performed for 100% of the tube expansion roll transitions in regions of the steam generator where the tube expansion zones are susceptible to PWSCC. Performing these inspections will provide assurance that the PWSCC is within limits such that the safety margins used in the structural integrity evaluation are maintained during service conditions and steam generator primary to secondary leak rates during normal and postulated accident condition loads remain within required limits.

1.2.6 GDC Summary

Section 2 of this report defines the burst pressure for tubes with PWSCC in roll transition expansion zones, while sections 4, 6 and 7 define the allowable crack length, including consideration of material properties and in-service crack growth, that will ensure adequate margins against rapidly propagating failure and nonbrittle fracture. The information in sections 2 and 4 provide the bases for compliance with GDC 14, 15, and 31.

Section 3 of this report describes the examination methods, including provisions for inspection error, that will be used to detect and size PWSCC in tube expansion zones. Implementing the methods described in section 3 provides bases for compliance with various requirements in GDC 14, 15, 30, 31, and 32.

Sections 5, 6 and 7 describe the leak rate and crack distribution limits that will ensure adequate margins against abnormal leakage during normal and postulated accident conditions. Implementing the leak rate and crack length limits as described in section 5 will ensure compliance with GDC 14, 15, 30, and 32.

1.3 BACKGROUND

1.3.1 Steam Generator Tube Degradation

Experience shows that steam generator tubes may be susceptible to degradation from a variety of mechanisms. As degradation progresses, the affected tubes (or tube segments) are repaired based on in-service inspection (ISI) results, or when primary to secondary leakage exceeds a pre-established limit during power operation. Defective segments are repaired either by taking the entire tube out of service, plugging, or by installing internal sleeves in the area of local degradation. If degradation progresses and more segments are repaired, core cooling requirements ultimately may dictate that either the plant be derated or that steam generators be replaced.

Guidelines for evaluating steam generator tube integrity are contained in Regulatory Guide 1.83, (Revision 1, July 1975), "Inservice Inspection of Pressurized Water Reactor Steam Generator Tubes" (2), and Regulatory Guide 1.121, (Draft for Review and Comment, July 1976), "Bases for Plugging Degraded PWR Steam Generator Tube," (3).

In the United States, the current application of the depth-based guidelines for steam generator tube defect management can be broadly characterized as follows:

1. Assume each degradation form is of equal concern;
2. Determine the allowable degradation size based on part-through-wall crack depth regardless of defect length, volume of material loss or cause of the degradation;
3. Establish a shutdown leak rate to help ensure an orderly shutdown prior to tube rupture should degradation penetrate through-wall during an operating cycle;
4. Assume that the combined application of known remedial measures, the inherent leak-before-break nature of alloy 600 for many degradation-types and the mandated inspection protocol provide assurance that the consequences of tubing damage will be acceptable.

While the depth-based approach has proved acceptable, [and experience shows that there have been few tube ruptures, and that the consequences of those ruptures are acceptable (4)] in certain cases it has led to excessive and unnecessary tube plugging (specifically in the case of small volume degradation such as isolated pits and primary-water-initiated stress corrosion cracks). In such cases, a more degradation-specific approach has been developed to provide significant benefit to affected plants while still maintaining acceptable margins. Several examples of these degradation-specific criteria include :

1. P* and F* Criteria - permit through-wall cracks to remain in service within the steam generator tubesheet region (5-8). A more detailed discussion of the P*/F* criteria is provided in Appendix A.
2. Tube Support Plate Primary Water Stress Corrosion Cracking - proposed a justification for through-wall axially oriented cracks to remain in service at the support plate elevation with denting present (9).
3. Pitting Degradation - justifies a 64% of wall thickness repair limit for tubes experiencing pitting (10, 11).
4. Tube Support Plate Outside Diameter (OD) IGA/SCC - justifies an allowable wall loss of 82%; implementing Reg. Guide 1.121 considerations the corresponding tube repair limit was conservatively limited to 51% wall thickness (12, 13).
5. Wastage - justifies a 47% of wall thickness repair limit for steam generator tube thinning (14, 15).

In each of these examples, a degradation-specific limit has been developed that satisfies the intent of Reg. Guide 1.121. The justification for degradation-specific criteria integrates concern for structural capability and leakage of the degraded tubing with nondestructive examination accuracy, tube crack tolerance, and leak detection capability. Appendix A provides a more detailed discussion of the generic degradation-specific approach to developing tube repair limits.

1.3.2 EZ PWSCC

PWSCC has been observed in steam generators with mill-annealed alloy 600 tubing. It can be caused by denting at tube support plates or top of the tubesheet, and/or processes associated with tubesheet expansion zone or inner row U-bend fabrication.

PWSCC due to denting is controlled by eliminating denting through improved secondary water chemistry, and inner-row U-bend cracking is controlled by local in situ stress relief or by preventively plugging susceptible tubes. Thus, the current area of concern is EZ PWSCC which is the focus of this document.

Many plants have experienced EZ PWSCC. Appendix B provides tables summarizing EZ PWSCC experience at plants with partial-depth and full-depth rolls. Plants with full-depth roll expansion that have experienced EZ PWSCC are listed in Table 1-1.

Table 1-1

FULL-DEPTH ROLLED PLANTS WITH EZ PWSCC *
(Ref. 16)

Experience shows that EZ PWSCC cracks are generally short, axially oriented and confined to the expansion zone, and may be through-wall; the cracks generally have been found in tubes in the steam generator hot leg. Pulled tube and RPC data from standard roll plants show that cracks grow slowly, if at all, after they have grown through the high residual stress field in the roll transition zone. Laboratory testing and some field experience indicates that circumferential cracks, or axial cracks with circumferential components, may develop as well. In the field, expansion zone crack leakage has been low and has increased gradually over time, and there are no cases of sudden tube rupture with expansion zone cracks.

1.4 CURRENT INTERNATIONAL PRACTICES

1.4.1 EdF Practices for EZ PWSCC

EdF is not governed by USNRC regulations and, as such, has developed an alternate approach through interactions with the French regulatory authorities. Specifically, the EdF approach uses a leak-before-risk-of-break (LBRB) argument, characterized as follows: (a) uses analysis to show leak-before-break for most axial cracks; (b) completes 100% RPC inspection in the sludge pile region (because of circumferential cracks) at each outage; (c) utilizes sensitive on-line leak detection capability (steam line N16 monitors); (d) applies plant-specific Technical Specification leakage limits; (e) uses sensitive off-line helium leak location methods; (f) applies 100% RPC on steam generators affected by EZ PWSCC every other outage; and (g) in the other outage, performs generally 12.5% bobbin coil inspection with RPC follow-up on bobbin coil signals that are indicative of "long" cracks. Tubes are repaired: (a) if helium tests indicate potential operational leakage exceeds the Technical Specification value, (b) if RPC inspection locates any crack long or longer above the tubesheet, (c) any dented tube in the sludge zone, or (d) if any circumferential crack is indicated and not otherwise dispositioned.

1.4.2 Belgian Practices for EZ PWSCC

The Belgian utility (Electronucleaire) is required to conform to USNRC Regulatory Guides. However, their proposed use of a modified version of Regulatory Guide 1.121 to develop an alternate tube repair limit has been reviewed and accepted by the Belgian safety authorities. Essentially, they use at-temperature material properties for ultimate and yield stresses and develop an approach using safety margins on crack length rather than pressure (load) for analysis, supplemented with field data for axial crack growth rate, and with testing to take credit for tubesheet reinforcement. Using this approach, they have an axial crack length plugging limit of 7/8 in. tubing. This is coupled with a 100% inspection of the tubesheet region with RPC technology at each refueling outage.

1.4.3 Spanish Practices for EZ PWSCC

The repair limits at one Spanish utility are primarily based on EdF's leak-before-risk-of-break (LBRB) method. However, limits are also placed on crack length, as determined by inspections, for operational reliability reasons, i.e., to protect against forced outages. For this reason, axial cracks in roll transition zone of tubes with normal roll geometries require repair if the crack length above the top of the tubesheet (TTS) is _____ or more. One hundred percent of steam generator tubesheet areas must be inspected each refueling outage using RPC. Allowable leak rates for the different units were selected by the safety authorities based on evaluations of the possible interactions of various defect mechanisms (e.g., OD IGSCC) with PWSCC, and based on concerns that actual leak rates through individual cracks may be lower than predicted.

1.4.4 Swedish Practices for EZ PWSCC

The Swedish utility initially followed an axial crack-depth-based 50% through-wall tube repair limit. Shortly after the PWSCC problem was detected and determined to be significant at the lead plant with Model D3 steam generators, Ringhals 3, the U.S.-developed P* criteria were adopted. These criteria allow axial cracks to remain in service if tubes or the tube support structure prevent tube pull-out even if the tube severs at the indication location.

An additional change was also adopted soon after discovery of EZ PWSCC at Ringhals. This change allows axial cracks of any length to remain in place if they were located below the top of the tubesheet. This position is justified on the basis that axial cracks do not affect pull out strength, or significantly impact leakage. Circumferential degradations in the P* regions, and all indications above the top of the tubesheet, were still governed by the 50% through-wall rule.

In 1988 and 1989, new criteria were developed and adopted using Framatome assistance. These new criteria are based on a degradation identification and monitoring approach. The criteria are based on a critical crack size under accident conditions of _____ based on tube minimum properties and worst case dimensions. To protect against growth of cracks to beyond this value, allowable crack length as determined during inspection is less than the critical size to allow for degradation growth and length measurement uncertainty.

1.5 REFERENCES

1. P. Hernalsteen. Steam Generator PWSCC In Service Leakage Experience in Belgium. LABORELEC Report M00-90-022/R-PH, May 1990.
2. U.S. Nuclear Regulatory Commission Regulatory Guide 1.83. "Inservice Inspection of Pressurized Water Reactor Steam Generator Tubes." Revision 1, July 1975.
3. U.S. Nuclear Regulatory Commission Regulatory Guide 1.121. "Bases for Plugging Degraded PWR Steam Generator Tubes." Draft for Comment, August 1976.
4. NRC Integrated Program for the Resolution of Unresolved Safety Issues A-3, A-4, and A-5 Regarding Steam Generator Tube Integrity. NUREG-0844, September 1988.
5. Tubesheet Region Plugging Criterion for Full Depth Hardroll Expanded Tubes. WCAP-10950, September 1985.
6. Tubesheet Region Plugging Criterion. WCAP-11225, July 1986.
7. Tubesheet Region Plugging Criterion. WCAP-11225, Rev. 1, October 1986.
8. Docket Nos. 50-369 and 50-370. Issuance of Amendment No. 59 to Facility Operating License NPF-9 and Amendment No. 40 to Facility Operating License NPF-17 for the McGuire Nuclear Station, Units 1 and 2, August 1986.
9. North Anna Unit 1 Steam Generator Tube Integrity Safety Evaluation. WCAP-11311, October 1986.
10. Docket No. 50-286. Request for Amendment to Facility Operating License DPR-64. "Proposed Changes to Technical Specifications Regarding Steam Generator Tube Plugging Limit." J. P. Bayne (New York Power Authority) to W. R. Denton (US NRC), September 1984.
11. Docket No. 50-286. Issuance of Amendment No. 55 to Facility Operating License DPR-64 for Indian Point Nuclear Generating Unit No. 3, May 1985.
12. Docket No. 50-255. Facility Operating License DPR-20. "1983/1984 Steam Generator Evaluation and Repair Report, Palisades Plant." D. J. VandeWalle (Consumers Power Company) to D. H. Crutchfield & US NRC), April 1984.
13. Docket 50-225, LS05-84-06-015. "1983/1984 Steam Generator Inspection, Re: Palisades Plant." D. J. Crutchfield (US NRC) To D. J. VandeWalle (Consumers Power Company) June 1984.

14. Docket No. 50-261. Facility Operating License No. DPR-23. "Supplemental Request for License Amendment for Cycle 9 Operation." P. W. Howe (Carolina Power and Light) to S. A. Varga (US NRC), July 1982.
15. Docket No. 50-261, Issuance of Amendment No. 71 to Facility Operating License No. DPR-23 for the H. B. Robinson Steam Generator Electric Plant, Unit No. 2, July 1982.
16. "Steam Generator Progress Report, Revision 7." September 1991. (Available from EPRI Steam Generator Reliability Project staff.)

Section 2

CRACKED TUBE BURST DATA

2.1 INTEGRITY CRITERIA

To ensure compliance with the General Design Criteria of 10CFR50 for tubes with EZ PWSCC, several criteria are used to assess the integrity of steam generator tubes and develop a length-based acceptance criterion for axial cracks in the roll transition region. These include: (1) a crack length limit (allowable crack length) which assures margins against structural tube failure, (2) enhanced NDE of 100% of the tubes that may be affected by EZ PWSCC to provide a high level of confidence that tubes exceeding the allowable crack length are repaired, (3) controlling the distribution of potential leaking tubes to preclude exceeding the site boundary dose limits during postulated faulted loads, and (4) reduced allowable leak rate from 500 to 150 gpd to enhance defense-in-depth and increase the potential for leak-before-break.

The remainder of this section identifies conditions and bases that can be used to determine the axial crack length corresponding to tube rupture. Allowable crack lengths are developed in section 4, while crack distribution and leak rate limits are discussed in section 5. Restrictions on spacing between axial cracks based on the potential for the presence of combined axial and circumferential cracks are developed in section 6. Repair criteria for cracks that exist in partial-depth rolled tubes (see figure 1-1B) are presented in section 7.

2.2 TUBE RUPTURE

2.2.1 Axial Through-Wall Cracks

Tube rupture is the condition of a tube segment with a crack at the maximum pressure it can support under actual steam generator conditions. Rupture occurs by significant tube deformation followed by crack tip extension.

The rupture behavior of alloy 600 steam generator tubes with axial cracks has been studied previously by a number of investigators (1-4). These studies have generally involved tests with tubes containing electrodischarge machine (EDM) slits to simulate cracks, with a patch or bladder in the tube to prevent leakage from the through-wall slit while the tube is pressurized until rupture occurs. A limited number of tests have been conducted on cracked tubes removed from service. These tests show that the rupture behavior of tubes with in-service cracking is comparable to tubes with EDM slits.

In addition to reporting experimental results, investigators have developed burst behavior relationships and correlated them with experimental results. These relationships are in terms of tube parameters that control burst behavior and can be used for predicting tube burst performance. Parameters used in the correlations are tube and crack dimensions, material properties and load. A brief description of these previously developed correlations is presented in the next several paragraphs.

The Belgian agency, BELGATOM, has conducted an experimental investigation of burst behavior of alloy 600 tubes with axial defects. Early work concentrated on a single heat of 7/8-inch diameter tube (1). Later work included tests with different heats and tube diameters. These tests confirmed the earlier burst behavior correlation (1).

BELGATOM has correlated the burst test results with a limit load equation which, for a flat plate, is written as

$$\sigma = \bar{\sigma} \quad (2-1)$$

where σ is the applied stress and $\bar{\sigma}$ is the material flow stress.

The critical length of an axial crack in a tube can be found by considering the stress magnification factor, m , associated with the bulging of the tube. In this case,

$$\sigma = m \bar{\sigma} \quad (2-2)$$

Different forms of the bulging factor have been proposed and used. BELGATOM found that the bulging factor expression due to Erdogan (5) best fit their data. This equation is

$$m = \frac{a}{t} \quad (2-3)$$

where a is the through-wall crack length, R is the tube mean radius, and t is the tube wall thickness. Further, BELGATOM used a flow stress of

$$\bar{\sigma} = \frac{S_u - S_y}{2} \quad (2-4)$$

and expressed the applied stress as a function of the differential pressure

$$\sigma = \frac{P R}{t} \quad (2-5)$$

where S_u is the ultimate strength, S_y is the yield strength, and P is the differential pressure. BELGATOM's initial correlation with burst test data is shown in figure 2-1. Later work with additional data supports this correlation (1).

Figure 2-1. Belgian (BELGATOM) Axial Defect
Burst Test Data and Correlation (3)

Additional burst tests have been carried out by Framatome and EdF (2) on alloy 600 and alloy 690 tubing with nominal diameters of 3/4 inch and 7/8 inch. These burst tests have been performed with various types of degradation located in the straight portion of tubes away from supports, in the roll transition, in the vicinity of supports and in U-bends.

These tests demonstrate that the burst behavior of tubes with through-wall cracks can be correlated with the expressions similar to those used by BELGATOM with slightly different correlation parameters. These include for the flow stress

$$\bar{\sigma} = \quad (2-6)$$

and for the bulging factor,

$$m = \quad (2-7)$$

Figure 2-2 shows the French tube burst behavior correlation plotted with through-wall burst data (2).

Like other investigators, the French have pointed out that the tube hoop stress due to internal pressure controls the burst behavior of tubes with axial cracks, and that axial stresses are relatively unimportant (2). In addition, their experiments confirm that the burst pressure for a tube with a crack near the top of the tubesheet is higher than that of a tube with the same defect remote from supports.

Westinghouse (3) has also conducted burst tests with both 3/4-inch and 7/8-inch diameter tubes. Further, they have correlated the burst behavior of tubes with through-wall axial cracks with the following two dimensionless terms

$$\lambda = \quad (2-8)$$

$$\bar{P} = \quad (2-9)$$

Figure 2-3 shows normalized burst data correlated with a ninth order polynomial fit shown below.

$$\bar{P} = \quad (2-10)$$

Figure 2-2. French (EDF/Framatome) Axial Defect
Burst Test Data and Correlation (2)

Figure 2-3. Westinghouse Axial Defect Burst Test
Data and Correlation (3)

The British (4) have recently reported the results of burst test data for tubes with through-wall axial corrosion cracks and compared their results with their proprietary tube burst and leak code TUBELEAK. TUBELEAK is reportedly based on a correlation with the burst test results of other researchers, and predictions with this code are indistinguishable from the Westinghouse correlation shown in figure 2-3.

A comparison of the correlations previously developed in Belgium, France, UK, and US is presented in figure 2-4. Because there were significant differences between some of the burst correlations determined from the various test programs (1-4), the relationship between burst pressure and crack length used to determine the PWSCC repair limit originally was defined as the lower bound of the available correlations, as indicated in figure 2-4 (i.e., the curve labeled tube rupture equation).

Figure 2-4. Comparison of Several Tube Burst Correlations Along with Lower Bound Tube Rupture Equation

Subsequently, it was determined that the difference between correlations resulted from the different techniques used to preclude flow through the throughwall crack prior to tube rupture. In general, tubes that had metal foil patches as the sealing system had higher burst pressures than tubes with elastomer type sealing systems.

To determine which sealing system was more representative of actual service conditions and assess the degree of conservatism of the burst curve initially defined for establishing the PWSCC repair limit, LABORELEC conducted burst tests using a flow source of 100 gpm and no crack sealing system (6). These tests were performed at room temperature and used 7/8 inch diameter, 0.050 inch wall thickness, and 3/4 inch diameter, 0.043 inch wall thickness tubes with axial throughwall machined slots ranging in length from _____ mm.

Figure 2-5 presents a comparison between the burst data obtained from tubes with no sealing system (6) and the initial rupture curve used to bound the previously obtained correlations. The figure shows normalized burst pressure,

_____ , versus normalized crack length, _____ , for: (1) the individual data points for tubes without a sealing system, (2) the mean curve determined for the data using the analytical form represented by Eqs. 2-2 through 2-4, and (3) the rupture curve used to bound the correlations shown in figure 2-4. Also included in figure 2-5 are data for non degraded tubes (_____ , see Table C-1).

The equation for the mean burst curve is

$$\bar{P} = \text{_____} \quad (2-11)$$

where

The equation for the rupture curve used to bound the correlations _____ , valid for _____ , is

$$\bar{P} = \text{_____} \quad , \text{ or} \quad (2-12)$$

$$\lambda = \text{_____}$$

Currently, work is still in progress to evaluate relevant tube burst data, define the rupture correlation, and assess the probability of tube rupture associated with the PWSCC repair criteria. This assessment will demonstrate that the combination of the rupture correlation, and adjustments for NDE uncertainty and crack growth used to define the repair criteria provides adequate margin against tube rupture. The results from this evaluation will be presented in a subsequent revision to this report.

Figure 2-5. Comparison of Tube Rupture Equation
With Data and Best Fit Curve for Axial
Throughwall Cracks Having No Sealing System

2.2.2 Multiple Axial Through-Wall Cracks

The effect of multiple axial cracks on steam generator tube burst behavior has been studied by a number of investigators (7-10). Westinghouse conducted burst tests with tubes containing multiple axial cracks and concluded that the longest crack controls the burst behavior and the presence of multiple cracks does not have a deleterious effect (table C-2 of appendix C). Framatome conducted similar tests with tubes containing multiple artificial defects and reached a similar conclusion (7, 9). Framatome concluded that burst pressure was not influenced by the presence of up to _____ cracks located in the same tube section. Finally, EdF has performed burst test with tubes removed from service which contained up to _____ service cracks (10). These tests confirm the conclusion that burst behavior is controlled by the longest crack and is not influenced by the presence of multiple cracks.

2.2.3 Axial Part-Through-wall Cracks

Because part-through-wall cracks may also exist in the roll transition region, data were collected to determine if the critical through-wall crack lengths obtained from Eq. 2-12 would bound the critical part-through-wall crack burst lengths. Figure 2-6 presents a comparison of part-through-wall crack burst data with the through-wall burst curves obtained using Eqs. 2-11 and 2-12. The individual data points shown in figure 2-6 and their sources are listed in tables C-3 and C-4 of appendix C.

Values for S_y and S_u were not reported for the experimental data in Tables C-3 and C-4 at the tube test temperatures, and computed or estimated values were used to determine the normalized burst pressures in figure 2-6. The values of $S_y + S_u$ for the data in Table C-3 were determined using the average burst pressure reported for non degraded tubes from the same heats of material and test temperatures (11), and an estimated mean for the normalized burst pressure at _____, i.e., _____ (see Table C-1); these values of $S_y + S_u$ are listed in Table C-3. The value of $S_y + S_u$ for the data in Table C-4 was estimated conservatively based on the material properties defined in the purchase specification as indicated in Table C-4.

Figure 2-6 shows that the through-wall crack tube rupture curves from Eqs. 2-11 and 2-12 provide conservative representations of the data part-through-wall axial cracks in steam generator tubes. This information demonstrates that a length based allowable crack criterion is acceptable for predicting burst conditions for both through-wall and part-through-wall cracks in the roll transition region of steam generator tubes.

Figure 2-6. Comparison of Throughwall Crack Tube
Burst Relationships With Data for Axial Part-throughwall
Cracks

2.3 REFERENCES

1. G. Frederick, P. Hernalsteen, and D. Dobbeni. Belgian Approach to Steam Generator Tube Plugging for Primary Water Stress Corrosion Cracking. Palo Alto, Calif.: Electric Power Research Institute, March 1990. NP-6626-SD.
2. B. Cochet and B. Flesch. "Application of the Leak-Before-Break Concept to Steam Generator Tubes." 10th SMIRT Conference, Volume G, August 1989.
3. J. A. Begley and J. L. Houtman. Inconel Alloy 600 Tubing - Material Burst and Strength Properties. WCAP-12522, January 1990.
4. P. McIntyre. "Procedures for Specimen Preparation, Leak Rate Measurement and Burst Testing of PWR Steam Generator Tubing Containing Axial Through-Wall Cracks and Preliminary Results for Tests on Fatigue Precracked Specimens." CEGB Draft Memorandum, March 1988.
5. F. Erdogan. "Ductile Fracture Theories for Pressure Riser Pipes and Containers." International Journal of Pressure Vessels and Piping, vol. 4, pp. 253-283, 1976.
6. Hernalsteen, P., "The Influence of Testing Conditions on Burst Pressure Assessment for Inconel Tubing", Int. J. Pressure Vessel and Piping 52 (1992).
7. B. Cochet. Assessment of the Integrity of Steam Generator Tubes - Burst Test Results - Validation of Rupture Criteria (Framatome Data). Palo Alto, Calif.: Electric Power Research Institute, June 1991. NP-6865-L, vol. 1.
8. B. Cochet. PWR Steam Generator Tube Plugging Criteria - Leak-Before-Break Analysis for Primary Water Stress Corrosion Cracking Near the Tubesheet (Framatome Data). Palo Alto, Calif.: Electric Power Research Institute, June 1991. NP-6865-L, vol. 2.
9. B. Flesch and B. Cochet. "Leak Before Break in Steam Generator Tubes." International Journal of Pressure Vessels and Piping, 1989.
10. P. Berger, F. Cattant, P. Calle, and J. P. Hutin. Characteristics of Roll Transition Cracks in Steam Generator Tubes. EdF Report.
11. J.M. Alzheimer, et. al., "Steam Generator Tube Integrity Program Phase I Report", NUREG/CR-0718, U.S. Nuclear Regulatory Commission, Washington, DC, September 1979.

Section 3

CRACK LENGTH MEASUREMENT

3.1 BACKGROUND

Nondestructive evaluation (NDE) is a critical element in implementing a degradation-specific tube repair approach, and the inspection method must provide a reliable measurement of critical crack dimensions. Additionally, the inspection process can provide crack growth rate data which is required to establish allowable crack length (see paragraph 4.6).

Conventional bobbin coil technology used for routine steam generator examination has limitations in inspecting roll expansions. Because of the change in tube diameter, this region is the source of a large extraneous signal which can mask signals associated with expansion zone cracking. Other limitations of the bobbin coil include the inability to determine flaw type (volumetric or crack-like), to estimate the number of cracks present or to determine crack orientation and length. These limitations can be overcome by using rotating pancake coil (RPC) eddy current technology which is the recommended method for inspecting the roll expansion zone when using a length-based repair limit. Other inspection methods can be used when they are qualified by an acceptable qualification program.

This section discusses industry experience in measuring crack length using RPC technology. Crack length measurement uncertainty, an important consideration in establishing the allowable crack length, is discussed in paragraph 4.7.

3.2 ROTATING PANCAKE COIL (RPC)

3.2.1 Data Acquisition

The development and use of RPC eddy-current technology in conjunction with a stable probe delivery system provides an important field diagnostic tool for measuring EZ PWSCC crack lengths.

RPC tube inspection is accomplished using a surface-riding coil which is rotated around the tube axis. Figure 3-1 shows the probe body with details of the coil shown in end-view in the enlarged schematic. The coil is spring-loaded to maintain contact with the tube inner surface as it moves through the expansion transition region. Lift-off variations between the coil and the tube surface caused by a change in tube diameter due to the roll expansion are significantly reduced when compared with the bobbin coil.

Figure 3-1. Typical Rotating Pancake Coil

As the probe coil is translated and rotated through the tube it describes a helical path, shown in figure 3-2(a). A linear discontinuity within the tube will be scanned once during each rotation of the probe. The coil output voltage from a given rotation is used to generate a line scan which represents signal amplitude as a function of coil position around the tube circumference (see figure 3-2(b)). Image formation (two-dimensional cylindrical coordinate system) is accomplished by plotting a series of consecutive line scans with the line-scan generation synchronized with probe rotation. This allows for the reconstruction of an image in perspective format as shown in figure 3-2(c). Crack presence is determined by recognizing linear features present in the reconstructed image, and orientation is inferred by noting the direction of the major axis of the image.

Essential acquisition test variables include coil diameter and coil excitation frequency. Multiple-frequency eddy-current instrumentation is utilized so that the coil is driven over a range of frequencies in order to independently optimize detection, characterization and measurement. Coil diameter which is typically in the range of _____, along with driving frequency, determine detection and resolution capability. Based on pulled-tube experience, a lower bound estimate on through-wall crack length detection capability for axial or circumferential cracking is approximately _____. Multiple through-wall axial cracks must generally be separated by approximately one coil diameter before the separate cracks are readily distinguishable (see section 6).

3.2.2 RPC Data Analysis

Crack length measurement is discussed with the aid of figure 3-3 which shows the display screen following automatic analysis of a selected tubescan. In the display shown, all measurements are in millimeters. The numbered indications represent crack sequences by axial location of the upper crack tip. The compass orientation shown on the left of the screen denotes the circumferential position of the crack. The vertical dotted line passing through +00 at the bottom of the screen shows the position of the top of tubesheet which is automatically detected using a low frequency applied to the test coil. The measurement shown in the upper right portion of the screen (labeled TTS) is the measured distance from the tube end to the top of the tubesheet. This absolute dimension is recorded to provide a reference for future inspections.

Figure 3-2. RPC Data Acquisition/Analysis

Figure 3-3. Zetec SM-15 Analysis Display (1)

A list of detected cracks appears below the tubesheet thickness number. **CK#** is the sequence number of the crack beginning with the uppermost crack tip. **Start** is the location of the crack's upper tip with respect to the top of the tubesheet, **LEN** is the length of the indication. **DEG** is the circumferential position. **P/T** is the ratio of the highest signal peak within a given crack indication to the signal threshold value used for detection. The signal displayed as a horizontal chart at the very top of the screen represents the lift off component of the test coil signal caused by the roll transition present in the tubing. The signal displayed as a horizontal chart at the very bottom of the screen represents the signal offset caused by the tubesheet interface used to automatically locate this axial position. To the right of that chart is a smaller chart showing the signal used to locate the tube end with the differential bobbin coil positioned on the rotating shaft.

Crack length estimates are accomplished by counting the number of line scans for a given crack. The axial length is then the coil pitch multiplied by the total number of hits or line scans. For crack lengths much greater than the coil diameter, the apparent eddy-current length will, in general, be longer than the true length because of the finite coil diameter. Thus, in practice, the total number of line scans is adjusted downward to compensate for this effect. The actual adjustment value is a function of the particular eddy-current procedure used for measuring crack length.

3.3 DEMONSTRATED CRACK LENGTH MEASUREMENT ACCURACY

The ability to reliably measure crack length in the roll expansion region of steam generator tubing is an important consideration. This has been assessed using tubes removed from operating plants, a detailed listing of which is provided in appendix D. Results from these studies have compared eddy-current RPC predictions of crack length with results determined destructively from metallographic examinations and, in some instances, with dye penetrate estimates of crack length. This section focuses on crack length measurement accuracy using this industry wide pulled tube database. Linear regression equations relating true crack length (the crack length measured on the inner surface of pulled tubes) and eddy current measured crack length are derived for an overall industry composite data set and for individual organization's specific data sets. The industry composite data set is used to describe how the experimental data is used to arrive at a length measurement uncertainty for use in establishing a repair limit.

The impact of length measurement uncertainty on the repair limit is discussed in paragraph 4.7, with the uncertainty used as one element in the calculation of allowable crack length. Crack length measurement error for the various data sets discussed in this section is summarized in Table 3-1. Two values of error are given; these include the standard error and the error calculated at a confidence limit. The latter value for the industry composite data set is used in paragraph 4.7 to calculate allowable crack length.

Table 3-1
Crack Length Measurement Accuracy

In general, crack length measurement uncertainty will be a function of eddy current instrumentation, probe type, calibration procedures and analysis methods. Accordingly, the uncertainty statistics presented in this section may not necessarily be the appropriate basis for establishing a repair limit for a specific plant. As an alternative, specific in-service inspection vendor acquisition and analysis procedures may be qualified/demonstrated using pulled tubes or other appropriate approaches.

3.3.1 Industry Composite Data Set

A scatter-plot showing RPC-measured eddy-current crack length versus true crack length for a composite data set comprised of _____ data points based on tube pulls from France, Belgium, Sweden, Spain and the United States (2-8) is shown in figure 3-4. The data set is described by the regression equation $Y = \dots$ where Y is the NDE measured crack length and X is the true crack length with both Y and X measured in mm. The correlation coefficient is $r = \dots$. (Paragraphs 3.3.2 - 3.3.6 below discuss the individual data sets that are included in the composite.)

In establishing measurement uncertainty for repair limit calculations, the regression equation is used as a transfer function to first relate true length to an apparent or measured eddy current length. For the composite data set, $Y = \dots$. At a particular Y value, which in this case is the measured eddy current length equivalent to the maximum allowable length, confidence limits are then calculated using standard statistical methods. For the composite data set shown in figure 3-4 the standard deviation is _____. As discussed in paragraph 4.7, the industry composite plot regression equation and the error calculated at a _____ confidence limit are used to calculate NDE error used in the allowable crack length calculation.

Figure 3-4. Crack Length Prediction - Composite Industry Experience

3.3.2 Electricité de France Data

The EdF data set (2) used in estimating crack length is shown in figure 3-5 and includes data points derived from pulled tubes from numerous French plants. These data are described by the regression equation $Y =$. The correlation coefficient is $r =$ and the standard deviation is $s =$. As can be seen from the figure, crack length measurements have been made over true lengths ranging from approximately . The scatter in the data is more pronounced at the shorter lengths with a tendency to decrease at lengths above approximately .

3.3.3 Laborelec Data

Figure 3-6 shows data (3-5) from tubes (data points) removed from two Belgian plants (Doel 2 and 3). These data are described by the regression equation $Y =$; the correlation coefficient is $r =$ and the standard deviation is $s =$. Cracks with true lengths ranging from approximately have been measured.

3.3.4 Swedish State Power Board Data

Figure 3-7 shows data (6) from tubes (data points) removed from two Swedish plants (Ringhals 3 and 4). These data are described by the regression equation $Y =$; the correlation coefficient is $r =$ whereas the standard deviation is $s =$. Cracks with true lengths ranging from approximately have been measured.

3.3.5 Spanish Data

Figure 3-8 shows data (7) from tubes (data points) removed from two Spanish plants (Almaraz and Asco 2). These data are described by the regression equation $Y =$; the correlation coefficient is $r =$ and the standard deviation is $s =$. Cracks with true lengths ranging from approximately have been measured.

3.3.6 U.S. Data

Figure 3-9 shows data (8) from tubes (data points) removed from one domestic U.S. plant (McGuire 1). These data are described by the regression equation $Y =$; the correlation coefficient is $r =$ and the standard deviation is $s =$. Cracks with true lengths ranging from approximately have been measured.

Figure 3-5. Crack Length Prediction - Electricité de France

Figure 3-6. Crack Length Prediction - Laborelec

Figure 3-7. Crack Length Prediction - Swedish State Power Board

Figure 3-8 Crack Length Prediction - Spanish Utilities

Figure 3-9. Crack Length Prediction - U.S. Utility

3.3.7 Discussion

A summary of regression equation parameters, measurement accuracy, and number of data points for the various data sets is given in table 3-2. All of the regression data is highly stable as evidenced by the high value of correlation coefficients. The most representative data in terms of assessing the ability to measure crack length are the EdF and Belgian data sets since they have the largest number of data points with crack length measurements accomplished over a fairly large dynamic range i.e., to approximately

Table 3-2
Eddy-Current Length Measurement Accuracy

The fundamental limit in length measurement accuracy is a dimension on the order of the eddy current coil diameter which ultimately determines system resolution. This dimension is on the order of several millimeters. Ultrasonic systems offer the potential for improved measurement accuracy since they utilize transducers with a smaller beam width, i.e., less than one millimeter. In addition, with a smaller beam width ultrasonics can in principle delineate more detail, i.e., resolve closely-spaced multiple axial cracks, and detect the presence of small circumferential cracks between closely-spaced axial cracks.

Ultrasonic systems have been deployed in Europe and the U.S. and are currently undergoing extensive evaluation. An example of recent ultrasonic inspection results for crack length measurement is shown in the upper part of figure 3-10 (5). Data from pulled tubes in 1989 (data points) with numerous axial cracks are presented. The data are described by the regression equation $Y =$ with a correlation coefficient of $r =$ and a standard deviation of $s =$. Eddy-current length measurement results for the same two tubes are shown in the lower part of figure 3-10. The data are described by the regression equation $Y =$ with a correlation coefficient of $r =$ and a standard deviation $s =$. The

Figure 3-10. Comparison of Eddy-Current and Ultrasonic Measurement of Crack Length

ultrasonic results do not correlate as well as the eddy current data, and exhibit a larger standard deviation about the regression line. Better results have been obtained with more recent instrumentation (9). These results indicate that current UT technology provides comparable length accuracy with RPC and also provides improved azimuthal resolution.

3.4 Compensating For Coil Diameter Effects in Measuring Crack Length

The basic principles of RPC data analyses were discussed in Section 3.2.2. This section expands on that discussion utilizing results from the EdF data set to illustrate an important correction factor (due to finite coil diameter effects) which can improve the overall accuracy in measuring crack length. This factor is identified in order to ensure that it is considered in the development of future eddy current data acquisition and analyses procedures for measuring crack length. All of the data presented in the previous section have been corrected. In addition, the various data set were taken using different data acquisition procedures e.g., test frequencies, test coils, etc. . Although the value of the correction factor is different for each data set, a recommended approach in obtaining the factor (described in this section) is identical.

Figure 3-11 is used to discuss the detailed interaction between a rotating coil and an axial crack. The upper part of the figure shows a coil scanning past an axial crack, whereas the lower part of the figure shows the coil output voltage (represented by an arrow of varying amplitude) during each rotation of the coil past the crack. Since the coil has a finite diameter (determined by its magnetic field) the coil responds to the leading edge of the crack before the coil center is aligned with the crack edge; this effect is often referred to as coil "look-ahead". Similarly, the coil continues to respond to the crack trailing edge after the coil center has traveled beyond the crack edge; this effect is often referred to a coil "look- behind". Looking at the details of the sampled coil output voltage, it is seen that the coil response is amplitude modulated (portrayed by the arrows of varying magnitude) increasing in amplitude as the coil magnetic field integrates more of the crack length reaching a constant value when the coil is centered within the crack away from the crack edges.

Crack length measurement is typically accomplished by counting the number of hits or line scans from a given crack (lower part of figure 3-11). The apparent length is then the coil pitch (assuming constant probe pull speed) multiplied by the total number of hits or line scans. For crack lengths much greater than the coil diameter, the apparent eddy-current length will, in general, be longer than the true length because of the finite coil diameter. In practice, the total number of line scans is generally adjusted downwards to compensate for this effect. The actual adjustment value will in general be a function of the particular eddy-current procedure used for measuring crack length.

Mathematically, the output response of a coil as it scans past a crack can be described as the convolution of the coil impulse response with the crack. For cracks with lengths much greater than the effective coil diameter, the output response is

Figure 3-11. Eddy-Current Crack Length Measurement
Showing Effects of Finite Coil Diameter

controlled by the crack; for crack lengths shorter than the coil effective diameter, the output is dominated by the coil impulse response. For crack lengths intermediate between the two extremes, the coil output will include effects from both the finite coil diameter and finite crack length. Notice that the crack leading and trailing edges tend to be smoothed or smeared by the impulse response of the coil. The coil diameter of interest is not the physical diameter of the coil but rather the effective coil diameter determined by the coil magnetic field which in turn is controlled by the coil excitation frequency and coil design features, e.g., shielding, etc. The effective diameter may be larger or smaller than the physical diameter of the coil.

Figure 3-12 shows the original EdF data set prior to compensation for finite coil diameter effects. The scatter plot shows the number of coil hits along the ordinate versus true length in mm along the abscissa. The EdF rotating probe scanner pitch is 1 mm which means that the number of coil hits also corresponds to the apparent length in mm. In figure 3-11 it was shown that in general, the true crack length should always be overestimated (look-ahead and look-behind) because of the finite coil diameter. This conclusion is borne out statistically by the data presented in figure 3-12 in which all crack lengths are overestimated. To arrive at a correction factor, a scatter plot of the number of coil hits (plotted along the abscissa) is made versus true crack length (plotted along the ordinate). This plot is shown in figure 3-13 where the data set is described by the equation $Y = \dots$. The Y-intercept value is rounded upwards to a value of \dots and then subtracted from the number of coil hits to correct for finite coil diameter. The data shown in figure 3-5 were generated by first subtracting this correction factor from the number of actual coil hits prior to plotting versus true crack length. Using the correction factor essentially removes a bias from the data leaving only a random error which must be accounted for in the margin allowance for sizing accuracy.

Figure 3-12. EdF Data Set Prior to Correction for Coil Diameter

Figure 3-13. EdF Data Set Showing How Coil Diameter Compensation Factor is Determined

3.4 REFERENCES

1. H. Houserman et al. "Development and Field Use of a Tubesheet Scanner System for Primary-Side Crack Detection and Measurement." EPRI Eighth Annual Steam Generator NDE Workshop, August 1989.
2. F. Cattant. "Mesure de la Longueur des Fissures Longitudinales de Corrosion Sous Contrainte en Milieu Primaire Situées dans la Zone de fin de Dudgeonnage Mécanique des Tubes." Electricité de France Report D.5004/CTT/RB.90.52, May 1990.
3. D. Dobbeni. "Implementation of a Fast and Accurate RPC Method for a 100% Inspection of Roll Transitions." EPRI Workshop on PWSCC Remedial Measures, Clearwater Beach, Florida, February 1989.
4. F. Cattant, J.M. Thomas, and P. Hubert, "Examen de deux tubes de generateur de vapeur extraits d'une unite beige." EdF - GdL Service controle des materiaux irradies, D.5004/CTT/R.84.37.
5. D. Dobbeni, D et, al., "Comparison between Destructive and Nondestructive Examinations on Tubes Pulled From Steam Generator B of Doel 3 in 1989." Laborelec M01-90-085/R-DDo-DDe-CI-CR, December 1990.
6. B. Wilson. Qualification of New MRPC Equipment for Crack Length Measurement in Roll Transition Zone in Ringhals 3 and 4 Steam Generators. Swedish State Power Board Report, November 1989.
7. L. Gonzalo. Results of the Pulled-Out Tubes from Steam Generators of Spanish Nuclear Power Plants. Tecnatom Report CI-21-01, November 1989.
8. D. Mayes. "Catawba 1 and McGuire 1 Tube Pull Experience", presentation given at EPRI SGRP TAG Meeting, October, 1990.
9. D. Dobbeni, "Fast UT Inspection of ID and OD IGSCC at Doel 4 and Tihange 3", Laborelec M01-92-077/N-DDo-CR, July 1992

Section 4

ALLOWABLE CRACK LENGTH

4.1 APPROACH

This section presents methods and criteria for calculating the allowable axial length of EZ PWSCC roll transition cracks in recirculating steam generator tubes made of alloy 600. The allowable axial crack length is the length of the largest axially oriented crack that can be left in service until the tube is next inspected. This length includes margins on load, consideration of variable material properties, a correction for tubesheet constraint, an allowance for crack growth during the time period between inspections and an allowance for crack length measurement uncertainty.

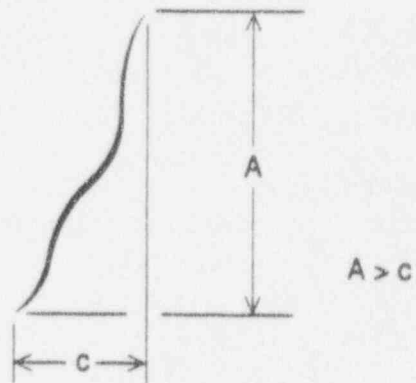
The methods described in this section apply to axial cracks and inclined axial cracks that are located near or above the top of the tubesheet (figure 1-1, cases A and C). This document can be used for inclined axial cracks when the circumferential extent of the inclined crack is equal to or less than the axial extent of the inclined crack. The applicable crack conditions are illustrated in figure 4-1. This document cannot be used for evaluation of NDE indications evaluated to be distinct circumferential cracks. Tubes with identified distinct circumferential cracks should be repaired.

For tubes having multiple axial cracks, additional conditions on spacing between cracks apply as described in section 6. Evaluation of cracks in partial-depth rolled tubes (figure 1-1, case B) is described in section 7.

The steps for calculating the allowable axial crack length are shown schematically in figure 4-2. The first step is to define the tube rupture equation which describes the relationship between crack length, tube dimensions, loads, and material properties. With appropriate input parameters, including safety factors, the tube rupture equation is used to calculate a reference crack length, \bar{a} . Three corrections to the reference crack length \bar{a} are needed. These are a correction for tubesheet constraint (a_{TS}), an allowance for crack growth until the tube is next inspected (a_{CG}) and an allowance for crack length measurement uncertainty (a_{NDE}). The allowable crack length, A , is found by adding the correction for tubesheet constraint and subtracting the allowances for crack growth and crack length measurement uncertainty from the reference crack length, \bar{a} .



Case A: Axial Crack



Case B: Inclined Axial Crack

Figure 4-1. Illustration of Allowable Crack Lengths for Axial and Inclined Axial Cracks

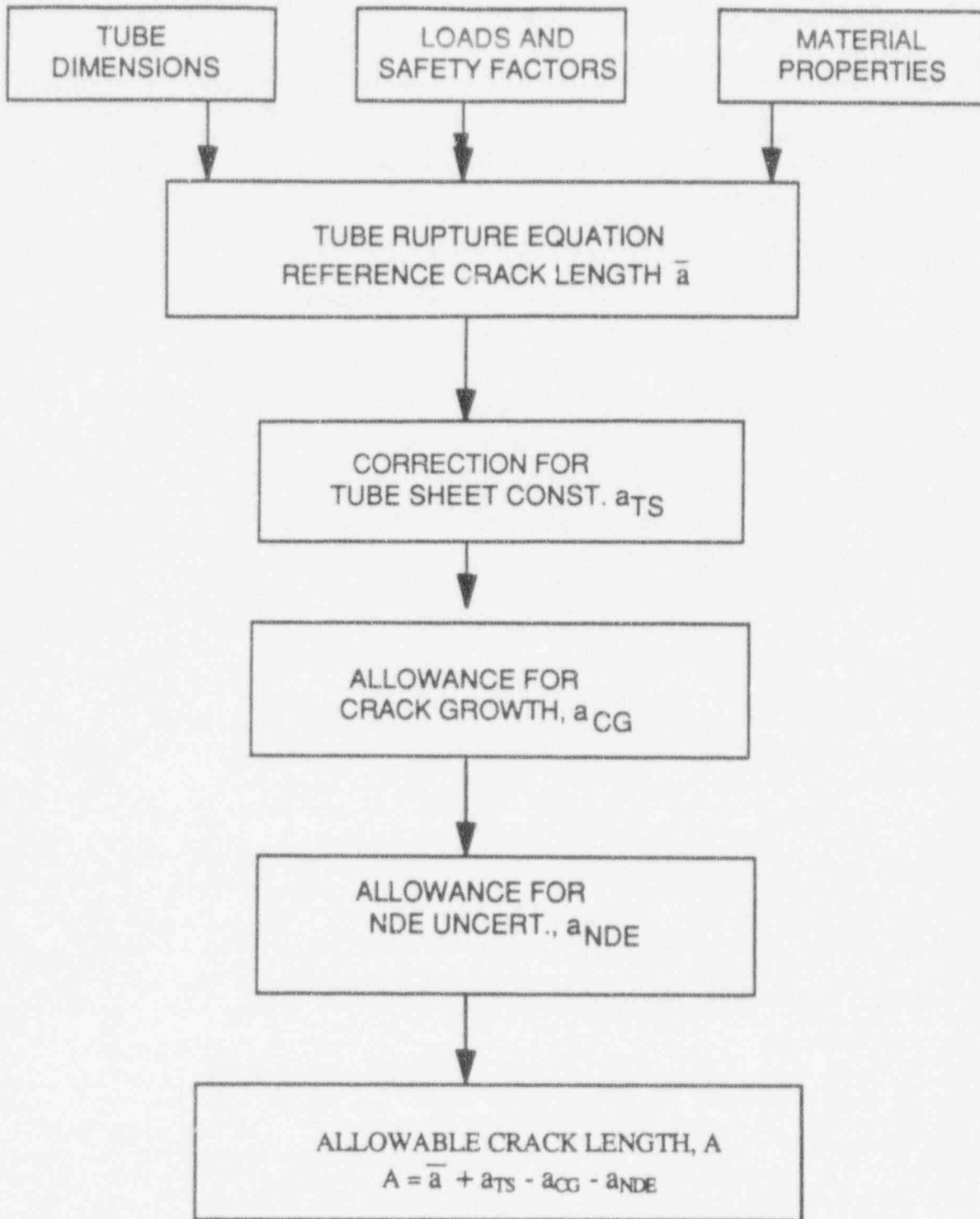


Figure 4-2. Allowable EZ PWSCC Axial Crack Length Calculation Steps

4.2 TUBE RUPTURE EQUATION

In section 2, major tube burst studies were reviewed and summarized. In addition, several tube rupture equations developed by the different investigators were presented. The equations were plotted using a common format, and a mean curve representative of field conditions and a curve that bounds various experimental burst relationships were described.

Currently, work is still in progress to determine the combination of burst correlation, and adjustments for NDE measurement uncertainty and crack growth that will be used to provide an adequate margin against tube rupture for the PWSCC repair criteria. Until the tube rupture evaluation is completed, the tube rupture relationship in Eq. 2-12 will be used to illustrate the process for determining allowable axial crack length; for convenience, the following summarizes this relationship.

Key parameters for the tube rupture equation are dimensionless pressure, \bar{P} and dimensionless crack length, λ .

$$\bar{P} = \quad (4-1)$$

where P is the tube differential pressure, S_u and S_y are the material ultimate and yield strength, respectively. R and t are the tube mean radius and thickness as shown in figure 4-1.

$$\lambda = \quad (4-2)$$

where \bar{a} is the reference crack length.

For an axial crack in the free span of a straight tube away from the tubesheet, the steam generator tube burst correlations can be bounded by the equation:

$$\bar{P} = \quad \text{or} \quad (4-3)$$

$$\lambda =$$

This equation is shown plotted in figure 4-3 and is valid for

Eqs. (4-1) through (4-3) or Eqs. (4-1) and (4-2) in combination with figure 4-3 can be used to solve for the burst pressure given an axial crack length or the critical axial crack length given the tube differential pressure.

Figure 4-3. Tube Rupture Equation in Terms of
Dimensionless Burst Pressure and Critical Crack Length

4.3 LOADS AND SAFETY FACTORS

Tube rupture depends on hoop membrane stress. In addition, for straight tube sections, hoop membrane stress is almost entirely due to the differential pressure between the inside and outside of the tube (2). For normal operating conditions, tube differential pressure is the difference between the primary system pressure and the secondary system pressure. Maximum differential pressure for faulted conditions is generally associated with the design basis accident of a main steam line break (MSLB) or feedwater line break (FWLB). In these accidents, the primary system pressure could be higher than normal operating conditions with secondary system pressure effectively ambient.

USNRC Regulatory Guide 1.121 (3) recommends that when establishing tube plugging limits based on depth, that safety factors be applied to the tube load. Recommended safety factors are:

- 3 under normal service conditions.
- A value consistent with the limits set by the ASME Code, Section III, paragraph NB-3225 for accident conditions. In compliance with NB-3225, this factor is taken as $\sqrt{2}$ for accident conditions (emergency and faulted conditions, service levels C and D).

In calculating the reference crack length, it is recommended that safety factors of 3 be applied to normal operating differential pressures and a factor of $\sqrt{2}$ be applied to accident differential pressures. The smaller of the crack lengths calculated with these two pressure terms is the reference crack length, \bar{a} .

4.4 MATERIAL PROPERTIES AND TUBE DIMENSIONS

The material property controlling tube rupture is the flow stress, $\bar{\sigma}$. As discussed in section 2, the flow stress is a simple function of the sum of the material yield and ultimate strengths. The tube rupture equation is in terms of the tube material yield plus the ultimate strength ($S_y + S_u$).

Three sources of tube yield and ultimate strength values are suitable for calculation of allowable axial crack lengths. If properties of the actual tube have been measured, these should be used for that tube. Further, if these properties were measured at room temperature, they should be adjusted for steam generator operating temperatures. Operating temperature yield strength should be taken as of room temperature yield strength while ultimate strength at temperature should be of room temperature ultimate strength (4).

A second possibility is to use a lower bound estimate* of yield and ultimate strengths for the different heats of material found in a steam generator. This eliminates the need to identify the heat of each individual tube. If lower bound room temperature yield and ultimate strength properties are used, the properties should be corrected for temperature as is the case where individual tube properties are used.

A third source of steam generator tube mechanical properties is the lower bound estimate based on Westinghouse testing of multiple heats of material (4). If steam generator specific data are not available, these properties can be utilized. Westinghouse mean and lower bound estimates of mechanical properties for mill-annealed tubing are given in tables 4-1 and 4-2.

In the absence of an identified wall thinning mechanism, it is recommended that nominal tube dimensions be used for calculating the reference axial crack lengths. For 3/4-inch diameter tubes, these dimensions are $R =$ and $t =$. For 7/8-inch diameter tubes, $R =$ and $t =$.

4.5 CORRECTION FOR TUBESHEET CONSTRAINT**

The tube rupture equation described in paragraph 4.2 describes the burst behavior for an axial flaw in a straight section of tube away from the tubesheet or support plates. With appropriate safety factors and tube mechanical properties, the tube rupture equation yields the reference flaw length, \bar{a} .

The presence of the tubesheet near EZ PWSCC influences the tube burst behavior. For a given flaw length, the tubesheet presence results in higher burst pressure; for a given tube pressure, the presence of a tubesheet results in larger critical flaw sizes. The effect of tubesheet constraint decreases as the distance from the crack tip to the tube-to-tubesheet contact point increases.

*Limit above which of data would be expected with confidence.

**Alternate tube repair limits have been proposed which would modify the substance of this section and the basic methodology presented in the body of the report. For example, an alternate criteria for all indications could consist of only comparing the crack length above the top of the tubesheet to an allowable crack length based on an associated, smaller tubesheet constraint factor than that recommended in this document. The smaller tubesheet constraint factor would need to be demonstrated by burst testing of tubes with EDM slots or SCC that extends below the top of a simulated tubesheet at least, for example, as far as the length of the exposed crack. NDE error and crack growth rates would also need to be addressed.

Table 4-1

ALLOY 600 STRENGTH PROPERTIES
3/4 X 0.043-INCH MILL-ANNEALED TUBING (4)

Table 4-2

ALLOY 600 STRENGTH PROPERTIES
7/8 X 0.050-INCH MILL-ANNEALED TUBING (4)

To take credit for tubesheet constraint, the crack must be in the vicinity of the tube-to-tubesheet contact point. In the calculation of the allowable crack length, it is assumed that the reference axial crack effectively spans the roll transition.* In this case, the lower end of the crack will be at the bottom of the roll near the contact point.

If during in-service inspection it is noted that a crack indication does not extend to the bottom of the roll transition:

- The tubesheet constraint term should be neglected (assumed to be zero) in the calculation of the allowable crack length, or
- The distance from the lower end of the crack indication to the bottom of the roll transition should be added to the indicated crack length and this length compared to the allowable crack length calculated with tubesheet constraint.

The effect of tubesheet constraint has been experimentally studied and an empirical relationship describing the strengthening effect developed. The French (5) and Spanish (6) have accounted for tubesheet constraint by modifying the bulging factor in the limit load equation based on the length of crack outside the tubesheet and an effective tube thickness which accounts for the interaction with the tubesheet. The Belgians (1) developed an empirical fit to their tubesheet constraint data using an exponential fall-off of reinforcement with crack length. This fit is shown in figure 4-4.

A tubesheet constraint correction for 3/4-inch and 7/8-inch diameter tubes was derived from the tubesheet constraint relationship developed by BELGATOM (1). This correction is designated as a_{TS} and is the crack length to be added to the reference crack length to account for tubesheet constraint.

For 3/4-inch diameter tubes:

$$\begin{aligned} & \qquad \qquad \qquad ; \qquad \qquad \qquad (4-4) \\ & \qquad \qquad \qquad ; \\ \text{or} & \qquad \qquad \qquad ; \end{aligned}$$

For 7/8-inch diameter tubes:

$$\begin{aligned} & \qquad \qquad \qquad ; \qquad \qquad \qquad (4-5) \\ & \qquad \qquad \qquad ; \\ \text{or} & \qquad \qquad \qquad ; \end{aligned}$$

*This is a reasonable assumption given the size of the reference crack length, on the order of

These relationships are also shown in figure 4-4.

Figure 4-4. Allowance for Tubesheet Reinforcement

4.6 ALLOWANCE FOR CRACK GROWTH

As discussed in section 3, inspection with the RPC eddy-current probe will identify EZ PWSCC and provide information on location, orientation and length. The reported length will subsequently be compared with the allowable crack length, and if longer than the allowable, the tube will be removed from service.

There are two corrections to the reported crack length that need to be considered. These are a correction for crack growth that is expected to occur until the time the tube is next inspected and a correction for the crack length measurement uncertainty. These corrections could be handled by adding an incremental crack length for each correction to the indicated crack length, or alternatively, subtracting the incremental crack lengths from the reference crack length in the allowable crack length calculation. It is this latter approach which has been used by others and is used here. The allowance for crack growth is discussed below and the allowance for crack length measurement uncertainty is discussed in paragraph 4.7.

The allowance for crack growth is developed by estimating EZ PWSCC crack growth rate and multiplying the rate by the time interval until the next planned inspection. Further, EZ PWSCC crack growth rates can be estimated from sequential measurement of EZ PWSCC cracks in service. Individual growth rate data points obtained in this manner are given by

$$\frac{a_2 - a_1}{\Delta \text{ time}} \tag{4-6}$$

where a_2 is crack length at time 2, a_1 is crack length at time 1 and Δ time is the operating time interval between inspections performed at time 1 and time 2.

Crack growth data for kiss and standard-roll transitions are available from Belgium because of the Belgian practice of performing RPC examinations of 100% of roll transitions at each annual outage.

The most recent inspection results for standard roll transitions indicate an average annual growth rate of _____ with a standard deviation of _____ for all crack sizes. In the crack range from _____ the growth rate was _____; this value is used as the crack growth rate for determining the PWSCC repair limit. Crack growth rates for EZ PWSCC also have been obtained for kiss-roll transition data; these data indicate growth rates that are higher than those for standard-roll transitions for small cracks and about the same for larger cracks in the range from _____.

Crack growth rate versus crack length curves for standard and kiss-roll transitions are presented in figure 4-5. Note that growth rates are in terms of effective full-power years (EFPY). Appendix E discusses the EZ PWSCC crack growth data in more detail.

Figure 4-5. Estimate of EZ PWSCC Average Crack Growth Rate Curves

4.7 ALLOWANCE FOR CRACK LENGTH MEASUREMENT UNCERTAINTY

Eddy-current measurement of EZ PWSCC crack length is discussed in section 3. Crack length measurement capability is presented in terms of a sizing model where the sizing model is a regression equation developed from NDE performance data relating true crack length for cracks of various sizes to an NDE measured dimension obtained using the applicable NDE equipment, procedure and analysis method. These data are generally developed from tube pulls and/or round robin exercises. The regression line is defined by the equation

$$y = \dots \dots \dots (4-7)$$

where

- y is the NDE measured value of the crack length,
- x is the true I. D. crack length (or corrected reference crack length),
- b is the intercept of the regression line with the y axis,
- k is the slope of the line defined by the regression equation, and
- s is the standard deviation or data scatter about the regression.

The sizing model regression line is shown schematically in figure 4-6.

Figure 4-6. Definition of Crack Length Measurement Correction, Δ_{NDE}

From the standpoint of efficiency in tube repair, i.e., repair only those tubes that could fail unacceptably, the ideal sizing model would have a slope, k , of 1.0 and a y-axis intercept, b , of 0, with no data scatter; however, from the standpoint of reliability, i.e., assuring that all such tubes be removed, it is only necessary to know what the slope, intercept and data scatter are. These are then accounted for in the determination of the allowance for NDE uncertainty, discussed below.

As is the case with the allowance for crack growth between inspections, the allowance for crack length measurement uncertainty, a_{NDE} will be one of the terms subtracted from the reference crack length to obtain the allowable crack length. Further, as the regression formula shows, the eddy current measured crack length depends on the true crack length. Consequently, the first step in calculation of a_{NDE} is to calculate the allowable crack length without an allowance for crack length measurement uncertainty to use as the true crack length in Eq. 4-7.

This crack size is the reference crack size, \bar{a} , plus the correction for tubesheet constraint, a_{TS} , minus the allowance for crack growth, a_{CG}

$$x = \bar{a} + a_{TS} - a_{CG} \tag{4-8}$$

Referring to figure 4-6, for a given true crack length x (which in our case is the corrected reference crack length), the regression equation can be used to calculate the expected NDE crack length, y , and the lower bound NDE crack length, y_{LB} . The systematic NDE error is the difference between the true crack length and the expected NDE crack length, $x-y$. The random error is the difference between the expected NDE crack length and the lower bound NDE crack length, $y-y_{LB}$. Taking t times the standard deviation, s , as the confidence interval, the NDE crack length measurement uncertainty is the sum of the systematic error, $x-y$, and the random error, $y-y_{LB}$.

$$a_{NDE} = (x - y) + (y - y_{LB}) \tag{4-9}$$

Calculated in this way, the lower bound NDE crack length is, by definition, the allowable crack length, A , since

$$A = y_{LB} \tag{4-10}$$

4.8 ALLOWABLE CRACK LENGTH SAMPLE CALCULATION

Currently, work is still in progress to determine the combination of burst correlation, and adjustments for NDE measurement uncertainty and crack growth that will be used to provide an adequate margin against tube rupture for the PWSCC repair criteria. The remainder of this section illustrates the process that will be used to define the repair criteria. Upon completion of the tube rupture evaluation, final values for the tube rupture correlation, and adjustments for NDE measurement uncertainty and crack growth will be defined and applied in a subsequent revision to this report. Consequently, the values presented in this section are for illustration purposes only and should not be considered typical or representative of any particular steam generator.

Calculation of allowable EZ PWSCC crack length follows the process shown in figure 4-2. The first step is to calculate a reference crack length, \bar{a} . Information needed to establish reference cracks length includes steam generator tube nominal dimensions, tube mechanical properties and normal operating and faulted condition tube primary-to-secondary differential pressures. Applying a safety factor of 3 to normal operating differential pressure and a factor of $\sqrt{2}$ to faulted condition differential pressure, a reference crack length is calculated from Eqs. 4-1, 4-2, and 4-3, or from Eqs. 4-1 and 4-2 and figure 4-3. The smaller of the calculated crack length from the two differential pressure terms is utilized as the reference crack length. Generally, normal operating differential pressure will be the controlling load.

As an example of this calculation, consider a 7/8-inch diameter tube with nominal dimensions of $R =$ _____ and $t =$ _____. Further, assume that mechanical properties for neither the particular tube nor the steam generator are available and that industry lower bound properties (provided in paragraph 4.4) are used. In this case, $S_y + S_u =$ _____. Assuming that the normal operating differential pressure is _____ and faulted load differential pressure is _____, the controlling load will be three times the normal operating differential pressure. Using this load, the reference crack length (\bar{a}) from Eqs. 4-1 through 4-3 or figure 4-3 is _____.

Correction for tubesheet constraint (a_{TS}) is found from Eq. 4-5 or figure 4-4. For this example of a 7/8-inch diameter tube with \bar{a} equal to _____, a_{TS} is _____.

In the absence of plant specific crack growth data, allowance for crack growth (a_{CG}) is found from table 4-3 or figure 4-5. Assuming that it will be one effective full-power year until the tube is next inspected and utilizing the result that $\bar{a} + a_{TS} =$ _____, $a_{CG} =$ _____. The allowable crack length without an allowance for crack length measurement uncertainty is _____.

$$A = \bar{a} + a_{TS} - a_{CG} = \text{_____} \quad (4-11)$$

For this example, the composite crack length measurement error statistics presented in Section 3 are used for calculating an allowance for crack length measurement uncertainty (a_{NDE}). Substituting the value of allowable crack length calculated above in equation (4-11) for x into the regression equation presented in paragraph 3.3.1 gives

$$y =$$

As pointed out in paragraph 3.3.1, the random error in measuring crack length is characterized by the standard deviation of . Thus, the
 The NDE crack length measurement uncertainty is from Eq. 4-9, the sum of the systematic error ($x-y$) which for the allowable crack length is equal to plus the random error or

$$a_{NDE} = -0.39 \text{ mm} + 2.12 \text{ mm} = 1.73 \text{ mm}.$$

Thus the allowable crack length, A , is the reference crack length, \bar{a} , plus the correction for tubesheet constrain, a_{TS} , minus allowances for crack growth, a_{CG} , and crack length measurement uncertainty, a_{NDE} . For the 7/8 inch diameter tube example

$$A = \tag{4-12}$$

The results of this sample calculation for a 7/8-inch diameter tube are provided in table 4-3. A similar sample calculation for a 3/4-inch diameter tube is included in this table as well. These results demonstrate how the calculations should be performed. Plant-specific calculations may be carried out using the information available in this report supplemented by available plant-specific data.

Table 4-3

SAMPLE CALCULATIONS OF ALLOWABLE
CRACK LENGTH FOR 7/8-INCH AND 3/4-INCH DIAMETER TUBES

4.9 REFERENCES

1. G. Frederick, P. Hernalsteen, and D. Dobbeni. Belgian Approach to Steam Generator Tube Plugging for Primary Water Stress Corrosion Cracking. Palo Alto, Calif.: Electric Power Research Institute, March 1990. NP-6626-SD.
2. P. DeRosa et al. Evaluation of Steam Generator Tube, Tube Tubesheet and Divider Plate Under Combined LOCA Plus SSB Conditions. WCAP-7832, April 1978.
3. U.S. Nuclear Regulatory Commission Regulatory Guide 1.121. "Bases for Plugging Degraded PWR Steam Generator Tubes." Draft for Comment, August 1976.
4. J. A. Begley and J. L. Houtman. Inconel Alloy 600 Tubing-Material Burst and Strength Properties. WCAP-12522, January 1990.
5. B. Cochet and B. Flesch. "Application of the Leak-Before-Break Concept to Steam Generator Tubes." 10th SMIRT Conference, Volume G, August 1989.
6. C. Cueto-Felgueroso and J. M. Garcia Alonso. Criteria for Plugging of SG Tubes in Model D3 Steam Generators Based on the Leak-Before-Break Criterion Applicable to Stress Corrosion Cracking. Tecnatom Report: EPRI-CT-D3, July 1989.

Section 5

LEAK RATE CONSIDERATIONS

5.1 LEAK RATE UNDER NORMAL LOADS

5.1.1 Leak Rates

To evaluate the potential for leak-before-break (LBB), axial through-wall crack length is correlated with leak rate for normal operating pressure.

A number of laboratory leak tests with primary water stress corrosion cracks have been conducted at normal operating pressure using tubes with axial corrosion cracks in the tube expansion zones, and the results are presented in figure 5-1. Also shown in figure 5-1 are data representing in-service leaks from tubes with axial corrosion cracks in the expansion zone. The leak rate data and the data sources are listed in appendix F. The indicated crack lengths are the reported nominal values or the average of the reported ID and OD crack lengths.

The data in figure 5-1 include experiments conducted on several heats of 3/4-inch and 7/8-inch diameter tubes at pressures ranging from . No effort was made to normalize these data in a manner similar to that shown in figure 2-4.

The data in figure 5-1 indicate a wide range of leak rates at crack lengths of interest in this work. This range may be due individually or in combination to effects such as tube sheet reinforcement, location within the sludge pile, and/or crud buildup at the crack. Additional in-service experience indicates that even some relatively long cracks in the roll transition region may not leak at all during normal operation (1).

To assess the potential for LBB behavior over the leak rate range indicated in figure 5-1, two curves are presented. One is the best fit mean curve (using the laboratory data and assuming a relationship in the form $Q =$), while the other represents the mean leak rate divided by 10 at any specified crack length. The lower curve encompasses most of the data and represents tubes where the leak rate may be restricted due to crud build-up, etc. Both curves are considered in the following LBB assessment.

Figure 5-1. Leak rate versus nominal or average axial crack length for steam generator tubes with corrosion cracks in the expansion zone roll transition region, 600°F (data from appendix F).

5.2.2 Leak-Before-Break

To establish the allowable leak rate at normal operation that provides a low probability of failure at faulted load, the critical crack length at faulted pressure first must be determined from Eq. 2-11 (or figure 2-9). This crack length is then used to enter figure 5-1 and determine a leak rate at normal operation. If this leak rate is greater than the plant allowable leak rate limit then leak-before-break at faulted load is likely.

As an example, consider a typical 7/8-inch diameter tube where mean radius, R , equals 0.413 inch and wall thickness is 0.050 inches. A conservative value for the sum of the yield and ultimate stresses at temperature for this size tube has been determined as (2) (see table 4-2). Substituting these values into Eq. 2-12 and including the tubesheet constraint correction described in paragraph 4.5, the critical crack size at a faulted pressure of is . Using similar procedures and a value of for the sum of ultimate and yield stress (2) (see table 4-1), the critical crack size for a 3/4-inch diameter tube is . Using average material properties, critical flaw sizes at a faulted pressure of are and for 7/8-inch and 3/4-inch diameter tubes, respectively.

If the conservative assumption is made that the leak rate at normal operation is produced by a single crack, then critical crack sizes determined from Eq. 2-12 can be used in figure 5-1 to define the allowable leak rate at normal operation for a corrosion crack in any region of the tube bundle.

As seen from the mean curve in figure 5-1, crack lengths of and correspond to leak rates of about respectively. For these conditions, the typical Technical Specification limit of 0.35 gpm generally ensures LBB at faulted load.

However, when the leak rate at normal operation is determined from the lower curve, which is more representative of most in-service leak rates of cracks in a roll transition, the indicated allowable leak rate at normal operation ranges from about for a long crack to for an long crack. This leak rate range is significantly less than typical Technical Specification limits. To impose such leak rate limits from the lower edge of the leak rate data may cause undue restrictions on plant operation and result in unnecessary plant outages, radiation exposure, and cost of repair. In addition, because some or longer cracks may not leak at normal operation (1) it is not feasible to ensure LBB for all tubes by reducing the leak rate limit.

While it is not feasible to have a leak rate limit that ensures LBB for all tubes, leaks may occur during service (even from cracks in regions other than the roll-transition). This possibility requires an assessment to be made of an appropriate leak rate limit. To determine this limit consider the potential for LBB at normal

operating pressure. Eq. 2-12 gives a critical through-wall crack length at normal operation of about _____ for both the 3/4- and 7/8-inch diameter tubing.

Using the _____ curve of figure 5-1, the leak rate at normal operation for a long through-wall crack is about _____. To ensure margin exists for LBB at normal operation when an in-service leak is detected, a leak rate limit of 150 gpd is recommended. Using a 150 gpd leak rate as the leak rate limit assures a crack length of _____ using the _____ curve in figure 5-1. Using Eq. 2-12 the minimum burst capability would exceed _____ for either size tube for this crack length. On the basis of the mean burst curve (Eq. 2-11), the burst capability of the 3/4-inch tubing with a _____ long crack is at least _____. LBB at postulated accident pressure levels therefore is essentially satisfied.

To provide a high level of confidence that tubes that may not exhibit LBB behavior at faulted load are removed from service, RPC inspection will be performed for 100% of the tube roll transitions of expansion zones in regions of the steam generator (i.e., the hot leg) that are affected by EZ PWSCC. Tubes with crack lengths greater than a conservative allowable length (see section 4) will be repaired.

5.2 LEAK RATE AT POSTULATED FAULTED LOADS

5.2.1 Background

The Standard Technical Specifications and many plant Technical Specifications limit the allowable primary to secondary leakage through all steam generators not isolated from the reactor coolant system (RCS). The allowable limits are based on the following considerations:

- The total steam generator tube leakage limit of 1.0 gpm for all steam generators not isolated from the RCS ensures that the dosage contribution from the tube leakage will be limited to a small fraction of 10 CFR 100 limits in the event of either a steam generator tube rupture or steam line break event. The 1.0 gpm limit is consistent with the assumptions used in the analysis of these accidents.
- The limitations on the specific activity of the primary coolant in the plant technical specification ensure that the resulting 2 hour doses at the site boundary will not exceed an appropriately small fraction of 10CFR100 limits following a steam generator tube rupture in conjunction with an assumed steady state primary-to-secondary leakage rate of 1.0 gpm.
- The 500 gpd (0.35 gpm, 79 l/hr) leakage limit per steam generator is intended to assure that steam generator tube integrity is maintained in the event of a main steam line rupture or under LOCA conditions. Permitting operation with leakage in excess of this limit increases the

potential that steam generators may be vulnerable to tube rupture during a postulated steam line break event.

Because current tubing plugging criteria are aimed at precluding penetration of the tube wall, significant leakage is not expected even at faulted load. However, because the objective of this work is to justify the presence of through-wall and/or deep part through-wall cracks, it is recommended that the leakage at faulted load be assessed. This assessment would identify the leak rate that must be tolerated when determining if the site boundary dose remains within 10CFR100 limits during postulated accidents. This leak rate is site-specific and, among other factors, will depend on the number and length of the cracks allowed to remain in the steam generator tubes subsequent to inspection.

The accidents that should be considered are those that assume that primary to secondary leakage is combined with secondary steam release to the environment (e.g., steam line break, locked reactor coolant pump rotor, SG tube rupture, control rod ejection, loss of load/loss of off-site power). For many plants, the limiting event with regard to primary to secondary leakage will be steam line break. For some plants, the locked rotor event may be more limiting depending upon the number of assumed fuel failures and the assumed iodine partition coefficient. To ensure that the most limiting condition is addressed relative to primary to secondary leakage, all accidents which combine leakage with steam release should be considered.

This section outlines a method that can be used to assess the leak rate during a postulated steam line break (SLB) for any specified crack distribution (number and length of cracks). Several examples are evaluated to illustrate its application and obtain an estimate of the range of leak rates that can be expected for various EZ PWSCC distributions.

5.2.2 Leak Rate Calculations

The method used to predict leak rate uses elastic plastic fracture mechanics analysis to estimate the crack opening for pressure loading. Thermal-hydraulic analysis is used to predict the mass flow through the crack opening. The analysis includes consideration of crack opening area, resistance to flow through the crack opening, and effective differential pressure.

There are several uncertainties associated with the analysis methods, including plastic crack opening area and the flow discharge coefficient (the resistance to flow through the crack). To obtain an accurate assessment of these variables, it is necessary to bench mark the leak rate calculational methods with experimental data. Available experimental data from tubes with corrosion cracks were used to bench mark computational procedures and define the flow discharge coefficient for PWSCC.

The deterministic model for leakage from an axial crack in a tube with internal pressure is given by the following formula:

$$Q = \tag{5-1}$$

The representation of the flow discharge coefficient, K , in Eq. 5-1 was determined from experiments where both leak rate and crack opening area had been measured experimentally. These experiments included tubes with laboratory induced corrosion cracks, either in free span or in EZ roll transitions (simulated tube sheets), and tested at normal and faulted differential pressures.

The K value and the computational procedure in Eq. 5-1 were benchmarked using experimental data where leak rate was measured as a function of ID axial crack length. These data include: (1) PWSCC in EZ roll transitions of pulled tubes at faulted differential pressure, (2) doped steam SCC in laboratory roll transition mock ups of Alloy 600 MA at normal operating differential pressure, (3) polythionic acid SCC in laboratory straight run and roll transition mock ups of sensitized Alloy 600 MA at normal operating and faulted differential pressures, and (4) polythionic acid SCC in laboratory straight run sections of sensitized Alloy 600 MA at normal operating differential pressure.

The data used to define the flow discharge coefficient and benchmark the leak rate computational procedure are provided in appendix F; the procedures used to determine K and benchmark the computational procedure are described in appendix G. The information in appendix G demonstrates that Eq. 5-1 provides a conservative procedure to predict total leakage from steam generators with PWSCC degraded tubes.

Plots of the leak rate versus crack length obtained from Eq. 5-1 for 3/4 and 7/8 diameter tubes are presented in figure 5-2. The primary coolant pressure and temperature conditions shown on figure 5-2 were obtained from reference 3 for a main steam line break and a total leak rate from the steam generator tubes of

Application of Eq. 5-1 requires that the leakage be computed for each distinct crack in each degraded tube. The sum of all these leak rates (plus leakage from other DSM mechanisms) will be used to determine the number of degraded tubes that can remain in service to ensure that 10CFR100 dose limits are satisfied. Work is still in progress to determine the combination of radiological assumptions, leak rate prediction methods, and adjustments for NDE uncertainty and crack growth that will provide an adequate level of confidence that 10CFR100 limits will be maintained during postulated faulted loads. The results from this work will be applied in a later revision to this report.

The leak rate versus crack length relationship in Eq. 5-1 also has been incorporated into a statistical computational routine based on a systematic combination of random variables (4,5); this computational procedure is described in more detail in appendix G.

Figure 5-2. Predicted leak rate versus axial throughwall crack length for steam generator tubes with corrosion cracks in the expansion zone roll transition region, 515F.

5.3 REFERENCES

1. P. Hernalsteen. Steam Generator PWSCC In Service Leakage Experience in Belgium. LABORELEC Report M00-90-022/R-PH, May 1990.
2. J. A. Begley, and J. L. Houtman. Inconel Alloy 600 Tubing - Material Burst and Strength Properties. WCAP-12522, January 1990.
3. N. Norris, et. al., "Thermal-Hydraulic Evaluation of Pressurized Water Reactor Transients During Steam Line and Feedwater Break Events with Induced Steam Generator Tube Leakage, SAIC Rpt. No. 93/6503, June 1, 1993.
4. P. Hernalsteen. LABOLEAK: Laborelec Leakrate Probabilistic Assessment Program for PWSCC Cracks in Steam Generator Tube Roll Transitions - User's Manual. LABORELEC Report M00-90-023/R-PH, May 1990.
5. P. Hernalsteen. LABOLEAK: Laborelec Leakrate Probabilistic Assessment Program for PWSCC Cracks in Steam Generator Tube Roll Transitions - Description and Validation. LABORELEC Report M00-90-024/R-PH, May 1990.

Section 6

COMBINATION AXIAL AND CIRCUMFERENTIAL CRACKS

6.1 INTRODUCTION

While this degradation-specific tube repair document addresses axial PWSCC in tube roll transition zones, field experience indicates that circumferential cracks and occasionally combinations of circumferential and axial cracks can occur.

Pulled tube experience (see appendix D) from European plants indicates that combination axial and circumferential cracks can occur in the EZ roll transition. In several instances, the circumferential cracks were through-wall, although not always in locations where interaction with axial cracks would have occurred. In almost all cases where there were through-wall circumferential cracks, the cracks were detected by RPC inspections even though the inspections were not being performed specifically to detect circumferential flaws.

The field experience in the United States with combination axial and circumferential cracking indicates significantly fewer confirmed indications of combined cracking. There have been several instances where through-wall circumferential cracks have been confirmed in U.S. plants. In one case, the through-wall crack was in a tube that also contained an axial crack, while in the other instance, there were no axial cracks present. The through-wall circumferential cracks were detected by RPC and confirmed when tubes were pulled. There has been one instance where a tube contained an axial crack in combination with a part-through-wall circumferential crack.

While more tubes may develop combined axial and circumferential cracks in the future, it is expected that combined cracking will not be widespread or may take significant time to develop.

When distinct circumferential cracks are identified during in-service inspection, the repair limits in this document do not apply. In these cases, the tube should be repaired.

To ensure that if circumferential cracks should develop in combination with axial PWSCC, structurally significant circumferential cracks will be readily detected by NDE and that undetected circumferential cracks will be small and would not leak significantly under faulted conditions, an additional repair limit is defined. Because there are few incidents of confirmed combined circumferential and axial cracking that can be used to evaluate in-service circumferential crack growth rates, the added

repair limit was developed using postulated final crack sizes. These include through-wall axial cracks in combination with circumferential cracks. The detection capability and pressure capacity of these postulated combination cracks were measured in laboratory tests. The repair limit resulting from these considerations requires a minimum spacing between axial cracks that are greater than the allowable axial length defined in section 4. Tubes with axial cracks longer than the allowable length requirements of section 4 must be repaired.

The ability to detect circumferential cracks in combination with axial cracks is discussed in section 6.2 and appendix H. Tests which measured the pressure capacity of tubes with combination cracks are reviewed in section 6.3 and appendix I. The additional repair limit to ensure that postulated combination cracks will not be structurally significant is described in section 6.4.

6.2 DETECTION OF CIRCUMFERENTIAL CRACKS BETWEEN AXIAL CRACKS

A series of laboratory experiments were conducted to assess the ability of the RPC eddy-current inspection to detect circumferential cracks in the presence of axial cracks (see appendix H). These experiments utilized tubes with combination axial and circumferential EDM notch configurations. Inspections utilizing different coil diameters were carried out and the detection of part-through-wall circumferential components in the presence of through-wall axial components was evaluated.

These experiments show that the conventional diameter unshielded pancake coil RPC can readily detect a through-wall circumferential defect in the presence of two through-wall axial defects spaced or more apart. With a smaller coil diameter, circumferential defects can be reliably detected between axial defects closer than

6.3 PRESSURE CAPACITY OF TUBES WITH COMBINATION CRACKS

A number of pressure tests have been conducted with steam generator tubes containing combination axial and circumferential defects (see appendix I). These tests involved pressurizing a section of steam generator tube containing either machined notches or stress corrosion cracks. For through-wall degradations, a crack sealing system was used to maintain tube pressure. Tubes were pressurized and the maximum pressure that the tube could support was recorded. Generally, maximum pressure was achieved when part-through crack ligaments tore or the crack sealing system was lost. This would result in a tube leak. With a limited flow capacity pressurization system, higher pressures could not be applied.

These tests show that with the axial component of the combination crack through-wall and with length equal to approximately the allowable length defined in section 4, combination cracks, with part-through-wall circumferential components less than through-wall, support maximum pressures greater than 3 times normal operating differential pressure. In fact, most combination crack configura-

tions supported pressures above the burst curve which characterizes the behavior of axial cracks alone in the absence of tubesheet constraint. Even completely through-wall "U" shaped cracks with axial components approximately equal to the allowable length will support pressures greater than MSLB pressures. Finally, the test show that stress corrosion combination cracks have significantly higher pressure capacity than EDM notches with similar lengths.

6.4 ADDITIONAL REPAIR LIMIT TO PRECLUDE SIGNIFICANT COMBINATION CRACKS

While plant experience suggests that combination axial and circumferential cracks are unlikely, for conservatism, it will be assumed that small circumferential cracks can exist together with through-wall axial cracks.

To assure that structurally significant circumferential cracks are readily detected by NDE and that undetected circumferential cracks in combination with axial cracks are small and would not cause a significant leak under faulted conditions, axial cracks longer than the allowable length defined in section 4 and whose circumferential separation* is less than should be removed from service. The spacing requirement of between axial cracks need not be applied to axial cracks with lengths less than

By requiring that axial cracks with length greater than be spaced further than or more apart to remain in service, one can be assured that circumferential cracks through-wall or deeper will be detected by standard RPC methods. In the absence of significant vibration loads, circumferential cracks through-wall and completely around the tube circumference will not compromise structural safety margins.

By limiting the length of axial cracks spaced more closely than to, one is assured that even a through-wall circumferential crack connecting the two through-wall axial cracks will not leak significantly at MSLB pressures and, based on limited data for real cracks, likely support much higher pressures.

A smaller crack spacing limit can be used if justified by qualification tests. This qualification should demonstrate that circumferential cracks ranging from to of wall thickness can be detected reliably when located between adjacent axial through-wall cracks of length approximately equal to A and separated by the proposed spacing limit.

*Circumferential separation is defined as the shortest circumferential distance between axial cracks as measured on any circumferential plane.

Section 7

REPAIR LIMITS FOR THE EXPANDED REGION OF PARTIAL-DEPTH ROLLED TUBES

This section presents repair limits for PWSCC in the expanded region, including the transition, of partial-depth rolled tubes (see figure 1-1B).

7.1 TUBE BURST AND ALLOWABLE CRACK LENGTH

Experimental results (1) have been performed to determine the burst pressure for tubes having outside diameter initiated axial cracks that are contained within a support with relatively small annular distances. The results from these experiments show that tube burst below the burst pressure for an unflawed tube is precluded by the constraint of the tube radial displacement when the cracked section of the tube remains within the tubesheet and the diametral gap is less than approximately

Further experiments have been performed using combined axial and circumferential cracks, where the axial crack was above the tubesheet and circumferential cracks were either above or below the tubesheet (2). The results from these experiments indicate that there is no influence of circumferential cracking on the axial crack burst curve when the circumferential cracks are located below the top of the tubesheet. Consequently, the structural integrity of partial-depth rolled tubes is defined by axial separation and tube pull out (which depends on the extent of circumferential cracking) rather than burst from the presence of axial defects.

Experimental data (3) indicate that the extent of circumferential cracking needed to produce axial separation of the tube is very large (i.e., approximately a through-wall crack extending around the circumference, or a part-through-wall crack of the wall thickness and around the circumference). These crack sizes are readily detectable by standard NDE methods for tube inspection.

Because circumferential cracks can be difficult to detect by standard NDE methods when they are located between closely spaced axial cracks (see section 6.2), it is assumed for partial-depth rolled tubes that a circumferential crack exists between two adjacent axial cracks less than apart (see section 6.2). An additional conservative assumption is made that the postulated circumferential cracks are through-wall. Circumferential cracks need not be postulated between adjacent axial cracks separated by or more. Circumferential cracks need not be assumed between axial flaws less than the allowable defined in

section 4. Tubes having NDE indications evaluated to be distinct circumferential cracks cannot be evaluated using this document and should be repaired.

The maximum allowable circumferential crack extent should be conservatively determined using a continuous through-wall flaw and the R.G. 1.121 margins. The tube is acceptable for continued service if the allowable circumferential extent is greater than the extent required to be postulated by the axial spacing indicated by the NDE results. The postulated circumferential extent is determined by the sum of the circumferential distances between adjacent axial cracks that have spacings less than

7.2 LEAK RATE CONSIDERATION

Leakage from cracks within the tubesheet will be restricted at both normal and faulted loads compared to cracks located in the free span of the tube. Although the leakage is expected to be smaller compared to the leakage from a crack in the free span, no analytical methodology or laboratory testing is available to quantify the level of leakage expected. Therefore, it is suggested that the leak rate at faulted loads for partial-depth rolled tubes can be computed conservatively using the methods defined in section 5 for cracks above the tubesheet. The leak rate calculated from each tube need not exceed the maximum leak rate possible through the annulus between the tube and tubesheet.

7.3 SUMMARY OF REPAIR LIMITS FOR PARTIAL-DEPTH ROLLED TUBES

The following repair limits are applicable for plants with partial-depth rolled tubes:

1. The cracks must be located within the defined expansion zone, which includes the expanded portion of the tube, the transition between the expanded and unexpanded portions of the tube, and a short distance (e.g.,) of the unexpanded portion of the tube above the transition.
2. The length of the axial and inclined axial cracks are only restricted by leakage considerations. Leakage shall be calculated based on the requirements in section 5. To be considered an inclined axial crack, the axial extent of an inclined crack must be equal to or greater than the circumferential extent of the crack. Indications evaluated to be distinct circumferential cracks cannot be evaluated using this document.
3. Circumferential cracks should be postulated to be present between the identified axial cracks due to nondestructive detection limitations. The extent of cracking retained in service should be limited such that the postulated circumferential crack extent in the presence of axial cracks does not exceed a portion of the tube circumference

that would provide adequate margin against axial separation of the tube. This provides assurance that axial separation of the tube can not occur. Circumferential cracks need not be postulated between axial cracks that are more than apart or whose lengths are less than the allowable defined in section 4.

7.4 REFERENCES

1. T. A. Pitterle et al. Steam Generator Tubing Outside Diameter Stress Corrosion Cracking at Tube Support Plates: Data Base for Alternate Repair Limits. Palo Alto, Calif.: Electric Power Research Institute. NP-7480-L (to be issued in December 1991).
2. Evaluation of the Impact of the Pressure of Circumferential Orientation Fissures in the Transition Zone of the Expanded Portion of Steam Generator Tubes. Tecnom Report, December 1990.
3. Northeast Utilities Tube Specimen Burst Tests. Westinghouse Report WCAP-12916, May 1991.

Section 8

SUMMARY

8.1 OVERVIEW

This document provides guidance and the supporting technical bases which may be used by a utility to justify leaving small, axially oriented, EZ PWSCC roll transition cracks in service. These cracks are typically through-wall, short, and are expected to grow slowly, if at all, with continued service.

Current technical specifications require repairing a tube if the ECT measured crack depth exceeds a specified limit, typically 40% of the wall thickness. Use of this tube repair limit for EZ PWSCC cracks would result in removal of many tubes from service which neither challenge steam generator tube burst capability nor leak a significant amount.

The justification for leaving some EZ PWSCC in service is based on a safety-related defense in depth approach. Elements in this defense include:

1. Performing enhanced eddy-current inspection (RPC) of 100% of tube roll transition expansion zones in regions of the steam generator (i.e., the hot leg) where the tube expansion zones are susceptible to PWSCC.
2. Repair of tubes with axial defects longer than a conservatively established repair limit.
3. Limiting total number of cracked tubes in service based on crack size distribution to limit leakage during postulated accidents.
4. Implementing reduced primary-to-secondary leak rate limit to enhance defense-in-depth and supplement leak-before-break detection.

The effectiveness of elements 1 and 2 is due to the ability to reliably detect and measure EZ PWSCC cracks, and the ability to establish allowable axial crack length (tube repair limits) which preclude tube rupture during normal operation or accident loading conditions. Elements 3 and 4 provide additional assurance that small EZ PWSCC left in service will not be a significant safety concern.

Inspection of tube expansion zones with the rotating pancake coil (RPC) probe is discussed in section 3. RPC eddy-current inspection methods will both detect and size EZ PWSCC axial cracks. Further, based on a comparison between measured and actual crack lengths, crack length measurement uncertainty can be calculated.

Guidance for calculation of an allowable EZ PWSCC axial crack length or tube repair limit is developed in section 4. Allowable crack length is based on a tube rupture curve which bounds published tube burst test correlations, Reg. Guide 1.121 safety factors applied to tube loads, lower bound tube material properties, a correction for tubesheet constraint, an allowance for crack growth between inspections and an allowance for crack length measurement uncertainty. Although some data are provided and sample calculations of allowable crack sizes are included in section 4, this was done to show how the calculation is made. It is expected that a utility user will perform plant-specific calculations using parameters and data applicable to the particular plant.

As proposed, EZ PWSCC tube repair criteria will leave short, possibly through-wall, axial cracks in service. The leak-before-break (LBB) nature of EZ PWSCC roll transition axial cracks is discussed in paragraph 5.1. Based on tube burst test and leak rate data, it is shown that some but not all EZ PWSCC cracks which could burst under faulted loading conditions would leak a detectable amount during normal operation. Although lowering of the allowable primary-to-secondary leak rate limit would further enhance LBB, due to the variable nature of tube leak rate data, LBB cannot be guaranteed. To provide a high level of confidence that tubes that may not exhibit LBB behavior at faulted load are removed from service, NDE will be performed on 100% of the tube roll transition expansion zones in regions of the steam generator where the tube expansion zones are susceptible to PWSCC. Tubes with crack lengths greater than a conservatively calculated allowable crack length will be repaired.

In addition, estimates of expected leak rate during faulted loading conditions are required. Calculation of leak rates for cracks left in service is discussed in paragraph 5.2. These calculations depend on the distribution of cracks in a generator (number and size) as well as other hydraulic parameters. The number and size of cracks allowed to remain in service will be limited to ensure that the site boundary dose will not exceed 10CFR100 limits for postulated accident conditions.

Section 6 defines an additional requirement to ensure that adequate margins for tube rupture and leakage at faulted load are maintained in the unlikely event that combined through-wall axial and circumferential flaws develop simultaneously in service. Repair limits for tubes with partial-depth roll expansion zones are defined in section 7.

The combination of the inspection scope and procedure, repair limits, crack distribution limits, and leak rate limits ensure that conservative margins exist against failure and abnormal or excessive leakage at normal and faulted loads. Using these elements to evaluate acceptance for return to service of tubes with EZ PWSCC will provide levels of structural and leakage integrity that are in compliance with GDC 14, 15, 30, 31, and 32.

8.2 COMPARISON WITH EUROPEAN PRACTICES

The repair limits that result from the European practices, together with pertinent input assumptions, are summarized in table 8-1. European practices are discussed in section 1. The EPRI recommended sample calculation values from section 4 are also shown. The main conclusions drawn from review of table 9-1 and from the review of European practices and experience, are as follows:

- Alternate repair criteria have been in effect for up to about eight years in France and Belgium. These criteria have allowed the continued operation of many thousands of steam generator tubes with short, through-wall axial cracks. This has resulted in substantial economic savings and reduced personnel exposure. More importantly, no tube ruptures or other safety problems have resulted.
- A variety of approaches have been used to develop alternate repair criteria to ensure that they provide necessary margins of safety. All of the approaches have resulted in the conclusion that operation with short axial through-wall cracks at roll transitions is acceptable from both safety and operational standpoints.
- Two main approaches have been used in development and application of alternate repair criteria. One approach has relied on leak-before-break (leak-before-risk-of-break in French terminology), and the other on expanded inspections of the roll transition area. While both approaches have attractive features, these guidelines emphasize the inspection-based approach. However, leak-before-break is considered and provides useful additional assurance of safety.

Table 8-1

COMPARISON OF LENGTH-BASED REPAIR LIMITS FOR AXIAL EZ PWSCC ROLL TRANSITION CRACKS

Appendix A

STEAM GENERATOR DEGRADATION-SPECIFIC MANAGEMENT

A.1 STEAM GENERATOR MANAGEMENT

The goal of steam generator management is to develop tools to optimize steam generator operation relative to safety, reliability, and cost-effective maintenance. This section presents a management approach that can be applied by utilities to deal with EZ PWSCC, which is one element of an overall steam generator management plan.

The strategy supported by this document uses the relationship between degradation, remedial measures, leakage during operation and inspection as the basis for changes to steam generator tube repair limits for EZ PWSCC. The strategy maintains a defense-in-depth concept to assure that steam generator tube leakage is minimized and that safety issues are adequately addressed. The approach is utility-specific and will require application of the techniques outlined in other portions of this document to the situation and the condition of the plant under consideration.

Broadly stated, the specific advantages of this strategy are:

1. Avoiding premature/unnecessary tube repair
2. Optimizing steam generator availability
3. Applying the ALARA principle
4. Maintaining flexibility for long-term repair options
5. Maximizing the available heat transfer area
6. Optimizing the cost-effectiveness of the steam generator repair and inspection program

A.2 STEAM GENERATOR MANAGEMENT STRATEGY

Managing steam generator tube degradation requires attention in three areas:

1. Mechanism management (preventive maintenance)
2. Degradation management (near-term corrective maintenance)
3. Life extension/replacement (long-term corrective maintenance)

A.2.1 Mechanism Management

Mechanism management determines the cause of and remedies for the steam generator degradation forms applicable to a particular plant. The remedies are mechanism-specific, may be applied at various times in the plant's operational period, and include such items as enhanced water chemistry, in situ thermal stress relief, application of stress modification processes (peening), etc.

A.2.2 Degradation Management

The goal of degradation management is to remove only those tubes from service that are required to be removed for reliability and/or safety considerations. Support for this area is generated from in-service inspection, tube repair limits and the capability to monitor primary-to-secondary leakage. (This document focuses on the elements of degradation management as they apply to EZ PWSCC.)

A.2.3 Life Extension/Replacement

Life extension/replacement is targeted toward long-range planning involving the economic analysis surrounding the repair/replacement decision. The ability to make an appropriate repair/replacement decision depends on information generated as part of the mechanism and degradation management elements of the program.

A.3 DEFENSE IN DEPTH

The defense-in-depth concept is used to assure that components which form the reactor coolant pressure boundary have a high degree of integrity in order to minimize the transport of radioactivity from the fuel and maintain core coolant inventory under a variety of assumed failure or accident modes.

Defense-in-depth is based on using multiple elements to minimize the potential for catastrophic failures, and is broadly addressed by: applying proper principles; selecting appropriate materials; specifying design loads, limits and safety factors; and identifying nondestructive evaluation and maintenance requirements.

For steam generator tubing, defense-in-depth has the following elements:

1. Initial design and material selection
2. Application of remedial measures for known degradation mechanisms
3. Limits on the maximum allowable primary-to-secondary leakage
4. Periodic in-service inspection (eddy-current testing) to monitor the steam generator tubing for degradation
5. Repair of those tubes exceeding a specified degradation limit by:
 - Removal from service (plugging).
 - Repair of the defective tube segment by sleeving or similar techniques.

Historically, specific interrelated criteria and requirements have been developed for each element of the defense-in-depth approach to steam generator tube degradation. In principle, it should be acceptable to change the relationship among the five elements without impacting defense-in-depth or changing the overall outcome of steam generator tube integrity assurance; i.e., with fixed design and material conditions, a change in the tube repair limit is acceptable assuming suitable analyses are completed to establish new allowable leak rate and to identify new steam generator tube inspection requirements.

Figure A-1 is a decision tree/logic chart that could be applied to any steam generator tube degradation mechanism to assure that defense-in-depth is adequately addressed. Table A-1 is a definition of the terms used in figure A-1, and table A-2 describes the management options. The following is a general discussion of the application of figure A-1 to the management of any specified degradation form.

For existing steam generators the design features and material selection were established as part of the original design. Tube degradation is monitored by periodic in-service inspection (ISI). Flaw-types are characterized using specialized inspection techniques and are further quantified through tube removals and laboratory tests. A cause can be postulated for the mode of tube degradation and degradation progress can be assessed.

The result of this combined field inspection and laboratory assessment is the development of a degradation-specific progression correlation, and the prediction of future steam generator tube degradation. The progression correlation serves as the input to the decision-analysis process regarding the impact of the degradation on tube rupture potential, the effectiveness of remedial measures, primary-to-secondary leak potential and the adequacy of inspection requirements.

The results of the inspection program are then used to improve the quantitative flaw assessment model which then can be used to improve the overall tube degradation progression correlation.

As shown in figure A-1, there are 12 possible outcomes as a result of application of the decision tree and each outcome could be distinct with appropriate methods for managing a specific steam generator tube degradation mode.

A.4 EZ PWSCC DEGRADATION MANAGEMENT

Application of the decision tree of figure A-1 to EZ PWSCC, using existing laboratory and field data, is shown in figure A-2 and leads to the following: (1) multiple axial cracks can form in the roll transition region of alloy 600 tubes hard rolled into the tube sheet; (2) operating experience has shown these cracks are short, often less than long, and (3) the cracks generally do not propagate upward beyond the stressed region of the roll transition. With appropriate analysis and approved alternate tube repair criteria, tubes containing these short, axial cracks can be safely left in service.

Leaving such tubes in service is predicated on the following:

- Application of EZ PWSCC remedies to limit the number of cracks expected in service
- Evaluation of the primary-to-secondary leak rate limit with respect to leak-before-break (LBB) capability
- Commitment to perform rotating pancake coil (RPC) eddy-current inspections of 100% of tube expansion zones in regions of the steam generator (i.e., the hot leg) where the tube expansion zones are susceptible to PWSCC
- Repairing of tubes with axial defects longer than a conservatively established repair limit, which includes the following elements:
 - Use of a tube rupture curve which bounds published tube burst test correlations.
 - Reg. Guide 1.121 safety factors applied to tube loads.
 - Use of lower bound tube material properties.
 - Correction for tubesheet constraint.

- Allowance for crack growth between inspections.
- Allowance for eddy-current crack length measurement uncertainty.
- Calculation of the leak rate expected during postulated accident loads from the cracked tubes that remain in service.

While this document and the logic described above is focused on permitting the existence of through-wall EZ PWSCC cracks up to and including the final expansion roll transition, earlier industry work has allowed revised limits for EZ PWSCC cracks that exist more than a specified depth below the tubesheet secondary face. These criteria are referred to as P* and F* criteria and are discussed in paragraphs A.4.1 and A.4.2 below.

A.4.1 Tubesheet Region Repair (P*) Criterion

Existing tube repair criteria apply throughout the tube length and do not take into account the reinforcing effect of the tubesheet on the external surface of the tube. The presence of the tubesheet constrains the tube and improves its integrity in that region by essentially precluding tube deformation beyond its initial outside diameter. The resistance to both tube rupture and tube collapse behavior is strengthened by the tubesheet, and the use of an alternate plugging criterion is justified.

The tubesheet repair criterion applies to steam generators that have been full-depth mechanically rolled in the tubesheet and obviates the need to repair a tube (by sleeving) or to remove a tube from service (by plugging) due to eddy-current indications for most of the length of tubing within the tubesheet. The basic premise is that if a severed tube is constrained such that it cannot come clear of the tubesheet, the integrity of the tube bundle is conserved, and if leakage is limited, the safety consequences of leakage have been appropriately addressed. In the development of the tubesheet repair criterion, three aspects of bundle integrity are addressed: (1) maintenance of a fixed tube end condition in the tubesheet with the limiting case of a circumferential indication near the top of the tubesheet, (2) limitation of primary-to-secondary leakage consistent with accident analysis assumptions, and (3) maintenance of tube integrity under postulated conditions of primary-to-secondary and secondary-to-primary differential pressure.

The tubesheet repair criterion for repairing and removing tubes from service is considered to be conservative. The basis for the analysis is the assumption that tube degradation is oriented circumferentially. If an indication on a tube within the tubesheet has been determined to be axially oriented, the structural integrity of the tube would be maintained, and tube pullout from the tubesheet is not an issue. Additional margin is provided by the resistance to vertical displacement of a separated tube that develops due to interference between the tube and the tubesheet,

the tube support plates and antivibration bars. However, no credit is taken for this in the development of the tubesheet plugging criterion.

The tube sheet repair criterion identifies a distance (1-4), designated P^* , below the top of the tubesheet for which tube degradation of any extent does not necessitate remedial action since even a severed tube is constrained by other tubes such that it cannot come clear of the tubesheet. The uncertainty in position of the eddy-current indication must be included in the final calculation of P^* criterion. For example, for a standard bobbin coil probe, a conservative eddy-current uncertainty would be ; therefore, P^* would have a value of between

A.4.2 F* Criterion

An alternate steam generator tube repair criterion, designated the F^* criterion (1-4), has been developed for use in determining whether or not repairing or plugging of hardroll expanded tubes is necessary for degradation which has been detected in that portion of the tube located within the tubesheet. The F^* criterion represents a length, F^* , of a mechanically rolled tube in the tubesheet which provides for sufficient engagement of the tube in the tubesheet hardroll such that tube pullout during both normal operating and postulated accident condition loadings would be successfully resisted by the elastic preload between the rolled tube and the tubesheet.

Existing steam generator tube repair criteria apply throughout the tube length but do not take into account the reinforcing effect of the tubesheet on the external surface of the tube. The presence of the tubesheet acts to constrain the tube and complement its integrity in that region by essentially precluding tube deformation beyond its expanded outside diameter. In addition, the proximity of the tubesheet significantly affects the leak behavior of through-wall tube cracks in this region; the joint is expected to be leak-tight. The conservativeness of the F^* criterion has been demonstrated to result in tube integrity consideration commensurate with R.G. 1.121 criteria, both empirically and analytically.

In developing the F^* criterion, it is postulated that the circumferential severance of the tube can occur. Implicit in assuming a circumferential severance to occur in the development of the F^* criterion is the consideration that degradation of any extent or orientation within the tubesheet is demonstrated to be acceptable below the F^* regions.

The required engagement length, F^* , below the bottom of the hardroll transition or the top of the tubesheet, whichever is greater relative to the top of the tubesheet, is calculated from a derived preload force, as well as an indirect measure of the static coefficient of friction. The F^* criterion varies with tube size and has been verified as conservative based on tube pullout and hydraulic proof testing. Also, in assessing the F^* criterion, it is postulated that the radial preload resulting from the hardroll would be sufficient to significantly restrict leakage during normal operating and

postulated accident-condition loadings. No leakage from any of the hydraulic proof tests for pressures in excess of faulted condition loadings has been detected.

A.5 REFERENCES

1. "Tubesheet Region Plugging Criterion for Full Depth Hardroll Expanded Tubes." WCAP-10950. September 1985.
2. "Tubesheet Region Plugging Criterion." WCAP-11225, July 1986.
3. "Tubesheet Region Plugging Criterion." WCAP-11225, Rev. 1, October 1986.
4. Docket Nos. 50-369 and 50-370. Issuance of Amendment No. 59 to Facility Operating License NPF-9 and Amendment No. 40 to Facility Operating License NPF-17 for the McGuire Nuclear Station, Units 1 and 2, August 1986.

Figure A-1. Degradation-Specific Management Decision Tree

Figure A-2. EZ PWSCC Degradation Management Decision Tree

Table A-1

DEFINITIONS

Terms

Degradation Management: Remove only those tubes (or tube segments) from service which are required to be removed for safety and/or reliability and no others.

Elements/Decision Points

Progression Correlation: Relates material condition, fabrication/techniques and environmental factors to determine degradation initiation point, growth rate and orientation as a function of time. (The degree of sophistication/complexity of this element is dictated by the need to separate rupturable from nonrupturable tubes, which, in turn, is dictated by the need to pursue defect-specific degradation management.)

Rupture Potential: Flaw-type can grow over time and reach a length that would allow tube to "rupture" under a specified load condition (e.g., typical steam line break or normal operating condition with safety factors).

Effective Remedies: Remedial measures such as improved water chemistry, sludge removal, stress relief, stress redistribution (peening), plating, sleeving, etc., exist that prevent flaw-type(s) from reaching a rupture-critical size.

LBB: Flaw-types that can grow to a rupture-critical length will reach a length that will produce a reliably detectable leak under normal operating loads (with a suitable response interval) prior to reaching the rupture-critical length such that the plant can be shut down.

Effective Inspection: The capability exists to accurately detect, characterize and size the flaw-type at a specified inspection interval such that flawed tube sections can be removed from service prior to reaching a rupture-critical length.

Regulatory Issues: The existence of the flaw-type regardless of rupture potential or capability for preventing rupture by LBB considerations or effective inspection procedures, violates a regulatory and/or technical specification position such as maximum through-wall penetration.

Leak Potential: Flaw-types that cannot rupture can leak at measurable/detectable rates during normal operation.

Table A-2

MANAGEMENT OPTIONS

Management 1

Conditions:

- (a) Flaw-type(s) can rupture
- (b) Effective remedial measures (exclusive of plugging) prevent flaw-types from growing to a rupture-critical condition.

Actions:

- (a) Apply appropriate remedial measures
 - (i) environmental control
 - (ii) stress alteration
 - (iii) sleeving
- (b) Manage as a "nonrupture" flaw type

Management 2

Conditions:

- (a) Flaw-type(s) can rupture
- (b) Remedial measures not effective or are not used
- (c) LBB argument is technically sound
 - (i) acceptable analysis method
 - (ii) supporting leak model data
 - (iii) supporting rupture/burst data
- (d) Acceptable leak rate less than that for existing Tech Specs (e.g., 0.35 gpm)

Actions:

- (a) Accept lower leak limit
 - (i) Tech Spec change
 - (ii) administrative limit
- (b) Install suitable leak-detection equipment
- (c) Develop (plant-specific) leak-monitoring/response procedures
- (d) Solve any regulatory issue(s) per Management 4

Table A-2 (Cont'd)

Management 3

Conditions:

- (a) Flaw-type(s) can rupture
- (b) Remedial measures not effective or are not used
- (c) LBB argument is technically sound
 - (i) acceptable analysis method
 - (ii) supporting leak model data
 - (iii) supporting rupture/burst data
- (d) Acceptable leak rate less than that for existing Tech Specs (e.g., 0.35 gpm)

Actions:

- (a) Manage as a "nonrupture" flaw-type

Management 4

Conditions:

- (a) Flaw-type(s) can rupture
- (b) Remedial measures not effective or are not used
- (c) LBB argument is technically sound
 - (i) acceptable analysis method
 - (ii) supporting leak model data
 - (iii) supporting rupture/burst data
- (d) Acceptable leak rate less than that for existing Tech Specs (e.g., 0.35 gpm)
- (e) Operation with identifiable/locatable through-wall flaws not accepted by USNRC

Actions:

- (a) Obtain NRC acceptance of the position or proceed to Management 5 or 6

Table A-2 (Cont'd)

Management 5

Conditions:

- (a) Flaw-type(s) can rupture
- (b) Remedial measures not effective or are not used
- (c) LBB argument is a supporting basis (defense-in-depth)
- (d) Effective inspection capability exists
- (e) Operation with identifiable/locatable through-wall flaws acceptable to USNRC (i.e., length-based plugging limit @ 100% TW is accepted)

Actions:

- (a) Commit to conduct required inspection
 - (i) plug/sleeve as required
 - (ii) leak reduction measures (such as nickel plating) may be acceptable to reduce total primary-to-secondary leakage

Management 6

Conditions:

- (a) Flaw-type(s) can rupture
- (b) Remedial measures not effective or are not used
- (c) LBB argument is a supporting basis (defense-in-depth)
- (d) Effective inspection capability exists
- (e) Operation with identifiable/locatable through-wall flaws not acceptable to USNRC (i.e., length-based plugging limit \geq 100% TW is not accepted)

Actions:

- (a) Obtain NRC acceptance of the position or proceed to Management 7 or 8

Table A-2 (Cont'd)

Management 7

Conditions:

- (a) Flaw-type(s) can rupture
- (b) Remedial measures not effective or are not used
- (c) LBB argument is a supporting basis (defense-in-depth)
- (d) Effective inspection capability not used
 - (i) doesn't exist
 - (ii) choose not to use
- (e) Consequence analysis shows that the probability of a tube rupture and resultant consequences are acceptable

Actions:

- (a) Obtain NRC acceptance of the position
- (b) No further action

Management 8

Conditions:

- (a) Flaw-type(s) can rupture
- (b) Remedial measures not effective or are not used
- (c) LBB argument is a supporting basis (defense-in-depth)
- (d) Effective inspection capability not used
 - (i) doesn't exist
 - (ii) choose not to use
- (e) Consequence analysis shows that the probability of a tube rupture and resultant consequences are not acceptable

Management 9

Conditions:

- (a) Flaw-type(s) can't rupture
 - (i) during life of plant
 - (ii) during next operating cycle
- (b) Flaw-type(s) can leak at rate that could result in a forced shutdown by approaching Tech Spec leakage limit

Actions:

- (a) Apply appropriate remedial measures OR
- (b) Accept periodic shutdowns
- (c) Resolve any regulatory issues

Table A-2 (Cont'd)

Management 10

Conditions:

- (a) Flaw-type(s) can't rupture
 - (i) during life of plant
 - (ii) during next operating cycle
- (b) Flaw-type(s) can leak but not at a rate likely to result in forced shutdown
- (c) Existence of flaw-type(s) violates a technical specification position such as maximum TW penetration

Actions:

- (a) Obtain NRC acceptance of the position, OR
- (b) Apply appropriate remedial measures

Management 11

Conditions:

- (a) Flaw-type(s) can't rupture
 - (i) during life of plant
 - (ii) during next operating cycle
- (b) Flaw-type(s) can't leak
- (c) Existence of flaw(s) violates a technical specification position such as maximum TW penetration

Actions:

- (a) Obtain NRC acceptance of the position, OR
- (b) Apply appropriate remedial measures

Management Option 12

Conditions:

- (a) Flaw-type can't rupture
 - (i) during plant life
 - (ii) during next operating cycle
- (b) Flaw-type can't leak
- (c) Existence of flaw-type is acceptable to plant technical specifications

Actions:

- (a) Monitor flaws for growth

Appendix B

BACKGROUND OF PWSCC

B.1 CAUSES OF PRIMARY WATER STRESS CORROSION CRACKING (PWSCC)

Primary water stress corrosion cracking (PWSCC) of alloy 600, and the related phenomenon of pure water stress corrosion cracking, are both forms of intergranular stress corrosion cracking (IGSCC). This degradation has been studied extensively since originally observed by Coriou (1), and both laboratory research (2, 3) and plant experience (4) have shown that PWSCC occurs when a high tensile stress, a susceptible microstructure and an aggressive environment occur simultaneously. Each of the three necessary elements are discussed in more detail below:

B.1.1 Tensile Stress

PWSCC occurs most readily when the tensile stress at the exposed surface is above the yield strength of noncold-worked tube material, i.e., above about 55 ksi. Typically, such levels occur in areas where there are high residual stresses as a result of tube fabrication or installation processes. Regions experiencing these residual stresses include the expanded tubesheet region (particularly where rolling anomalies have occurred), the expansion transition zone into the unexpanded region of the tube, tube dents such as can occur at TSP intersections, and the small radius U-bends. The total stresses are due to pressure, and thermal and residual stress. The other stresses are usually not as high as the residual stresses which can be in some locations (5, 6).

B.1.2 Susceptible Material

Susceptibility of alloy 600 to PWSCC appears to be related to the carbide microstructure which is a function of the carbon content, heat treatment and cold-work history of the tubing. Highest susceptibility is characterized by a microstructure with few carbides at grain boundaries and many carbides within the grains (i.e., many intragranular carbides). High susceptibility also tends to correlate with small grain size and high yield strength. The susceptible microstructure is the result of low temperatures (within the acceptable range) used for the final mill anneal and for the mill annealing performed before the last stage of cold-work. The least susceptible condition is that associated with a microstructure characterized by continuous carbides at grain boundaries and few carbides within the grains (7, 8).

B.1.3 Aggressive Environment

With a susceptible microstructure and high tensile stresses, elevated temperature pure water is sufficiently aggressive to cause IGSCC of alloy 600, i.e., PWSCC. The main environmental factor that increases aggressiveness is high temperature (about 100°C increase in the progression of degradation for each 10°C) (9, 10). A secondary factor is the concentration of dissolved hydrogen. Current research indicates that at high temperatures (e.g., 300°C), increasing hydrogen concentration increases the rate of cracking (11). However, at operating temperatures characteristic of plant hot leg temperatures (e.g., 300°C), the occurrence of PWSCC does not appear to be strongly dependent on the concentration of dissolved hydrogen (12).

The effects of other environmental variables are not well known. The impact of lithium concentration on PWSCC--tests have yielded mixed results, with some data indicating that higher lithium accelerates cracking, while other data indicate that lithium has little effect (13). The most recent data indicate that higher lithium concentrations can accelerate PWSCC of alloy 600 in certain conditions (14). Recent studies have shown that the addition of zinc to primary coolant may increase the time to PWSCC initiation significantly, by altering the protective oxide film. Consequently, zinc additions may be useful for reducing the incidence of PWSCC as well as corrosion product buildup on the primary side. However, substantial additional study is required before such steps could be taken (15). There is also some information indicating that impurities such as sulfate can affect PWSCC; however, at the levels currently maintained in PWR primary system, the impact of such impurities is considered negligible when compared to the other factors discussed above (stress, material and temperature).

B.2 PLANT EXPERIENCE

This section provides a brief chronology of the more notable occurrences of PWSCC in PWR steam generators.

- The earliest occurrence of what is now considered PWSCC in a PWR steam generator was cracking observed at roll transitions and in row 1 U-bends at Obrigheim in 1971 (16). (In that case, lithium hydroxide was not added to the primary coolant, as is normally done to control the pH. Also, hydrogen was not added, and the tubing was pickled). Later, bulging occurred between expanded areas in the tubesheet and, in 1983, the Obrigheim steam generators were the first to be replaced (in 1983) as a result of PWSCC at roll transitions.
- About 1976, PWSCC was identified at U-bends and distorted TSP intersections at several plants affected by severe denting. This PWSCC with dents was associated with high dynamic straining

(e.g., up to), and occurred at plants with relatively low hot leg temperatures (and below).

- In 1978, Doel 2 experienced PWSCC at a roll transition (17) that was detected as a result of primary-to-secondary leakage. Doel 2 has part-depth-rolled tubes, and has low temperature mill-annealed tubing which appears to be especially susceptible to PWSCC. Since that time, a large percentage of the tubes in Doel 2 have been diagnosed by ECT as having PWSCC at the roll transition (17). However, tubes in Doel 2's sister unit, Doel 1, from the same manufacturer, have not experienced PWSCC.

Other plants around the world have also reported PWSCC at roll transitions (18). In many cases, PWSCC reported by eddy-current test (ECT) examination methods has been confirmed by destructive examination of pulled tubes (several hundred tubes pulled from U.S., Spanish, French, Belgian and Swedish plants). PWSCC has occurred in the standard roll transition found in both U.S. and European plants, as well as in "kiss roll" transitions found in many French and Belgian units and one Swedish unit (see figure B-1).

- In 1977 at Takahama 1, and in 1978 at Trojan, PWSCC was identified in row 1 U-bends (19, 20). The PWSCC was at the discontinuity that can occur at the location where the ball mandrel used to fabricate row 1 and 2 U-bends was located at the end of the bending operation. Measurements of the residual surface stresses at this location indicate that they are in the neighborhood of (6).
- Since the late 1970s, reporting of PWSCC has become more common. A number of plants with small radius row-1 U-bends, susceptible tubing material, and hot leg temperatures over have either experienced leaks due to PWSCC or have preventively plugged the row-1 tubes (18), and many plants with hot leg temperatures over have also reported PWSCC at hot leg roll transitions. This has been especially true in European plants with kiss-roll transitions, but has also been true in plants with standard rolls. As plants age, older plants with lower temperatures are starting to report roll transition cracking (18) (see table B-1).
- PWSCC has also been observed at explosive expansion transitions and at minor dents in a few plants with high hot leg temperatures (18).

Figure B-1. Standard and "Kiss" Roll Transitions,
With Typical PWSCC

Table B-1

REPORTED EXTENT OF EZ PWSCC AT PLANTS WITH \geq 10% TUBES AFFECTED
(September 1991)

- Recently, PWSCC has been reported in the expansion zone in the cold leg tubesheet region. Based on inspection information, the cold leg cracking is similar to the hot leg cracking, but the time to appearance of cold leg roll transition PWSCC is delayed as a result of the lower cold leg temperatures (21).
- While the large majority of EZ PWSCC degradations observed to date by ECT and/or destructive examination have been axially oriented, small but increasing numbers of circumferentially oriented PWSCC are also being observed in the EZ region. In France, isolated circumferential PWSCC has been identified in kiss roll transitions in tubes in the sludge pile region, and in tubes with dents at the top of the tubesheet. Isolated circumferential PWSCC has also been observed in standard roll transitions in some Spanish and Swedish units. These isolated circumferential cracks can typically be identified using RPC-type inspections. In addition to the occurrence of isolated circumferential cracking, some plants have experienced mixed mode, or combined axial and circumferential PWSCC in close proximity, in the EZ. Mixed mode EZ PWSCC has been identified in French, Swedish, and Belgian plants with kiss roll transitions, and in French, U.S., and Swedish plants with standard roll transitions. Mixed mode cracking can generally be identified using RPC-type inspections, if the circumferential component is of significant length (22).

B.3 IMPACT OF ROLL TRANSITION PWSCC

B.3.1 Number of Plants Affected

To date, reported roll transition PWSCC has been more extensive in Europe than in the United States. One reason for this is believed to be the fact that plants with the combination of susceptible mill-anneal material, mechanical rolls, and high hot leg temperatures came into operation in large numbers earlier in Europe than in the United States. Since the fraction of tubes affected by PWSCC increases with time, the longer operating times of the European plants results in more tubes with reported degradations. Another major factor is that many European units have kiss rolls. The cold work associated with kiss rolling appears to accelerate the development of detectable cracks.

Table B-2

STATUS OF PWSCC AT PART-DEPTH-ROLLED PLANTS IN USA
(September 1991)

Table B-3

STATUS OF PWSCC AT FULL-DEPTH-ROLLED PLANTS IN USA
(September 1991)

Plants that have reported roll transition PWSCC in the United States are listed in tables B-2 and B-3, respectively. The magnitude of reported PWSCC may increase with time as discussed below:

- Part-Depth-Rolled Plants. Older plants with low hot leg temperatures, e.g., Conn Yankee, San Onofre, Ginna, Zion, and Cook 1, have reported roll transition PWSCC in the past few years. Accordingly, other plants with part-depth rolls may eventually develop roll transition PWSCC.
- Full-Depth-Rolled Plants. The plants in table B-3 have material in the mill-annealed condition and many also have high hot leg temperatures. This combination is prone to PWSCC (18, 23). Expected behavior at these plants is as follows:

--Plants that operated prior to peening report EZ PWSCC. Depending on the length of operation before peening, this PWSCC may be severe.

--For plants that were shot peened before operation, PWSCC in the tubesheet area is expected to be negligible (24).

- Based on experience in Belgian plants (25), the occurrence of reported PWSCC will be limited to relatively low numbers of tubes, e.g., a few percent, at plants that rotopeened or shot peened prior to operation. This SCC is expected to occur mainly at relatively severe rolling abnormalities, and will probably become detectable early in life, within three or four cycles of operation, since rolling irregularities have high stresses and initiate defects earlier than other locations.

B. 4 REMEDIAL MEASURES FOR PWSCC IN EXPANDED AREAS

This section briefly describes remedial measures that have been developed or explored for PWSCC in expansion zones. Preventive measures are first described, and then the repair methods.

B.4.1 Peening

Peening of metal surfaces has been used for many years to change the stress state of the surface to increase resistance to stress corrosion cracking. This effect is achieved by developing a thin layer of compressively stressed material on the surface as a result of impacting by small balls or beads. Laboratory testing and experience show that if this compressive stress is uniform and is sufficiently high to overcome all in-service tensile stresses, SCC will not occur even in aggressive environments.

Peening is directed at preventing initiation of new cracks. If applied to a surface that has already developed cracks, it will be less effective. It is probable that shallow cracks, with a depth less than the thick compressive layer developed by peening, will be prevented from growing by peening. However, defects with depths of over probably can continue to grow since the crack tip is in a tensile area. If a plant has operated for a few years and peening is then performed, it is possible that there will be a population of cracks present with depths that exceed the thickness of the compressive layer.

Experience at many plants which peened after operation and which have now operated for cycles subsequent to peening show that the population of tubes with cracks present at the time of peening can be substantial. Some units have exhibited up to an additional of their tubes cracked following peening (26).

B.4.2 Stress Relief

Tests have shown that stress relief is effective at preventing roll transition PWSCC (27). However, a practical stress relief process has not been developed and qualified to the point where it is commercially available.

If performed, the stress relief would involve heating the roll transition area to about for up to . Such heat treatments have been found to be effective for U-bends and have been qualified for use at dented TSP intersections. The heat treatments reduce tensile residual stresses from over-yield levels to values of yield or less. This amount of stress reduction is expected to prevent PWSCC from occurring during the steam generator operation.

B.4.3 Plugging

Tube plugging has been the standard steam generator repair approach used in the United States for PWSCC degradations reported in the roll transitions. However, many plants have limited plugging margins, in the range of (the plugging margin is the fraction of tubes that can be plugged before plant power must be reduced because of reduced primary flow or reduced steam pressure). Since the number of tubes that may be affected by PWSCC at some plants will approach or exceed applicable plugging margins, and since other tube defect mechanisms are also likely to cause some level of plugging, plugging is not the desirable long-term solution.

B.4.4 Sleeving

Sleeving has been widely used for problems such as pitting and IGA/IGSCC in tube sheet sludge pile and crevice areas. Recently, several vendors have qualified sleeving for use in PWSCC susceptible tubing (28), and several plants are now using sleeving on a regular basis to repair tubes with roll transition PWSCC. These

sleeves involve stress relief of the top joint to prevent residual stresses associated with joint fabrication from causing PWSCC. The lower joint is not stress-relieved because the configurations result in a low potential for problems even without stress relief, as shown by mockup tests. Alloy 690 is used for sleeving because tests have shown it to provide additional resistance to PWSCC.

Sleeving, while useful, has some limitations:

- Installing sleeves is relatively expensive and slow (relative to plugs).
- Sleeves increase resistance to flow (though not as much as plugs) and reduce heat transfer area.
- Sleeves interfere with repairs that may become necessary in the future at higher elevations, for example, at TSP intersections.
- Some portions of the sleeved joint are difficult to inspect, especially the tube area immediately adjacent to the top joint.

B.4.5 Nickel Plating

Nickel plating of roll transitions with axial cracks has been developed by Belgatom and Framatome, and has been used on a trial basis in Doel 2 (part-depth-rolled) and Doel 3 (full-depth rolls) (29), and Ringhals 3. The nickel plating is typically applied for a length of about _____, including the roll transition, and has a thickness of _____. It is applied remotely using electroplating techniques.

Tubes with nickel plating have been in operation since 1985, and examination of pulled tubes shows that nickel plating can effectively seal PWSCC. Belgatom and Framatome indicate that it will provide long-term repair, but the possibility remains that crack growth might occur from the secondary side (29). Ultrasonic examination after three years of operation at Doel 3 has shown no evidence of such growth.

Because of its thinness, nickel plating has the advantage of not interfering with other repairs or with inspections of other areas. On the other hand, roll transitions with nickel plating are difficult to inspect using ECT techniques, and Laborelec together with Framatome, has developed an ultrasonic technique to monitor cracks in nickel-plated roll transitions (30). In addition, unlike sleeving, nickel plating is not considered a structural repair, and can only be used for tubes with relatively short axial cracks.

Nickel plating has been developed as an alternative repair method to plugging or sleeving. It can be used to seal PWSCC that has grown to a length that could lead to excessive leakage or, if further growth occurred, might impinge on allowed crack

length limits. Use of nickel plating is practical only where approved plugging limits allow short through-wall cracks to remain in service.

An alternate approach for nickel plating would be to use it in a preventative mode. In this mode, nickel plating would be applied to roll transitions in the absence of detected cracking in an effort to prevent cracking from occurring.

An additional repair approach using nickel plating has been used at Doel 2, which has part-depth rolls. At Doel 2, a new expansion was made above the original roll transition, and the ID surface was then nickel plated to prevent PWSCC.

B.4.6 Tube Section Replacement

KWU has developed, and demonstrated in nonnuclear heat exchangers, a technique for cutting out a defective length of tube and replacing it with a new tube section. The technique is applicable to tube sections extending to a short distance above the top of the tube sheet. The new tube section would be made of a more corrosion-resistant material, such as alloy 690, and would be installed in a manner to minimize residual stresses. The technique has not been used in operating PWR steam generators, and there is no experience on which to judge whether installing new tube sections would be practical and economical in nuclear applications.

B.4.7 Temperature Reduction

As described in paragraph B.2, PWSCC is strongly affected by temperature, with an activation energy of about . This means that a reduction in temperature would reduce the number of tubes initiating cracking to of the value experienced at the higher temperature. If plants have a sufficient design margin to accommodate such temperature reductions, the temperature reductions may be cost-effective. Some utilities (e.g., Commonwealth Edison at Byron) have implemented such temperature reductions. Temperature reduction as a PWSCC remedial measure is dependent on many plant-specific factors such as available design margins, secondary system design features, etc., and some utilities have concluded that it is not their preferred remedial approach.

B.5 REFERENCES

1. H. Coriou et al. "Corrosion Fissurante Sous Contrainte de l'Inconel Dans l'Eau a Haute Temperature." Third Colloque de Metallurgie Corrosion, Centre d'Etudes Nucleaires de Saclay, France. Amsterdam: North Holland Publishing Co., 1959, p. 161.
2. D. van Rooyen. "Review of the Stress Corrosion Cracking of Inconel 600." Corrosion, 1975, vol. 31, p. 327.

3. R. Bandy and D. van Rooyen. "Stress Corrosion Cracking of Inconel Alloy 600 in High Temperature Water—An Update." Corrosion, 1984, vol. 40, p. 425.
4. A. R. McIlree et al. "Primary Side Stress Corrosion Cracking." Chapter 7, Steam Generator Reference Book. Palo Alto, Calif.: Electric Power Research Institute, May 1, 1985.
5. R. Boudot, P. Vidal and G. Zacharie. "Evaluation of Residual Stresses Involved in PWSCC at Roll Transitions." In Proceedings: 1987 EPRI Workshop on Mechanisms of Primary Water Intergranular Stress Corrosion Cracking. Palo Alto, Calif.: Electric Power Research Institute, September 1988. NP-5987SP.
6. E. C. Ruud. "Residual and Applied Stress Analysis of Inconel Alloy 600 7/8-Inch U-Bend Tubing." Proceedings: 1987 EPRI Workshop on Mechanisms of Primary Water Intergranular Stress Corrosion Cracking. Palo Alto, Calif.: Electric Power Research Institute, September 1988. NP-5987SP.
7. S. M. Bruemmer et al. "Microstructure and Microdeformation Effects on IGSCC of Alloy 600 Steam Generator Tubing." Paper 88 presented at Corrosion 87, March 1987, San Francisco, California, NACE.
8. T. Yonezawa and K. Onimura. "Effect of Chemical Compositions and Microstructure on the Stress Corrosion Cracking Resistance of Nickel Base Alloys in High Purity Water." Proceedings: 1987 EPRI Workshop on Mechanisms of Primary Water Intergranular Stress Corrosion Cracking. Palo Alto, Calif.: Electric Power Research Institute, September 1988. NP-5987SP.
9. A. S. Stein. "Use of Activation Energy for SCC to Predict Life of Alloy 600 in Primary Water." Proceedings: 1985 Workshop on Primary-Side Stress Corrosion Cracking of PWR Steam Generator Tubing. Palo Alto, Calif.: Electric Power Research Institute, June 1987. NP-5158.
10. D. van Rooyen. "Update on SCC of Alloy 600 in High Temperature Water." Proceedings: 1985 Workshop on Primary-Side Stress Corrosion Cracking of PWR Steam Generator Tubing. Palo Alto, Calif.: Electric Power Research Institute, June 1987. NP-5158.
11. Preliminary results of Studsvik tests at 10 and 25 cc/Kg hydrogen (on file at Electric Power Research Institute, Steam Generator Project Office).

12. F. W. Pement et al. "Effect of Operational Dissolved Hydrogen Concentration on Alloy 600 PWSCC in PWR Reactor Coolant at 315 and 330°C (599 and 626°F)." Presented at Fifth International Symposium on Environmental Degradation of Materials in Nuclear Power Systems, August 1991, Monterey, California.
13. Report on May 9 and May 18, 1989, visits by Electric Power Research Institute representatives to Studsvik and Electricite de France, "Effect of Lithium on PWSCC of Steam Generator Tubing". (On file at Electric Power Research Institute, Steam Generator Project Office.)
14. R. B. Rebak and Z. Szklarska-Smialowska. "Stress Corrosion Cracking of Alloy 600 in Pressurized Water Reactors - Primary Water. The Influence of pH and Stress Intensity." Presented at Fifth International Symposium on Environmental Degradation of Materials in Nuclear Power Systems, August 1991, Monterey, California.
15. J. N. Esposito et al. "The Addition of Zinc to Primary Reactor Coolant for Enhanced PWSCC Resistance." Presented at Fifth International Symposium on Environmental Degradation of Materials in Nuclear Power Systems, August 1991, Monterey, California.
16. H. J. Schenk. "Investigation of Tube Failures in Inconel 600 Steam Generator Tubing at KWO Obrigheim." *Materials Performance*, March 1976, p. 25.
17. R. Houben and P. Hernalsteen. "Part Depth Rolled Plants, Status of the Doel 2 Unit." Proceedings: 1989 Electric Power Research Institute PWSCC Remedial Measures Workshop. Palo Alto, Calif.: Electric Power Research Institute, April 1990. NP-6719-SD.
18. A. R. McIlree. "Status of PWSCC-USA." Proceedings: 1989 Electric Power Research Institute PWSCC Remedial Measures Workshop. Palo Alto, Calif.: Electric Power Research Institute, April 1990. NP-6719-SD.
19. Steam Generator Progress Report. Palo Alto, Calif.: Electric Power Research Institute, November 1989. EPRI Research Project S405-3, Rev. 5.
20. J. W. Carter. "Operating History and Field Inspection Results of Trojan Steam Generators." Workshop Proceedings: U-Bend Tube Cracking in Steam Generators. Palo Alto, Calif.: Electric Power Research Institute, June 1981. WS-80-136.
21. D. B. Mayes. "When to Peen the Cold Leg Tubesheet." Proceedings: 1989 EPRI PWSCC Remedial Measures Workshop. Palo Alto, Calif.: Electric Power Research Institute, April 1990. NP-6719-SD.

22. Proceedings: 1990 EPRI Workshop on Circumferential Cracking of Steam Generator Tubes. Palo Calif.: Electric Power Research Institute, March 1991. NP-7198-S.
23. E. S. Hunt and J. A. Gorman. Status and Suggested Course of Action for Nondenting Related Primary-Side IGSCC of Westinghouse-Type Steam Generators. Palo Alto, Calif.: Electric Power Research Institute, May 1986. NP-4594-LD.
24. Discussion by G. Slama, Framatome, during 1989 EPRI PWSCC Remedial Measures Workshop, Clearwater Beach, Florida.
25. P. Hernalsteen and C. Leblois. "General Status of PWSCC in Belgian Plants." Proceedings: 1989 EPRI PWSCC Remedial Measures Workshop. Palo Alto, Calif.: Electric Power Research Institute, April 1990. NP-6719-SD.
26. P. Hernalsteen. Belgian Utility Experience Reports, October 1990 and June 1991, On File at EPRI.
27. J. Woodward and D. van Rooyen. Stress Relief to Prevent Stress Corrosion in the Transition Region of Expanded Alloy 600 Steam Generator Tubing. Palo Alto, Calif.: Electric Power Research Institute, May 1983. NP-3055.
28. Proceedings: 1989 EPRI PWSCC Remedial Measures Workshop. Palo Alto, Calif.: Electric Power Research Institute, April 1990. EPRI-6719-SD.
29. J. Stubbe and C. Leblois. "Belgian Utilities Experience with Nickel Electroplating and Sleeving." Proceedings: 1989 EPRI PWSCC Remedial Measures Workshop. Palo Alto, Calif.: Electric Power Research Institute, April 1990. NP-6719-SD.
30. D. Degreve and D. Dobbeni. "UT Developments for the Inspection of Electroplated and Sleeved Tubes." Proceedings: 1989 EPRI PWSCC Remedial Measures Workshop. Palo Alto, Calif.: Electric Power Research Institute, April 1990. NP-6719-SD.

Appendix C

BURST DATA AND STATISTICAL EVALUATION OF DATA FOR
THROUGHWALL FLAWS AND BURST DATA FOR
PART-THROUGHWALL FLAWS

Table C-1

NORMALIZED BURST PRESSURE FOR NON DEGRADED TUBES ($\lambda = 0$)¹

Table C-2

WESTINGHOUSE S/G TUBE BURST DATA, 70°F
EDM NOTCHES IN ROLL TRANSITION REGION
AXIAL THROUGH-WALL CRACKS¹

Table C-3

NRC PHASE II BURST TESTS 600°F, TUBES WITH AXIAL SCC ^a
(Nominal Tube Size: 7/8 OD, 0.050 in. Thickness)

Table C-4

CE S/G TUBE BURST DATA, 565F
AXIAL IGA CRACKS SIMULATING THOSE IN ST. LUCIE 1
(Nominal Tube Size : 3/4 OD, 0.048 in. Thickness)*

Appendix D

NDE OF ROLL TRANSITIONS—INDUSTRY EXPERIENCE

This appendix provides (1) a listing of tubes removed from operating steam generators that has been used to evaluate ECT reliability for detecting and sizing EZ PWSCC, and (2) a discussion of some specific and unique aspects of the information developed as a result of the tube pulls.

D.1 TUBE-PULL DATA

Table D-1 is an incomplete but representative listing of tubes removed from operating steam generators for investigation of PWSCC, principally from steam generators with standard roll expansions.* For each tube, all known references which discuss metallographic results and/or the correlation with inplant eddy-current results are also given. _____ tubes are identified, which represent the bulk of the tubes removed for possible PWSCC at a standard roll expansion. For tubes which are actually degraded, axial PWSCC is the predominant degradation. Several exceptions in which circumferential PWSCC has been observed include tubes from Ringhals 4, Ohi 1, and V. C. Summer.

D.2 SPECIFIC DETAILS

D.2.1 Correlation Between Pulled Tube Metallography and In-Plant Eddy-Current Data

D.2.1.1 Detection of Axial Cracking.

Ringhals 4 (SG2 Tube R22-C97). This tube was removed because of a long axial eddy-current indication at the roll transition (see figure D-1). The destructive exam confirmed a _____ axial crack from the roll transition zone downwards. The eddy-current crack length was approximately _____. No other cracking was identified during metallography. A comparison of test results using various examination methods is shown in figure D-2. The long length of the crack was probably the result of incomplete expansion of the tube in the region just below the top of the tubesheet, which lead to an abnormal tapered profile (see figure D-2). The whole length of crack was below the top of the tubesheet.

*Tubes from Ringhals 3, Doel 3, and Dampierre 1 have kiss-roll transitions.

Figure D-1. Ringhals 4 - Tube R22-C97. RPC Isometric - High and Low Sensitivity. Indication Just Below Roll Expansion.

Figure D-2. Ringhals 4 - Tube R22-C97. Comparison of Composite Test Results.

Dampierre 1 (SG2 Tube L12-C43). This tube (kiss-rolled) was removed because of multiple (seven) axial eddy-current indications. Eddy-current data was analyzed using the French 'ESTELLE' analysis system. Figure D-3 shows a comparison of the RPC graphic analysis of tube condition with that determined destructively. A direct comparison of crack lengths is given in the table shown in the figure. ESTELLE indicates the lengths of longitudinal cracks within accuracy, provided the cracks are through-wall in depth. System performance is such that it enables detection of isolated, longitudinal through-wall cracks in length or greater.

Doel 2 (SG Tube R13-C30). Figure D-4 shows a comparison of tube condition as determined using eddy-current RPC with destructive metallography results. The numbers at the upper part of the figure identify crack location whereas the individual cracks are identified by the numbers one through ten shown in mid-figure. The lower set of numbers are the eddy-current and metallography crack lengths. Correspondence between the two data sets is generally good both in terms of identifying individual cracks and predicting crack length. One crack (#10 on the far left of the figure) is not recognized by the eddy current because of masking effects by the larger crack adjacent to it (#1).

Doel 3 (SG Tubes R23-C32 & R27-C52). Figure C-5 shows the actual shape of two axial cracks from two tubes removed from the Doel 3 steam generators (a kiss-rolled unit). Both cracks were through-wall with different lengths on the tube inner and outer wall. Both cracks were detected using RPC eddy current with the length estimate shown below each crack cross-section for comparison with the "true length" which is different on the two sides of the tube. As expected, the eddy current provides some sort of estimate of crack length.

D.2.1.2 Detection of Circumferential Cracking.

Ringhals 4 (SG1 Tube R47-C50). This tube with a standard roll transition was selected for removal because of an eddy-current indication of an abnormal long circumferential crack, with a small axial component at one end. An isometric plot (end-on and oblique views) of the inplant eddy-current RPC data is shown in figure D-6. Flaw orientation is deduced by observing the orientation of the major axis of the eddy-current indications. In this case, two orthogonal indications are present, suggesting both axial and circumferential cracking. Metallography results did confirm the presence of both cracks; the length of the circumferential crack was —the axial crack length was not given. Figure D-7(a) shows the circumferential crack while figure D-7(b) shows the axial extension emanating from one end of the circumferential crack.

Figure D-3. Dampierre 1 - Tube L12-C43. Comparison of RPC and Destructive Test Results.

Figure D-4. Doel 2 Tube R13-C30. Comparison of RPC and Destructive Test Results.

Figure D-5. Doel 3 Tubes R27-C52 and R23-C53. Actual Shape of Through-Wall Cracks and Comparison with RPC Length Measurement.

Figure D-6. Ringhals 4 - Tube R47-C50. Axial and Circumferential
RPC Indications.

Figure D-7. Ringhals 4 - Tube R47-C50. Axial and Circumferential Cracks.

Dampierre 1 (SG Tube L8-C48). Another example of a tube kiss-rolled with an isolated circumferential crack is shown in figure D-8 removed from Dampierre 1. Shown is a comparison of the destructive analysis results and the initial inplant eddy-current prediction. For circumferential cracks, the detection threshold is approximately _____ arc length, with a depth of at least _____ of the tube wall thickness.

D.2.1.3 Nondetection of Short Axial Cracking.

Ringhals 3 (SG2 Tube R18-C79). This tube had been kiss-rolled. No eddy-current indications were reported by the field analyst. Metallography confirmed the presence of numerous ID-initiated cracks; they were located in the area between the top of the main roll and the kiss roll. Maximum crack length was approximately _____. Figure D-9 shows a view of the ID surface of the tube; the multiple short cracks are apparent. A pictorial summary of various test results for this tube are shown in figure D-10.

D.2.1.4 Masking Effects.

Ringhals 4 (SG1 Tube R17-C81). This tube was removed because it contained the greatest number of axial indications around the tube circumference. No circumferential indications were identified. Metallography revealed _____ axial cracks, the longest of which was _____, with another five approximately _____ in length. An unusual circumferential crack was also identified with a length of _____. Figure D-11 shows the RPC isometric; the presence of multiple cracking in close proximity is apparent with most indications appearing to have their major axes aligned in the axial direction. No clear evidence of circumferential cracking is indicated. In this case, the eddy-current coil is averaging over several coil diameters, causing a masking of individual indications. Figure D-12 shows composite test results for this tube, using various methods. The circumferential crack was only observed after the tube was flattened. It should be noted that short circumferential cracks of the type not detected in this tube do not significantly affect burst or leakage behavior.

Figure D-8. Dampierre 1 - Tube L8-C48. Circumferential Cracks in Kiss-Roll Transition Comparison of RPC and Destructive Test Results.

Figure D-9. Ringhals 3 - Tube R18-C79. Short ID Axial Cracking.

Figure D-10. Ringhals 3 - Tube R18-C79. Composite Test Results

Figure D-11. Ringhals 4 - Tube R17-C81. Multiple RPC Indications

Figure D-12. Ringhals 4 - Tube R17-C81. Composite Test Results

D.2.2 Improved Detection of Circumferential Cracks in the Presence of Multiple Axial Cracks

Observations derived from laboratory studies and tubes removed from operating plants have provided estimates on isolated crack detectability, resolution problems associated with the occurrence of multiple cracking, as well as highlighting special difficulties associated with the detection of circumferential crack initiation in the presence of multiple axial cracking.

The resolution properties of an eddy-current pancake coil are determined by the mean coil radius. The field of view of the coil—as determined by the average coil radius—is finite which means that multiple cracks present simultaneously within the coil field of view will be averaged as a single composite response. This effect can cause the output response to appear as a single crack even though several cracks are present. The occurrence of small circumferential cracks initiating and radiating from larger preexisting axial cracks has been a concern because of masking effects by the larger axial cracks. Similar to detection of single cracks, this situation can be improved somewhat by using coils of smaller diameter.

A series of laboratory experiments were conducted to define the ability of the RPC eddy-current probe to detect circumferentially oriented degradations in the presence of through-wall axial degradations. Those experiments are described in appendix H. They show that the conventional _____ diameter pancake coil clearly resolves a circumferential notch between axial notches separated by _____, with a degraded capability beginning at spacing between axial notches of _____ or slightly greater. The _____ (shielded, i.e. focused) pancake coil offers significantly improved resolution, with the _____ circumferential notch visible down to a _____ axial notch separation.

Table D-1

LISTING OF TUBES REMOVED FOR PWSCC

Table D-1 (Cont'd)

Table D-1 (Cont'd)

Table D-1 (Cont'd)

Table D-1 (Cont'd)

Table D-1 (Cont'd)

Table D-1 (Cont'd)

Table D-1 (Cont'd)

Table D-1 (Cont'd)

Table D-1 (Cont'd)

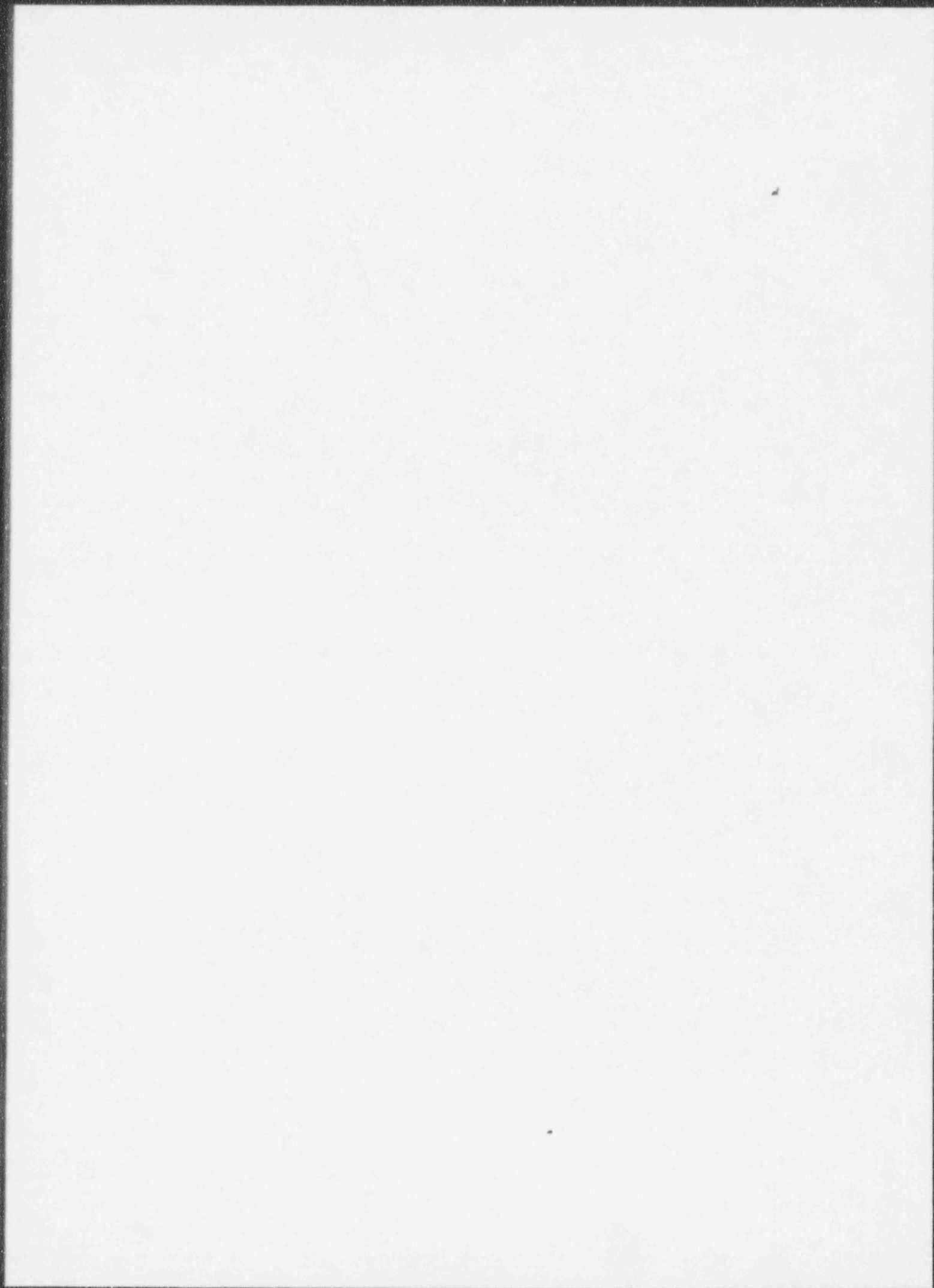
Table D-1 (Cont'd)

Table D-1 (Cont'd)

Table -1 (Cont'd)

Table D-1 (Cont'd)

Table D-1 (Cont'd)



Appendix E

CRACK GROWTH RATE DATA

E.1 INTRODUCTION

The crack growth rate of EZ PWSCC can be estimated from sequential measurement of EZ PWSCC cracks in service. Data to estimate crack growth are available for two plants with kiss roll transitions, and a program to generate data for a plant with standard roll transitions also has been completed (2, 3). This appendix summarizes the crack growth results. In the future, it is anticipated that utilities will generate plant specific crack growth rate data for estimating an allowance for crack growth based on repeated measurement of EZ PWSCC cracks left in service.

E.2 KISS ROLL DATA

The Belgians have performed 100% RPC of kiss roll transitions in Doel 3 and Tihange 2, using a highly accurate automated system, for five fuel cycles. These inspections provide EZ PWSCC crack length measurement data for five points in time. By taking the difference between crack length measurements and dividing by the time interval between measurements, crack growth rates have been calculated.

Statistical analysis of the resulting crack growth data has been carried out by LABORELEC. Their results are shown in table E-1 for the first two cycles. Table E-1 gives the average, standard deviation and maximum growth rates as a function of nominal crack length for individual plants, steam generators and time periods.

To develop a better picture of the growth rate of EZ PWSCC cracks as a function of crack size, the individual plant, steam generator and time period data points were combined in table E-2. In addition, these data were fitted to a quadratic equation using a least squares method. The values were weighted by the number of observations at each crack length. Growth values were converted to EFPY by dividing by 0.8, a typical capacity factor for Belgian plants. After reaching minimum growth rates at lengths of about 100 micrometers, the growth rate was modeled as being constant out to a length of 200 micrometers. The results of this "fitting" or "smoothing" are shown in figure E-1.

Table E-1

LABORELEC ANALYSIS OF EZ PWSCC CRACK GROWTH DATA
FROM DOEL-3 AND TIHANGE-2

Table E-2

CRACK GROWTH DATA FROM BELGIAN PLANTS WITH KISS ROLLS

Figure E-1. Average crack growth rates based on LABORELEC repeated measurements of kiss and standard roll transitions with EZ-PWSCC Indications.

It should be pointed out that there has been no attempt to separate from the apparent variability of crack growth rate data, the variability due to the uncertainty in crack length measurements. Referring to table E-2, the standard deviation in crack growth rate ranges from _____ to _____

E.3 STANDARD ROLL DATA

EPRJ contracted Belgatom to have three successive RPC inspections analyzed by LABORELEC on a large sample of standard roll transitions in a Doel 2 steam generator. The first of the three inspections was performed in 1989 (1), the second was performed in 1990 (2), and the third was performed in 1991 (3). Each time, a total of about _____ tubes with cracks were inspected in steam generator A.

Doel 2 steam generators have partial-depth roll tubes with the standard roll transition occurring well within the tubesheet. Roll transitions have not been shot peened and significant EZ PWSCC has been identified. As the PWSCC is confined by the tubesheet, crack indications have been allowed to remain in service. A total of _____ tubes with crack indications in steam generator A in 1989 were again inspected in 1990.

The most recent inspection results (3) for standard roll transitions indicate an average annual growth rate of _____ with a standard deviation of _____ for all crack sizes. In the crack range from _____ the growth rate was _____ . Based on the results from successive inspections the crack growth rate of _____ is used for computing the repair limit for standard-roll transitions.

Average crack growth rates as a function of initial crack length are shown plotted in figure E-1. The reported growth rates in terms of extension per year have been converted to extension per effective full-power year (EFPY) by dividing by 0.8.

Referring to figure E-1, note that growth rates for standard roll cracks are significantly lower at small crack lengths than that of cracks in kiss roll transitions. These differences are likely due to different residual stress patterns in kiss and standard roll transitions (4). The average growth rate for initial crack lengths in the range of _____ is similar to that observed in kiss rolls and is approximately _____

E.4 REFERENCES

1. D. Dobbeni, J. P. Benoit, and W. Ferket. Roll Transition Inspection of Doel-2 Steam Generator Tubes, Volume 1: June 1989 Inspection. Palo Alto, Calif.: Electric Power Research Institute, March 1990. NP-6716-L, vol. 1.
2. D. Dobbeni, J. P. Benoit, and W. Ferket. Roll Transition Inspection of Doel-2 Steam Generator Tubes, Volume 2: October 1990 Inspection. Palo Alto, Calif.: Electric Power Research Institute, June 1991. NP-6716-L, vol. 2.
3. D. Dobbeni, J.P. Bensoit, and W. Ferket, Roll Transition Inspection of Doel-2 Steam Generator Tubes, Volume 3: September 1991 Inspection. Palo Alto, Calif. Electric Power Research Institute, February 1991. NP-6716-L, Vol 3.
4. R. Houben and P. Hernalsteen. "Part Depth Rolled Plants, Status of the Doel 2 Unit." Proceedings: 1989 Electric Power Research Institute PWSCC Remedial Measures Workshop. Palo Alto, Calif.: Electric Power Research Institute, April 1990. NP-6719-SD.

Appendix F

LEAK RATE DATA FOR STEAM GENERATOR TUBES WITH SCC
IN THE EXPANSION ZONE ROLL TRANSITION REGION

Table F-1

CE S/G TUBE LEAKAGE TEST RESULTS, 600°F
AXIAL ROLL TRANSITION AND UNROLLED SECTION CRACKS
NORMAL OPERATING PRESSURE DIFFERENTIAL

Table F-2

CE S/G Tube Leakage Test Results, 600°F
Axial Roll Transition and Unrolled Section Cracks
Main Steam Line Break Differential Pressure

Table F-3

WESTINGHOUSE LEAK RATE TESTS
AXIAL ROLL TRANSITION CRACKS AT 600°F¹

Table F-4

IN-SERVICE LEAK RATES - AXIAL ROLL TRANSITION CRACKS

Table F-5

Crack Length and Measured Leak Rate at Normal and Faulted Pressure Differentials
for Pulled Tubes with Through-wall PWSCC in the EZ Roll Transition

Table F-5 continued

Table F-6

CEGB S/G TUBE LEAKAGE TEST RESULTS, 560°F
CRACKS IN UNROLLED TUBE SECTIONS
NORMAL OPERATING PRESSURE DIFFERENTIAL 1.2

Appendix G

ANALYSIS METHOD FOR LEAK RATE CALCULATION

G.1 INTRODUCTION

This appendix describes a methodology for evaluation of the primary to secondary leakage in a steam generator with a large number of through-wall axial cracks. The methodology comprises a probabilistic approach (Monte Carlo type) combined with a simple deterministic model for leakage from an axial crack.

G.2 BASE DETERMINISTIC MODEL

The deterministic model for leakage from an axial crack in a tube with internal pressure is given by the following formula:

$$Q = \quad \quad \quad (G-1)$$

S_u	=	ultimate stress (psi)
x^*	=	
m	=	
a_{TS}	=	tube sheet constraint adjustment (inches) (see section 4.5 and footnote)

Note:

The key parameters P_e , δ and K were established based on the following:

G.2.1 Effective Differential Pressure (P_e)

For "single-phase" flow of water, the formula holds true if P_e is taken as the actual differential pressure acting across the tube. When the secondary side is empty (vapor phase), as is the case for accident conditions, the leak flow will flash and the leak rate will be limited to a critical value by a choking process. A simple way to approximate this behavior is to use an "equivalent" or "effective" differential pressure by assuming a down stream back pressure equal to the saturation pressure; this approximation is valid for subcooling down to a range of 20 to 30°C.

G.2.2 Leakage Area (δ)

The leakage area is obtained by summation of an elastic and plastic component

$$\delta =$$

Elastic Component (δ_{el}). The elastic crack opening area (δ_{el}) of a through-wall axial crack is the sum of the pure elastic opening and a small scale yielding component, or

$$\delta_{el} =$$

Plastic Component (δ_{pl}). The plastic crack opening area of the crack (δ_{pl}) is a function of the tube material properties. This component gets larger when the differential pressure approaches the burst pressure. δ_{pl} can be expressed as a nonlinear function of crack length and the ratio of applied pressure to burst pressure, or

$$\delta_{pl} =$$

Typical values of δ_{pl} for a 7/8" diameter tube are illustrated in figure G-1. Section G.3.1 describes the development of this relationship

Figure G-1. Plastic Component of the Crack Leakage Area

G.2.3 Flow Discharge Coefficient (K)

Under normal operating conditions, the crack opening area is small and there is a major effect of the tortuosity of the leakage path on flow rate. This is caused by the intergranular nature of the stress corrosion process and is dependent on the material grain size, resulting in multiple flow restrictions and deviations. The consequence is a low apparent value of K which is difficult to estimate other than by curve fitting to the available data. Also, tight cracks under normal operating conditions can clog up to the point of being almost leak tight. For larger crack opening areas, as should be expected under accident conditions, the value of K will gradually increase up to a maximum value of about . Thus, the K value to be used is defined as a function of the calculated average crack width (leak area, δ , divided by crack length a).

The functional form used to model this behavior is

$$K =$$

where A and CW_0 are parameters to be determined from experimental data to obtain realistic leak rate estimates for this degradation mechanism. Conservative estimates can be obtained by taking $CW_0 =$ (even very small cracks leak) and A as a very large value ($K =$ maximum value of even at very small cracks). Figure G-2 shows two curves that illustrate conservative and realistic models for K over the range of interest in this work. Section G.3.2 describes the procedure used to determine the parameters A and CW_0 for PWSCC.

Figure G-2. Flow Discharge Coefficient Assumptions

G.3 MODEL VALIDATION

G.3.1 Crack Opening Area

The plastic component of the crack opening area (COA) was obtained over the full deformation range up to burst pressure. This was based on LABORELEC large scale testing of 7/8" and 3/4" diameter tube specimens with artificial flaws (3); the test rig used the feedwater pump of a Belgian fossil fueled plant and allowed bursting of test specimens with throughwall flaws, without any sealing bladder (pressure up to _____; flow rate in excess of _____).

Leak rate measurements were performed at various pressure levels, during the slow pressurizing process and, occasionally, during depressurization in those tests where the tube did not burst at maximum pressure.

Figure G-3 illustrates the results from two identical 7/8" diameter test specimens, each having a _____, through-wall EDM flaw. One specimen burst at _____. The other specimen did not burst at maximum pressure, so that it was possible to measure the leak rate during the pressure decrease; from comparison of the flaw deformation with prior laboratory experiments, it was concluded that _____ of the burst pressure had been reached. Figure G-3 also shows, in solid line, the leak rate predictions for the full-cycle (pressure up and down); the agreement with test data is quite good.

Figure G-3. Leakage Model Validation

A systematic assessment of the crack opening area for all tested specimens was made with the following procedure. The COA values were derived from the measured leak rates using Equation G-1, i.e.,

$$\delta =$$

where: (1) as the test were conducted at room temperature, P_e was taken equal to the actual differential pressure, (2) as EDM notches were used, with an initial flaw width of about , the discharge coefficient could realistically be valued at $K =$, and (3) the initial flaw area of the EDM slot () was subtracted from the calculated value of δ .

The resulting "measured" COA values were then fitted to obtain the δ_{pl} relationship presented in section G.2.2. Plots of the "measured" data and calculated fit are presented in figures G-4 and G-5 for linear and logarithmic coordinates, respectively. The agreement is quite good over the full range of plastic deformation.

Figure G-4. Comparison of Calculated Leak Areas With Measured Areas, Belgian Data from SCHELLE tests (Linear Coordinates)

Figure G-5. Comparison of Calculated Leak Areas With Measured Areas,
Belgian Data from SCHELLE tests (Logarithmic Coordinates)

G.3.2 Discharge Coefficient

The discharge coefficient K has been derived on basis of a theoretical model involving flow discontinuity ("elbows" simulating the tortuosity of the flow path in narrow cracks) and fictional losses. The result was approximated by the functional form proposed in section G.2.3, or

$$K =$$

To validate the model and determine realistically conservative values for the parameters A and CW_0 , K values were obtained from tubes where both leak rate and crack opening area had been measured experimentally. These tests included tubes with laboratory induced corrosion cracks, either in free span or in EZ roll transitions (simulated tube sheets), and are listed in Tables F-1 and F-2 for normal operating differential pressure and faulted differential pressure, respectively.

Most tubes had one crack per tube. In all cases the COA was measured both at the inner and outer surface of the tube, and the lower value was used, which results in higher (conservative) values of K .

The discharge coefficient was derived from equation G-1 by

$$K =$$

and the following: (1) as the leak was discharges into a water environment (single phase flow), P_e was taken as the differential pressure, (2) δ was obtained by increasing the measured COA (plastic component) by the calculated elastic component, δ_{el} , where a was taken as the average crack length (the ID length being usually somewhat larger than the OD length), and (3) the resulting K factor is associated with the average crack width w .

The results are illustrated by Figure G-6; measured K values in excess of K_{max} result from measurement inaccuracies (in either COA or leak rate). On this basis, the proposed model parameters are A and CW_0 . The experiment data clearly show the same trend as the proposed model, which provides an upper bound.

For the lower CW and K values, inaccuracies may result from an elastic crack not closing back upon unloading (not perfectly matching crack faces); this would unduly increase the assumed CW and decrease the assumed K . These data also were evaluated conservatively by assuming the "measured" (residual) COA to be the total δ value (no elastic correction); the modified data points (the \square data points in Figure G-6) are still bounded by the proposed model.

Figure G-6. Correlation Between Flow Discharge Coefficient, K ,
and Mean Crack Width, CW

G.3.3. - Leak Rate Validation

While the critical components of the model (K and δ) are validated as previously discussed, the full procedure was further benchmarked with leak rate data from pulled tubes and representative laboratory induced corrosion cracks. The following data were used for the benchmark:

1. PWSCC in EZ roll transitions of pulled tubes (see Table F-5), at both normal operating () and faulted () differential pressures.
2. Doped steam SCC in laboratory roll transition mock ups of ALLOY 600 MA (see table F-3), at normal operating differential pressure ().
3. Polythionic acid SCC in laboratory straight run and roll transition mock ups of sensitized ALLOY 600 (see tables F-1 and F-2), at both normal operating (psi) and faulted () differential pressures.
4. Polythionic acid SCC in straight run specimens of sensitized ALLOY 600 (see table F-6), at normal operating differential pressure ().

The measured leak rates from the four data sets are plotted against the predicted leak rates, as calculated by Equation 5-1, and the results are shown in figure G-7; in all cases the ID length of crack was used for calculation. The leak rates are calculated at the test temperature except for data set #4, which is explicitly stated to be normalized at room temperature.

The following data are not included in figure G-7:

- data for which either the predicted or measured leak rate is zero (not compatible with logarithmic scale).
- data from set #2 at normal operating conditions, because the integrated leak rate (all pulled tubes) was measured at a value times larger than the measured inservice leak rate of the plant, just prior to the outage. This results from (unavoidable) damage to the roll transition areas during tube pulling, which is likely to considerably increase the leak rate, especially when measured under conditions involving little to no additional plastic deformation (as is the case under simulated normal conditions).

Figure G-7. Comparison of Calculated Leak Rates (Eq. 5-1) With Measured Leak Rates From Various Test Programs

The following describes the tube and/or experimental conditions where zero leakage was either measured or predicted.

- For data set #1, under normal operating conditions:
 - 1 tube (26-69 with a long crack) is correctly predicted not to leak
 - 1 tube (22-31 with a long crack) is predicted not to leak while a minute leak (); is measured, likely as the consequence of tube pull deformation.
- For data set # 1, under faulted conditions
 - 1 tube (26-69) is predicted to slightly leak () while no leak rate is measured
- For data set #2, seven additional test specimens (HOUTM-7 to 14, from table F-3, with a long crack) are predicted to slightly leak () while the unquantified actual leak rate is stated to be below a threshold of
- For data set #4, one tube (n° 1023, with a long crack) is predicted to very slightly leak () while no leak rate is measured.

The non zero leak rate test results in figure G-7 where the predicted leakage is less than the measured leakage generally can be attributed to one or more of the following: (1) deformation induced by pulling, (2) a number of parallel axial cracks (of comparable length), combined with dominant, circumferential cracks (while the predicted value was based on a single crack), (3) low measurement accuracy (below sensitivity threshold). These data were included in the data base until more detailed information could be obtained concerning the exact crack and experimental conditions.

Examination of figure G-7 shows that the predicted values are conservative for the large majority () of the individual tests ; this applies to a very large range of leak rates (over orders of magnitude), three tube diameters (7/8", 3/4" and 11/16"), several heats of material, two metallurgical conditions (MA and sensitized), and various experimental conditions, including straight runs and rolls transitions, and NOP and SLB pressure differentials).

As a general conclusion, Equation 5-1 provides a conservative representation of available leak rate data from laboratory and field. While the measured leak rates are greater than the predicted leaks rates for some individual experiments, the relevant quantity for ensuring that 10CFR100 dose limits are maintained during the postulated faulted load is the sum of the leak rates from all degraded tubes in the steam generator. To demonstrate that the calculational method provides conservative values for assessing compliance with 10CFR100 limits, the sum of the predicted leak rate for each of the four data sets was compared to the sum of the measured values. The results are presented in Table G-1 and show that, while individual predicted leak rates may be less

than measured values, the sum of the predicted values is significantly more conservative than the sum of the measured values. Work is still in progress to provide an improved formulation (such as an increased CW_0 value), with less conservative but still acceptable margins with respect to best estimate behavior for the steam generator as a whole.

Table G-1

Comparison of Predicted Total Leak Rates With Total Measured Leak Rates

G.4 PROBABILISTIC METHODOLOGY

The probabilistic methodology consists of a stochastic combination of (1) the statistical distributions assumed for each of the parameters involved in the base deterministic model, and (2) the population of crack lengths established by in-service inspection of the steam generator. It results in a Monte Carlo type evaluation, with repeated calculation of the base formula for every possible combination of crack length and associated set of relevant parameters. Appropriate statistical distributions are used for:

- Mechanical properties ($S_y + S_u$) at operating temperature.
- Correlation coefficient between "flow stress" ($\bar{\sigma}$) and mechanical properties.

$$C_S =$$

- Tube wall thickness.
- Sizing uncertainty on crack length (based on RPC inspection technique).
- Expected crack lengths at the end of next (or current) operating cycle.

The first four distributions can be approximated by Gaussian curves while the last distribution needs inspection results and some knowledge of the crack growth of the population of interest.

Deterministic algorithms and input values are further used to take into account:

- Reinforcing effect of the tubesheet in accordance with figure 4-4 (Eqs. 4-4 and 4-5).
- Shape Factor. Empirical formula derived from LABORELEC laboratory experiments (plastic deformation of specimens with axial artificial flaws of trapezoidal shape).
- Repair Limit. Arbitrary value; in the examples a value of 11 mm has been used.

G.5 COMPUTER PROGRAM

A version of the above methodology has been developed into a software program, written in APL language and implemented on a personal computer (1, 2). The program is user-friendly and does not require any special computer training. A simple "input data screen" can be edited to select the particular set of parameters representative of the steam generator under consideration. These include:

- Mechanical Properties ($S_y + S_u$). Average and standard deviation values.
- Flow Stress Coefficient (C_s). Average and standard deviation values.
- Eddy-Current (RPC) Crack Length Sizing Error. Average and standard deviation values.
- Tube Wall Thickness. Average and standard deviation values.
- Crack Length Distribution. 3 options are available:
 - Uniform distribution. Used only to get information about the relative "weight" of each crack length in contributing to the total leak rate.
 - Given distribution of crack lengths (histogram). This allows the input of any kind of distribution expected at the end of the operating cycle, as derived from the inspection data at the start of cycle.
 - Probabilistic model of steam generator degradation. This includes input of the initial (start of cycle) crack length and crack growth distributions and the required repair limit.
- Flow Shape Factor. Coefficients of the linear relationship between ID and OD crack lengths.
- Flow Discharge Coefficient. Selection of either constant K value or an optional function of crack width (see Eq. G-1 and section G.3.2).
- Primary Pressure and Temperature; Secondary Pressure.
- Number of Cracks.

The LABOLEAK software generates a series of useful graphs; typical examples of these graphs are illustrated below in Figures G-8 through G-14, which were generated using the input summarized in Table G-2.

TABLE G-2 : Input Data Used for Sample Probabilistic Calculation

Fig. G-8 Distribution of Initial Crack Lengths
This is a graphic representation of the specified input (inspection results at the start of cycle).

Fig. G-9 Distribution of End of Cycle and Critical Crack Lengths
This illustrates the range of:

- Critical crack lengths for the specified conditions; variation is caused by variations in $(S_y + S_u)$, C_s , and t (tube wall thickness).
- Predicted crack lengths at the end of cycle.

Comparison of these two distributions gives a picture of the overall safety margin with respect to tube failure. The calculated "probability of steam generator tube rupture" is also indicated.

Fig. G-10 Mean Crack Width as a Function of Crack Length
This illustrates the nonlinear relationship between width and length of cracks under the specified conditions; the elastic component of the crack width is also indicated.

Fig. G-11 Distribution of Crack Width (For a Long Crack)
This illustrates, for any particular crack length, the variation of crack widths from the average value given by figure G-10.

Fig. G-12 Contribution of Each Crack Length Category to the Total Leak Rate
This illustrates the contribution of each crack length category to the total leak rate. No contribution is observed for the shorter cracks while the peak contribution is influenced by the crack length distribution (figure G-9). The "best-estimate" value of the total leak rate is also indicated.

Fig. G-13 Distribution of Tube Leak Rates
This illustrates the relative participation of individual leakers.

Fig. G-14 Distribution of Steam Generator Leak Rate (mean=)
This illustrates the expected variation of the total leak rate for the given number of cracks. It allows selection of leak rate values at any predefined confidence level.

Figure G-8. Distribution of Initial Crack Lengths

Figure G-9. Distribution of End of Cycle and
Critical Crack Lengths

Figure G-10. Mean Crack Width as a Function
of Crack Length

Figure G-11. Distribution of Crack Width (For a
Inch Long Crack)

Figure G-12. Contribution of Each Crack Length Category to the Total Leak Rate (Total = gpm)

Figure G-13. Distribution of Tube Leak Rates

Figure G-14. Distribution of Steam Generator
Leak Rate (mean= gpm)

G.7 REFERENCES

1. P. Hernalsteen. "LABOLEAK: Laborelec Leakrate Probabilistic Assessment Program for PWSCC Cracks in Steam Generator Tube Roll Transitions - User's Manual." LABORELEC Report M00-90-023/R-PH, May 1990.
2. P. Hernalsteen. "LABOLEAK: Laborelec Leakrate Probabilistic Assessment Program for PWSCC Cracks in Steam Generator Tube Roll Transitions - Description and Validation." LABORELEC Report M00-90-024/R-PH, May 1990.
3. P. Hernalsteen, "The Influence of Testing Conditions on Burst Pressure Assessment For Inconel Tubing", Int. J of Pressure Vessels and Piping 52 (1992).

Appendix H

COMBINATION AXIAL AND CIRCUMFERENTIAL CRACK DETECTION UTILIZING RPC EDDY-CURRENT PROBES

H.1 INTRODUCTION

A series of laboratory experiments were conducted to define the ability of the rotating pancake coil (RPC) eddy-current probe to detect circumferentially oriented cracks in the presence of through-wall axial cracks simulated by using EDM notches. The results of these experiments are summarized in this appendix.

In principle, the RPC is equally sensitive to both axial and circumferential cracking. Crack orientation is inferred by noting the direction of the major axis of the indication; an axial crack--of sufficient length--will have its major axis aligned or directed along the tube longitudinal axis. A circumferential crack--again of sufficient length--will have its major axis directed along the tube circumference.

H.2 NDE EXPERIMENTS

U-shaped EDM notch test samples in expanded tubes with tubesheet collars were fabricated in order to investigate the detection and resolution capability of the RPC. U-shaped notch geometry and dimensions were specified based on structural considerations. A drawing of the notch geometry showing typical shape and location relative to the upper roll expansion is shown in figure H-1. A summary of U-shaped notch dimensions for the test sample matrix is given in table H-1.

Test data was taken using three pancake coil configurations. These included and diameter unshielded coils and a diameter shielded coil.

Front and rear view oblique RPC graphics for the unshielded and shielded pancake coils--for five U-shaped EDM notch geometries summarized in table H-1--are shown in figures H-2 through H-11. A summary of the test results, e.g., whether the circumferential notch which links the two adjacent axial notches is discernible, as inferred from a review of the graphic area, is given in table H-2. The unshielded pancake coil data is not included since the results are not significantly improved over the coil data.

Figure H-1. Typical Test Sample Geometry
(Expanded Tube With U-Shaped Notch at Roll)

Table H-1

TEST SAMPLE MATRIX

U-Shaped Notch
Closed-End View

U-Shaped Notch
Open-End View

Figure H-2. Pancake Coil -

Diameter, Sample # Z-9300

U-Shaped Notch
Closed-End View

U-Shaped Notch
Open-End View

Figure H-3. Pancake Coil - Diameter (Shielded), Sample # Z-9300

U-Shaped Notch
Closed-End View

U-Shaped Notch
Open-End View

Figure H-4. Pancake Coil - Diameter, Sample # Z-9299

U-Shaped Notch
Closed-End View

U-Shaped Notch
Open-End View

Figure H-5. Pancake Coil - Diameter (Shielded), Sample # Z-9299

U-Shaped Notch
Closed-End View

U-Shaped Notch
Open-End View

Figure H-6. Pancake Coil -

Diameter, Sample # Z-9289

H-7

U-Shaped Notch
Closed-End View

U-Shaped Notch
Open-End View

Figure H-7. Pancake Coil - Diameter (Shielded), Sample # Z-9289

U-Shaped Notch
Closed-End View

U-Shaped Notch
Open-End View

Figure H-8. Pancake Coil - Diameter, Sample # Z-9281

U-Shaped Notch
Closed-End View

U-Shaped Notch
Open-End View

Figure H-9. Pancake Coil - Diameter (Shielded), Sample # Z-9281

H-10

U-Shaped Notch
Closed-End View

U-Shaped Notch
Open-End View

Figure H-10. Pancake Coil - Diameter, Sample # Z-9280

U-Shaped Notch
Closed-End View

U-Shaped Notch
Open-End View

Figure H-11. Pancake Coil - Diameter (Shielded), Sample # Z-9280

H.3 RESULTS

The conventional diameter pancake coil clearly resolves the circumferential notch at and spacings, with a degraded capability beginning at or slightly greater. The (shielded) pancake coil offers significantly improved resolution, with the circumferential notch visible down to a axial notch separation. Even the circumferential notch linking the two axial notches is resolvable.

Table H-2

SUMMARY OF PANCAKE COIL DATA

Appendix I

PRESSURE TESTS OF STEAM GENERATOR TUBES WITH COMBINATION AXIAL AND CIRCUMFERENTIAL CRACKS

I.1 INTRODUCTION

A number of pressure tests have been conducted with steam generator tubes containing combinations of axial and circumferential degradations. These tests included machined through-wall linear degradations inclined at an angle with respect to the tube axis, machined "L" shaped cracks with an axial and circumferential through-wall component, machined "U" shaped cracks with axial through-wall components, and part-through-wall and through-wall circumferential components. A limited number of tests with tubes containing laboratory-produced stress corrosion combination cracks have also been conducted.

Pressure tests involve pressurizing a section of steam generator tube containing either machined degradations or stress corrosion cracks. For through-wall degradations, a crack sealing system was used to maintain tube pressure. Tubes were pressurized until the maximum pressure that the tube can support was achieved. Generally, maximum pressure occurs when part-through-wall ligaments tore or the crack sealing system was lost. This would result in a tube leak, and with a limited makeup capacity pressurization system, higher pressures could not be applied.

I.2 LABORELEC DATA

LABORELEC pressure-tested the degradation geometries shown in figure I-1. Inclined axial crack specimens had through-wall electrodischarge-machined (EDM) slits with overall lengths from _____ to _____ inclined with the tube axis from _____. "L" shaped crack specimens had EDM through-wall slits with _____ axial components and _____ circumferential legs with gaps between the axial and circumferential components for _____ to _____.

The LABORELEC test results are provided in table I-1 and are shown plotted in figures I-2 and I-3. These figures show the dimensionless length (λ) of the axial component of the degradation plotted with dimensionless maximum pressure \bar{P} . These dimensionless parameters are defined in Eqs. 2-8 and 2-9.*

*See section 2.

Also shown in figures I-2 and I-3 is the "EPRI" burst curve for a simple through-wall axial crack. This curve is defined by Eq. 2-11.* For reference, the dimensionless pressure corresponding to 3 times normal differential pressure and MSLB differential pressure, along with the dimensionless axial crack length corresponding to the repair limit and the repair limit defined in section 4.0, are shown in each of these figures as well.

Referring to figure I-2, note that the inclined axial cracks all had maximum test pressures above the burst curve. This was true even for a degradation inclined to the tube axial by θ with a $L \sin \theta$ projected axial length and a $L \cos \theta$ projected circumferential length. Figure I-3 shows that the "L" shaped degradation tests also produced maximum pressures that fall on or above the burst curve. These tests show that for these geometries one could neglect the circumferential component of the "L" shaped degradations and estimate the tube maximum pressure using the burst curve for simple axial cracks.

I.3 TECNATOM DATA

TECNATOM tested the EDM degradation geometries shown schematically in figure I-4 (1). The test degradation configurations generally included two axial through-wall degradations separated by either L or $L/2$. The circumferential degradations were part-through-wall and intersected the axial defects. In a few of the TECNATOM tests, the circumferential degradation was at or below the top of a simulated tubesheet. TECNATOM test results are summarized in table I-2 and are shown plotted in figure I-5. Examination of figure I-5 shows that unless the depth of the circumferential crack was deeper than $t/2$ of the wall thickness, the maximum pressure was above the burst curve. The same conclusion is reached in all cases that the circumferential cracks are within the tubesheet.

I.4 WESTINGHOUSE DATA

Westinghouse pressure test results for "L" and "U" shaped cracks are summarized in table I-3 and are shown plotted in figures I-6 and I-7.

Through-wall "L" shaped cracks had an axial length of L with circumferential lengths of L or $L/2$. Figure I-6 shows that with circumferential length of the "L" shaped crack equal to L , the maximum test pressure falls above the burst curve, while with the $L/2$ circumferential lengths, they fall below the curve.

Westinghouse conducted tests with machined "U" shaped degradations where the circumferential component was not completely through-wall and where the circumferential component was through-wall with shims inserted in the circumferential slots to create slot face interference. The results of these tests are

shown in figure I-7. Maximum pressures for machined "U" shaped specimens through-wall and through-wall are below the burst curve. Specimens with machined "U" shaped degradations through-wall achieved maximum pressures equal to or above the burst curve. Note that in spite of being below the burst curve, "U" shaped specimens with axial through-wall components longer than the repair limit defined in section 4 and through-wall circumferential components supported pressures greater than MSLB differential pressures.

Westinghouse tested steam generator tubes with combination stress corrosion crack geometries produced in model boiler tests (2). Sketches of the resulting stress corrosion crack geometries are shown in figure I-8. Crack geometries which can be characterized as "L" and "U" shaped are included. The depth of the circumferential portion of the stress corrosion cracks was reported as through-wall. A collar was used to simulate the tubesheet. The specimens were fabricated with the roll transition flush, to slightly above (about), the simulated tubesheet. The test results are summarized in table I-3, and maximum test pressures are plotted in figure I-9. It is important to note that in all cases, maximum test pressure was above the burst curve and significantly above the maximum pressure supported by EDM degradations with similar dimensions.

1.5 REFERENCES

1. Evaluation of the Impact of the Presence of Circumferential Orientation Fissures in the Transition Zone of the Expanded Portion of Steam Generator Tubes. TECNATOM Report, December 21, 1990.
2. J. A. Begley. Evaluation of the Leak and Burst Characteristics of Roll Transitions Containing Primary Water Stress Corrosion Cracks. Palo Alto, Calif.: Electric Power Research Institute (publication pending). NP-7414.

Table I-1

LABORELEC COMBINED AXIAL AND CIRCUMFERENTIAL CRACK
PRESSURE TEST DATA

Table I-2

TECNATOM COMBINED AXIAL AND CIRCUMFERENTIAL
CRACK PRESSURE TEST DATA

Table I-3

WESTINGHOUSE COMBINED AXIAL AND CIRCUMFERENTIAL
CRACK PRESSURE TEST DATA

Figure I-1. LABORELEC Combination
Notch Geometries

Figure I-2. LABORELEC Through-Wall Angle
Degradation Pressure Tests

Figure I-3. LABORELEC Through-Wall "L" Shaped
Degradation Pressure Tests

Figure I-4. Spanish Combination Degradation
Pressure Test - Specimen Configuration

Figure I-5. TECNATOM Part-Through-Wall Degradation
Pressure Tests

Figure I-6. Westinghouse Through-Wall "L" Shaped
Degradation Pressure Tests

Figure I-7. Westinghouse Modified Through-Wall and
Part-Through-Wall "L" Shaped Degradation Pressure
Tests

Figure I-8. Sketches of Axial and Circumferential Cracks in Westinghouse RP301-9 Specimens

Figure I-9. Westinghouse Stress Corrosion Crack
Pressure Tests